The University Of Sheffield.

Clathrin light chains' role in Endocytosis: Cargo in Focus

By:

Hannes F. Maib

A thesis submitted in partial fulfilment of the requirements for the degree of Doctor of Philosophy

The University of Sheffield

Faculty of Science

Department of Biomedical Sciences

December 2018

1 TABLE OF CONTENTS

ABSTRACT

Clathrin light chains (CLCs) control selective uptake of a range of G protein-coupled receptors (GPCRs), although the mechanism by which this occurs has remained elusive thus far. In particular, site-specific phosphorylation of CLCb controls the uptake of the purinergic GPCR $P2Y_{12}$, but it is dispensable for the constitutive uptake of the transferrin receptor (TfR). We demonstrate that phosphorylation of CLCb is required for the maturation of clathrin-coated pits (CCPs) through the transition of flat lattices into invaginated buds. This transition is dependent on efficient clathrin exchange regulated by CLCb phosphorylation and mediated through auxilin. Strikingly, this rearrangement is required for the uptake of $P2Y_{12}$ but not TfR. These findings link auxilin-mediated clathrin exchange to early stages of CCP invagination in a cargo-specific manner. This supports a model in which CCPs invaginate with variable modes of curvature depending on the cargo they incorporate.

ACKNOWLEDGEMENTS

First of all I want to thank my supervisor Liz Smythe. Completing my PhD under her guidance was a great experience and she was always there for me to discuss ideas and motivate me when I doubted myself. It was a great pleasure to have her as my supervisor and be able to share my passion about science and clathrin with her.

I also want to thank the Marie Curie network for funding my PhD and giving me a great opportunity to travel across Europe, meet great people and build both a professional and personal network that will last for many years.

I also want to thank everyone who helped with my experiments and especially to the Roux lab in Geneva with their help in electron microscopy.

Of course I want to thank all of my friends that I met here in Sheffield. Moving to another country is always a big challenge, but with the help and support of my friends, I made it into my home. Without you all, this would not have been a very enjoyable time. Thank you for making me love this beautiful city that will always have a special place in my heart. Even though my journey though the world will continue, I am sure that we will keep in touch and I will visit Sheffield as often as I can.

Thanks to everyone in the Smythe labs who made me feel very welcome.

Cheers,

Hannes

LIST OF ABBREVIATIONS

aa	amino acid
AD	Alzheimers Diseas
AFM	Atomic Force Micrscopy
AP	assembly Proteins
AP2	Adaptor Protein 2
APP	Amyloid Precursor Protein
Arp2/3	Actin-related protein 2/3
ATP	Adenosine triphosphate
BSA	Bovine serum albumin
CALM	Phosphatidylinositol-binding Clathrin assembly protein
CCP	Clathrin Coated Pit
CCR5	C-C chemokine receptor type 5
CCV	Clathrin Coated Vesicle
CHC	Clathrin heavy Chain
CHC17	Clathrin Heavy Chain 17
CHC22	Clathrin Heavy Chain 22
CLCa	Clathrin light Chain A
CLCb	Clathrin Light Chain B
CLEM	Correlative light and electron microscopy
CXCR4	C-X-C chemokine receptor 4
CXCR5	C-X-C chemokine receptor 5
DMSO	Dimethyl sulfoxide
EDTA	Ethylenediamine tetraacetic acid
EEA1	Early endosome antigen 1
EGF	Epidermal Growth Factor
EGFR	Epidermal growth factor receptor
ELISA	enzyme-linked immunosorbent assay
EM	Electron Micrscopy
Eps15	Epidermal growth factor receptor substrate 15
FCHO1	F-BAR domain only protein 1
FCHO2	F-BAR domain only protein 2
FCS	Fetal Calf Serum
FRAP	Fluorescence recovery after photobleaching
GAK	Cyclin-G-associated kinase
GDP	Guanosine diphosphate
GFP	green fluorescent protein
GLUT4	Glucose transporter type 4
GPCR	G-protein-coupled receptors
GPI	Glycosylphosphatidylinositol
GRK2	G Protein-Coupled Receptor Kinase 2
GTP	Guanosine triphosphate
HA tag	hemagglutinin tag
HeLa	Henrietta Lack
Hip1	Huntingtin-interacting protein 1

hip1R	Huntingtin-interacting protein 1-related protein
Hsc70	Heat shock cognate 71 kDa protein
IgG-A	Immunoglobulin G - A
KO	Knock Out
LatA	Latrunculin A
LDL	low-density lipoprotein
LPA	lysophosphatidic acid
MAP kinase	mitogen-activated protein kinase
MOPr	mu opioid receptor
NT	nontargeting
o.n.	over night
PBS	Phosphate-buffered saline
PBS-T	Phosphate-buffered saline - Tween
PFA	paraformaldehyde
PIP2	Phosphatidylinositol 4,5-bisphosphate
PTEN	Phosphatase And Tensin Homolog
RIPA	Radioimmunoprecipitation assay
RT	Room Temperature
SD	Standard deviation
SDS	sodium dodecyl sulfate
SEM	Standard error of the Mean
siRNA	small interfering Ribonucleic Acid
SQUASSH	segmentation and quantification of subcellular shapes
TD	Terminal Domain
TfR	Transferrin Receptor
TGFbR2	Transforming growth factor receptor 2
TIRF	total internal reflection fluorescence
YAP	Transcriptional coactivator YAP1

1 INTRODUCTION

1.1 MAIB, H., E. SMYTHE, AND K. AYSCOUGH. 2017. "FORTY YEARS ON: CLATHRIN-COATED PITS CONTINUE TO FASCINATE". *MOL BIOL CELL*. 28:843-847.

Cells are surrounded by a lipid bilayer that separates them from their surroundings and the formation of this barrier has been an essential step for the development of life. However, for particles and nutrients to be taken into the cell, they have to cross this barrier without disrupting it. One of the key pathways that regulates this uptake is called Clathrin Mediated Endocytosis (CME) and has been studied extensively over the past four decades. In order to give a brief overview into the development of this field, we wrote a retrospective. This review focuses on key developments in the field of CME that have led to conceptual advances as well as future directions of CME and its importance to heath and disease. The initial draft was devised by me (as apparent by position of authors) with major contributions of Elizabeth Smythe and Kathryn Ayscough towards the finalisation of the manuscript. The article was aimed for a general audience, has been peer reviewed and was published in the journal "Molecular Biology of the Cell" in April 2017. Following this general introduction into CME, a more in depth introduction section will follow in order to prepare the reader for the research that has been conducted in this thesis.

_____ _____

Hannes Maib Elizabeth Smythe

_____

Kathryn Ayscough

Forty years on: clathrin-coated pits continue to fascinate

Hannes Maib, Elizabeth Smythe, and Kathryn Ayscough*
Department of Biomedical Science, Centre for Membrane Interactions and Dynamics, University of Sheffield, Sheffield S10 2TN, United Kingdom

ABSTRACT **Clathrin-mediated endocytosis (CME) is a fundamental process in cell biology and has been extensively investigated over the past several decades. Every cell biologist learns about it at some point during his or her education, and the beauty of this process has led many of us to go deeper and make it the topic of our research. Great progress has been made toward elucidating the mechanisms of CME, and the field is becoming increasingly complex, with several hundred new publications every year. This makes it easy to get lost in the vast amount of literature and forget about the fundamentals of the field, which are based on the careful interpretation of simple observations made >40 years ago, as exemplified by a study performed by Anderson, Brown, and Goldstein in 1977. We examine how this seminal study was pivotal to our understanding of CME and its progression into ever-increasing complexity over the past four decades.**

Monitoring Editor
David G. Drubin
University of California, Berkeley

Received: Nov 8, 2016
Revised: Jan 23, 2017
Accepted: Jan 30, 2017

THE PATH FROM THE PLASMA MEMBRANE TO THE LYSOSOME

In their landmark study, Roth and Porter (1964) were the first to describe the uptake of yolk protein through small "bristle-coated pits" at the plasma membrane of mosquito oocytes and rightfully predicted their importance for the uptake of extracellular material. In March 1977, when understanding of the process of endocytosis was still in its infancy, Anderson, Brown, and Goldstein performed a study that described the uptake of the low-density-lipoprotein (LDL) receptor from coated regions on the plasma membrane into endocytic vesicles that subsequently fuse with lysosomes (Anderson *et al.*, 1977a). In an era before the advent of fluorescently tagged proteins, relatively little was known about the uptake of cargo proteins by receptors. Goldstein and his colleagues realized the importance of specific cell surface receptor interactions from their studies following the internalization of ferritin-labeled LDL molecules. In a series of beautifully detailed electron micrographs, they observed that ~70% of LDL was located in small coated regions that made up only ~2% of the total surface (Figure 1). These regions would later become known as clathrin-coated pits (CCPs). By allowing LDL to bind to cells at 4°C (blocking receptor uptake) and subsequently warming the cells back to 37°C for various times before fixation, they we able to follow the uptake of LDL from these coated regions into the cell. By arranging the electron micrographs into a logical order, they concluded that LDL binds to its receptor in coated regions of the plasma membrane, which become deeply invaginated and then are pinched off to form intracellular vesicles. These vesicles are then trafficked through the cell to fuse with lysosomes, where LDL is degraded. As a control, they also visualized the uptake of horseradish peroxidase in the same manner. This protein is not recognized by specific receptors on the plasma membrane and so does not become concentrated in coated pits but is still taken up by the cell to some degree. These findings and the use of cells from a patient with hypercholesterolemia, whose fibroblasts were unable to bind LDL, led Goldstein and his colleagues to postulate the model of receptor-mediated endocytosis in a prescient review 2 years later (Goldstein *et al.*, 1979). This basic trafficking pathway is common knowledge for many of us today, but at the time it took tremendous conceptual insight and creativity to postulate it from a series of simple observations. Moreover, this model is still valid and includes the notion of high-affinity receptors, cargo selection, and recycling pathways. Strikingly, it also suggested the existence of additional, clathrin-independent endocytic pathways, which are increasingly recognized as having key physiological roles (Mayor *et al.*, 2014). It has become the framework for a whole field of research and has inspired scientists throughout the past 40 years.

DOI: 10.1091/mbc.E16-04-0213

*Address correspondence to: Kathryn Ayscough (k.ayscough@sheffield.ac.uk).

Abbreviations used: AD, Alzheimer's disease; AP, adaptor protein; CCP, clathrin-coated pit; CME, clathrin-mediated endocytosis; LDL, low density lipoprotein; TIRF, total internal reflection fluorescence.

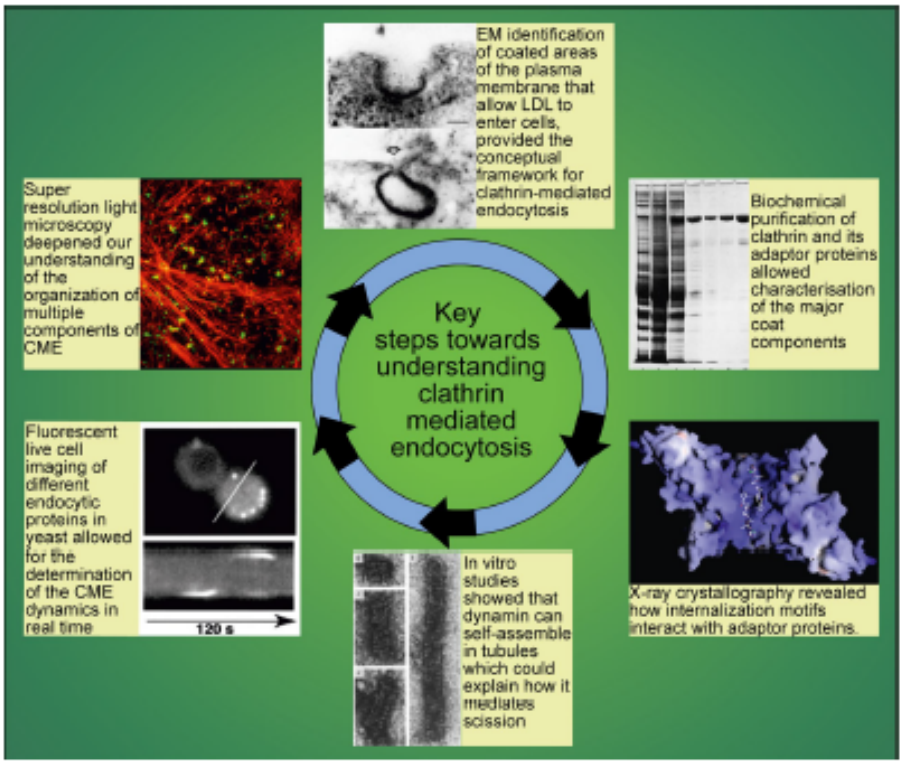

FIGURE 1: Key steps in our understanding of the CCV cycle. Clockwise from top: original images showing LDL-ferritin being internalized through coated structures on the surface of normal fibroblasts (Anderson *et al.*, 1977a); SDS–PAGE gel showing clathrin and adaptor proteins purified from pig brain (Pearse, 1975); x-ray crystallography studies revealing how tyrosine-based motifs interact with AP2 (Owen and Evans, 1998); in vitro studies showing that dynamin assembles into ring structures that suggest a mechanism by which dynamin might pinch off coated pits (Hinshaw and Schmid, 1995); studies in yeast pioneering live-cell imaging to understand dynamics of endocytic patch assembly (Kaksonen *et al.*, 2003); structured illumination imaging allowing unprecedented resolution to visualize the relationship of clathrin-coated structures (green) to the actin cytoskeleton (red; Li *et al.*, 2015).

KEY STEPS TO UNDERSTANDING THE MOLECULAR MACHINERY OF CCPs

The key protein component of these coated regions was purified by Pearse (1975), who named it clathrin (from the Latin *clatratus*, meaning "like a lattice"). This marked the beginning of the molecular era, and the key components of clathrin-mediated endocytosis (CME) were identified. Through biochemical purifications, "assembly" or "accessory" proteins (APs) were isolated (Zaremba and Keen, 1983; Pearse and Robinson, 1984; Ahle and Ungewickell, 1986), and by reconstituting clathrin-coated vesicles (CCVs) in vitro, it was shown that they connect the clathrin coat to the membrane, acting as adaptors (Vigers *et al.*, 1986). Progress in molecular biology made it possible to express and purify modified versions of proteins, and after years of painstaking research and contradictory results, investigators were able to identify internalization signals in cargo molecules and how they are recognized by the APs. This led to the discovery of a simple tyrosine motif as the first internalization sequence that is recognized by the adaptor molecule AP2 (Traub and Bonifacino, 2013). Elegant structural studies revealed that when AP2 is recruited to the plasma membrane, it undergoes a conformational change to enable it to bind to cargo-sorting signals and clathrin (Kelly *et al.*, 2014; reviewed in depth by Robinson, 2015). All of these discoveries are perfectly in line with the postulated model from Goldstein and colleagues, which predicted the existence of such a sorting motif after their study in 1977.

Despite these advances, the mechanism by which CCPs are pinched off from the membrane remained unresolved. The solution to this came from understanding why a temperature-sensitive *Drosophila melanogaster* mutant (called *shibire*) is paralyzed at high temperatures (Poodry *et al.*, 1973). Electron microscopy studies of this mutant revealed that coated pits at the neuromuscular junction were stalled at a late stage of CME as deep invaginations in the plasma membrane that could not be pinched off. After identification and cloning of the responsible gene, a defect in the GTPase dynamin was shown to be responsible for this phenotype (Chen *et al.*, 1991; Vanderbliek and Meyerowitz, 1991). It took additional years to discover that dynamin assembles into ring-like structures (Hinshaw and Schmid, 1995) around the neck of deeply invaginated coated pits (Takei *et al.*, 1995), and indeed the precise mechanism by which dynamin causes the final scission of CCPs is still not fully resolved and remains a major research focus (Antonny *et al.*, 2016). Having identified the key components of the fundamental model, from the concentration of cargo into CCPs by adaptor proteins, to their scission by the GTPase dynamin, more detailed analysis led to the discovery of many new factors that influence CME. This included many more adaptors, regulatory proteins, and components that sculpt the membrane, promoting and sensing increasing curvature as the pit buds inward to form a vesicle (Merrifield and Kaksonen, 2014).

A DYNAMIC PERSPECTIVE THROUGH LIVE-CELL IMAGING

The availability of fluorescent protein tags and the use of real-time fluorescence microscopy greatly affected how CME could be investigated. For the first time, the dynamics of the endocytic machinery and recruitment of several key components to growing CCPs could be visualized in real time. This meant that all the pieces of the model proposed by Goldstein and his colleagues could be put together to form a complete picture of CME in live cells. The ease of genetic manipulation of *Saccharomyces cerevisiae* made this model system extremely amenable to this new technology. Even though the process of endocytosis in yeast initially seemed to differ in some aspects from that of mammalian cells, the insights gained through these studies had a significant effect on understanding fundamental aspects of CME. In mammalian cells as well as in yeast, the sequential assembly and disassembly of protein modules during the early stages of endocytosis holds true and is similar in both systems (Goode *et al.*, 2015). By fluorescently labeling multiple key components of the endocytic pathway, kymographs of single endocytic patches could be assembled to visualize coat invaginations in real time for the first time (Kaksonen *et al.*, 2003). Through these early studies, the lifetime dynamics of single endocytic events were revealed and the dynamics and contribution of multiple endocytic proteins could be investigated. In particular, these approaches highlighted the importance of actin polymerization and filament

organization to driving membrane invagination when the plasma membrane is under pressure (Aghamohammadzadeh and Ayscough, 2009). In mammalian cells, although the role of actin is not fully resolved, a critical need for actin when the plasma membrane is under tension has also been demonstrated (Boulant *et al.*, 2011).

For the investigation of CME in mammalian cells, the development of total internal reflection fluorescence (TIRF) microscopy proved to be an extremely valuable tool, which allows the basal membrane of live cells to be imaged with a very low signal-to-noise ratio while keeping a high temporal resolution. This method was pioneered by Merrifield and his colleagues, who were able to detect single endocytic events and confirm that the GTPase dynamin is recruited to CCPs, peaking at the end of their lifetime and mediating their scission (Merrifield *et al.*, 2002). Shortly thereafter, many different investigators used this experimental approach to precisely dissect the lifetime dynamics of CCPs from their nucleation at the membrane to their uncoating in the cytoplasm (Ehrlich *et al.*, 2004; Perrais and Merrifield, 2005, Cocucci *et al.*, 2012; Aguet *et al.*, 2013). This allowed further refinement of the model proposed by Goldstein and colleagues and demonstrated the recruitment of different components to the growing clathrin lattice at different stages during its lifetime (Taylor *et al.*, 2011), thus helping to elucidate their mechanisms of action. It also became apparent that different cargo molecules can regulate CME through posttranslational modifications of the endocytic machinery for their efficient uptake (Ferreira *et al.*, 2012). This added an extra layer of intricacy to the system and resulted in the current situation in which the internalization of particular cargo molecules is sufficiently complex to warrant its own review.

FUTURE DIRECTIONS

After the use of electron microscopy to determine the morphology of CCPs and live-cell fluorescence imaging to dissect their dynamic behavior, the development of superresolution light microscopy enabled scientists to visualize CME in unforeseen detail. The resolution of conventional light microscopy is limited to ~200 nm in the horizontal and ~400 nm in the vertical direction. However, with a diameter of ~150 nm, CCPs are just below this resolution limit and have been a useful benchmark for the application of many novel superresolution methods, with each technique in turn being immensely useful to investigate new details of CME (Huang *et al.*, 2008; Miller *et al.*, 2015). This development has been very valuable for gaining more detailed insight into the organization of different components of the endocytic machinery and has been used to investigate the interplay of clathrin with the actin cytoskeleton in beautiful detail (Li *et al.*, 2015). Although superresolution microscopy is a powerful tool to investigate CME, the conventional methods used by Goldstein and his colleagues are still being used. One approach combining visualization of the morphology of CCPs by electron microscopy with the detection of coat components by fluorescent markers is correlative light and electron microscopy (CLEM). This method enables researchers to correlate the morphology of CCPs with the presence of different coat components and has been used with great effect to investigate the transition of flat clathrin lattices into spherical CCVs (Avinoam *et al.*, 2015). This shows that even 40 years after the article by Goldstein and colleagues, the methods that they used are still immensely valuable. With the use of biochemical purification, x-ray crystallography, live-cell fluorescence imaging, and superresolution microscopy researchers are able investigate almost every element of CME.

Notwithstanding the great advances that have been made in recent years, many challenging questions about CCV assembly and disassembly remain unanswered. One of these challenges is to understand precisely how the membrane is bent and curvature is generated to deform a flat membrane into a CCV. The delicate design and complex geometry of these vesicles has fascinated researchers since the first electron microscopy images were published. It was soon realized that the conversion of hexagonal arrangements into pentagons is essential for the transition of a flat clathrin lattice into a spherical vesicle (Kanaseki and Kadota, 1969). However, how this rearrangement takes place is still unclear, and understanding the generation of curvature during CME has proven to be a complex challenge. Two models have been proposed that aim to explain this process. In the model of "constant curvature," the CCP grows through the continuous polymerization of coat components and steadily increases in size with constant curvature, whereas in the "constant-area" model, the CCP starts as flat lattice that is continuously deformed into a vesicle (Lampe *et al.* 2016). In vitro, the stepwise polymerization of clathrin is sufficient to drive curvature in reconstituted membranes into vesicles (Dannhauser and Ungewickell, 2012; Kirchhausen, 2012), whereas in vivo, the clathrin lattice seems to start as a flat coat that is continuously deformed into a CCV (Avinoam *et al.*, 2015). Among the main differences between these systems is that the membrane composition of live cells differs in some aspects to that of in vitro model membranes and many components of the membrane cannot be effectively modeled in these systems. It is therefore possible that the different properties of the plasma membrane and the presence of different cargo molecules could influence the way it can be deformed. Answering these challenging questions will greatly improve our understanding of CME and will require the collaborative effort of biologists, physicists, and mathematicians.

IMPORTANCE OF CME IN DISEASE

Brown and Goldstein were motivated to understand the reasons why their patients suffered from hypercholesterolemia. The use of patient fibroblasts suggested the importance of high-affinity receptors (Anderson *et al.*, 1977a). Some patients with this disorder have a mutation in the cargo recognition sequence of the LDL receptor such that the protein is unable to bind to adaptor proteins and undergo endocytosis. This inability to take up LDL leads to an excessive amount of cholesterol in the bloodstream, which can cause coronary heart disease (Anderson *et al.*, 1977b; Marks *et al.*, 2003). It is therefore no surprise that the regulation of CME became crucial in understanding and battling some major healthcare challenges.

One of many examples of the importance of CME is in the development of Alzheimer's disease (AD; Nordstedt *et al.*, 1993; Cossec *et al.*, 2010). Differential processing of the amyloid precursor protein (APP) is crucial for the development of AD and the disposition of amyloid plaques that are found in the brains of AD patients. The subcellular localization of APP is an important factor for its processing and determines whether it is cleaved into its amyloidogenic (pathogenic) or nonamyloidogenic (nonpathogenic) product. Whereas amyloidogenic processing takes place after uptake through CME, the nonamyloidogenic cleavage occurs at the plasma membrane (Haass *et al.*, 2012). Inhibition of CME shifts the processing of APP toward the nonamyloidogenic pathway, and endocytic factors have been identified as risk factors for development of AD (Harold *et al.*, 2009; Kanatsu *et al.*, 2014). In the future, it will be interesting to see whether targeting endocytic uptake of APP could be a promising way to interfere with the development of AD (Schreiber *et al.*, 2012). In addition, CME is involved in many other diseases, such as cancer (Mellman and Yarden, 2013), viral uptake, and bacterial infections (Cossart and Helenius, 2014). This makes it

clear that the model of receptor-mediated endocytosis proposed by Goldstein and his colleagues is still at the core of developments that have the potential to affect the lives of many people.

CONCLUDING REMARKS

Anderson, Brown, and Goldstein observed the uptake of LDL though coated regions on the plasma membrane into the cytoplasm. From these simple observations, they were able to postulate a model of receptor-mediated endocytosis that has provided the conceptual framework for this pathway for researchers ever since. Understanding the pathway is of interest not only to those involved in elucidating fundamental endocytic processes but also to many other researchers. Owing to its central role in cell biology, CME is intimately connected to key advances in fields such as neuroscience, cell signaling, and immunology, as well as for mechanisms of development and adult homeostasis. Gaining a better understanding of it will benefit all of these fields. A challenge for the future is to understand how this key cellular pathway is regulated in cell- and tissue-specific contexts. Tremendous progress has already been made, and, with the development of new methods to investigate CME, the field is sure to progress even further. However, the findings from Goldstein and his colleagues will always be the foundations upon which this progress is being made. Therefore, when we feel overwhelmed by the ever-increasing complexity of the field, it is good to remind ourselves that its foundation is the clever interpretation of simple observations made >40 years ago.

ACKNOWLEDGMENTS

We apologize to colleagues whose work we were unable to cite due to the concise nature of this short review. H.M. is supported by the Biopol EU ITN network.

REFERENCES

Aghamohammadzadeh S, Ayscough KR (2009). Differential requirements for actin during yeast and mammalian endocytosis. Nat Cell Biol 11, 1039–1042.

Aguet F, Antonescu CN, Mettlen M, Schmid SL, Danuser G (2013). Advances in analysis of low signal-to-noise images link dynamin and ap2 to the functions of an endocytic checkpoint. Dev Cell 26, 279–291.

Ahle S, Ungewickell E (1986). Purification and properties of a new clathrin assembly protein. EMBO J 5, 3143–3149.

Anderson RGW, Brown MS, Goldstein JL (1977a). Role of the coated endocytic vesicle in the uptake of receptor-bound low density lipoprotein in human fibroblasts. Cell 10, 351–364.

Anderson RGW, Goldstein JL, Brown MS (1977b). Mutation that impairs ability of lipoprotein receptors to localize in coated pits on cell-surface of human fibroblasts. Nature 270, 695–699.

Antonny B, Burd C, De Camilli P, Chen E, Daumke O, Faelber K, Ford M, Frolov VA, Frost A, Hinshaw JE, *et al.* (2016). Membrane fission by dynamin: What we know and what we need to know. EMBO J 35, 2270–2284.

Avinoam O, Schorb M, Beese CJ, Briggs JAG, Kaksonen M (2015). Endocytic sites mature by continuous bending and remodeling of the clathrin coat. Science 348, 1369–1372.

Boulant S, Kural C, Zeeh JC, Ubelmann F, Kirchhausen T (2011). Actin dynamics counteract membrane tension during clathrin-mediated endocytosis. Nat Cell Biol 13, U1124–U1158.

Chen MS, Obar RA, Schroeder CC, Austin TW, Poodry CA, Wadsworth SC, Vallee RB (1991). Multiple forms of dynamin are encoded by shibire, a drosophila gene involved in endocytosis. Nature 351, 583–586.

Cocucci E, Aguet F, Boulant S, Kirchhausen T (2012). The first five seconds in the life of a clathrin-coated pit. Cell 150, 495–507.

Cossart P, Helenius A (2014). Endocytosis of viruses and bacteria. Cold Spring Harb Perspect Biol 6, a016972.

Cossec JC, Simon A, Marquer C, Moldrich RX, Leterrier C, Rossier J, Duyckaerts C, Lenkei Z, Potier MC (2010). Clathrin-dependent APP endocytosis and A beta secretion are highly sensitive to the level of plasma membrane cholesterol. Biochim Biophys Acta 1801, 846–852.

Dannhauser PN, Ungewickell EJ (2012). Reconstitution of clathrin-coated bud and vesicle formation with minimal components. Nat Cell Biol 14, 634–639.

Ehrlich M, Boll W, van Oijen A, Hariharan R, Chandran K, Nibert ML, Kirchhausen T (2004). Endocytosis by random initiation and stabilization of clathrin-coated pits. Cell 118, 591–605.

Ferreira F, Foley M, Cooke A, Cunningham M, Smith G, Woolley R, Henderson G, Kelly E, Mundell S, Smythe E (2012). Endocytosis of G protein-coupled receptors is regulated by clathrin light chain phosphorylation. Curr Biol 22, 1361–1370.

Goldstein JL, Anderson RGW, Brown MS (1979). Coated pits, coated vesicles, and receptor-mediated endocytosis. Nature 279, 679–685.

Goode BL, Eskin JA, Wendland B (2015). Actin and endocytosis in budding yeast. Genetics 199, 315–358.

Haass C, Kaether C, Thinakaran G, Sisodia S (2012). Trafficking and proteolytic processing of APP. Cold Spring Harb Perspect Med 2, a006270.

Harold D, Abraham R, Hollingworth P, Sims R, Gerrish A, Hamshere ML, Pahwa JS, Moskvina V, Dowzell K, Williams A, *et al.* (2009). Genome-wide association study identifies variants at CLU and PICALM associated with Alzheimer's disease. Nat Genet 41, 1088–1093.

Hinshaw JE, Schmid SL (1995). Dynamin self-assembles into rings suggesting a mechanism for coated vesicle budding. Nature 374, 190–192.

Huang B, Wang WQ, Bates M, Zhuang XW (2008). Three-dimensional super-resolution imaging by stochastic optical reconstruction microscopy. Science 319, 810–813.

Kaksonen M, Sun Y, Drubin DG (2003). A pathway for association of receptors, adaptors, and actin during endocytic internalization. Cell 115, 475–487.

Kanaseki T, Kadota K (1969). Vesicle in a basket—a morphological study of coated vesicle isolated from nerve endings of guinea pig brain, with special reference to mechanism of membrane movements. J Cell Biol 42, 202–220.

Kanatsu K, Morohashi Y, Suzuki M, Kuroda H, Watanabe T, Tomita T, Iwatsubo T (2014). Decreased CALM expression reduces A beta 42 to total A beta ratio through clathrin-mediated endocytosis of gamma-secretase. Nat Commun 5, 3386.

Kelly BT, Graham SC, Liska N, Dannhauser PN, Honing S, Ungewickell EJ, Owen DJ (2014). AP2 controls clathrin polymerization with a membrane-activated switch. Science 345, 459–463.

Kirchhausen T (2012). Bending membranes. Nat Cell Biol 14, 906–908.

Lampe M, Vassilopoulos S, Merrifield C (2016). Clathrin coated pits, plaques and adhesion. J Struct Biol 196, 48–56.

Li D, Shao L, Chen BC, Zhang X, Zhang MS, Moses B, Milkie DE, Beach JR, Hammer JA, Pasham M, *et al.* (2015). Extended-resolution structured illumination imaging of endocytic and cytoskeletal dynamics. Science 349, aab3500.

Marks D, Thorogood M, Neil HAW, Humphries SE (2003). A review on the diagnosis, natural history, and treatment of familial hypercholesterolaemia. Atherosclerosis 168, 1–14.

Mayor S, Parton RG, Donaldson JG (2014). Clathrin-independent pathways of endocytosis. Cold Spring Harb Perspect Biol 6, a016758.

Mellman I, Yarden Y (2013). Endocytosis and cancer. Cold Spring Harb Perspect Biol 5, a016949.

Merrifield CJ, Feldman ME, Wan L, Almers W (2002). Imaging actin and dynamin recruitment during invagination of single clathrin-coated pits. Nat Cell Biol 4, 691–698.

Merrifield CJ, Kaksonen M (2014). Endocytic accessory factors and regulation of clathrin-mediated endocytosis. Cold Spring Harb Perspect Biol 6, a016733.

Miller SE, Mathiasen S, Bright NA, Pierre F, Kelly BT, Kladt N, Schauss A, Merrifield CJ, Stamou D, Honing S, Owen DJ (2015). CALM regulates clathrin-coated vesicle size and maturation by directly sensing and driving membrane curvature. Dev Cell 33, 163–175.

Nordstedt C, Caporaso GL, Thyberg J, Gandy SE, Greengard P (1993). Identification of the alzheimer beta/A4 amyloid precursor protein in clathrin-coated vesicles purified from Pc12 cells. J Biol Chem 268, 608–612.

Owen DJ, Evans PR (1998). A structural explanation for the recognition of tyrosine-based endocytotic signals. Science 282, 1327–1332.

Pearse BMF (1975). Coated vesicles from pig brain-purification and biochemical characterization. J Mol Biol 97, 93–98.

Pearse BMF, Robinson MS (1984). Purification and properties of 100-Kd proteins from coated vesicles and their reconstitution with clathrin. EMBO J 3, 1951–1957.
Perrais D, Merrifield CJ (2005). Dynamics of endocytic vesicle creation. Dev Cell 9, 581–592.
Poodry CA, Hall L, Suzuki DT (1973). Temperature-sensitive mutations in drosophila-melanogaster 14. Developmental properties of shibire—pleiotropic mutation affecting larval and adult locomotion and development. Dev Biol 32, 373–386.
Robinson MS (2015). Forty years of clathrin-coated vesicles. Traffic 16, 1210–1238.
Roth TF, Porter RF (1964). Yolk protein uptake in the oocyte of the mosquito *Aedes aegypti*. L. J Cell Biol 20, 313–332.
Schreiber A, Fischer S, Lang T (2012). The amyloid precursor protein forms plasmalemmal clusters via its pathogenic amyloid-beta domain. Biophys J 102, 1411–1417.
Takei K, Mcpherson PS, Schmid SL, Decamilli P (1995). Tubular membrane invaginations coated by dynamin rings are induced by Gtp-gamma-S in nerve-terminals. Nature 374, 186–190.
Taylor MJ, Perrais D, Merrifield CJ (2011). A high precision survey of the molecular dynamics of mammalian clathrin-mediated endocytosis. PLoS Biol 9, e1000604.
Traub LM, Bonifacino JS (2013). Cargo recognition in clathrin-mediated endocytosis. Cold Spring Harb Perspect Biol 5, a016790.
Vanderbliek AM, Meyerowitz EM (1991). Dynamin-Like protein encoded by the drosophila-shibire gene associated with vesicular traffic. Nature 351, 411–414.
Vigers GPA, Crowther RA, Pearse BMF (1986). Location of the 100 Kd-50 Kd accessory proteins in clathrin coats. EMBO J 5, 2079–2085.
Zaremba S, Keen JH (1983). Assembly polypeptides from coated vesicles mediate reassembly of unique clathrin coats. J Cell Biol 97, 1339–1347.

1.2 CLATHRIN

The short review article was meant to give a brief overview about the last four decades of research regarding clathrin mediated endocytosis and was targeted at a general audience. In order to give a more precise introduction into CME, it is important to first delineate the structure and function of the core protein in CME: Clathrin. As mentioned in the review article, it is the main constituent of the vesicles purified by Pearse in 1975 (Pearse, 1975) and is the key component during CME; forming coated vesicles that appeared as baskets composed of a mixture of hexagons and pentagons, similar to the shape of a football. Using electron microscopy combined with rotary shadowing, it was discovered in 1981 that clathrin forms a three legged structure, forming the basic building blocks for these complex baskets (Ungewickell and Branton, 1981). It was proposed at that time that the triskelion is made out of three copies of the 180kDa clathrin heavy chain, associated with the three copies of the much smaller (25kDa) clathrin light chains. Therefore, in order to give a complete picture of CME, the structure and function of the clathrin heavy chain will be discussed first, followed by the roles of the clathrin light chains and the assembly of the complete triskelia.

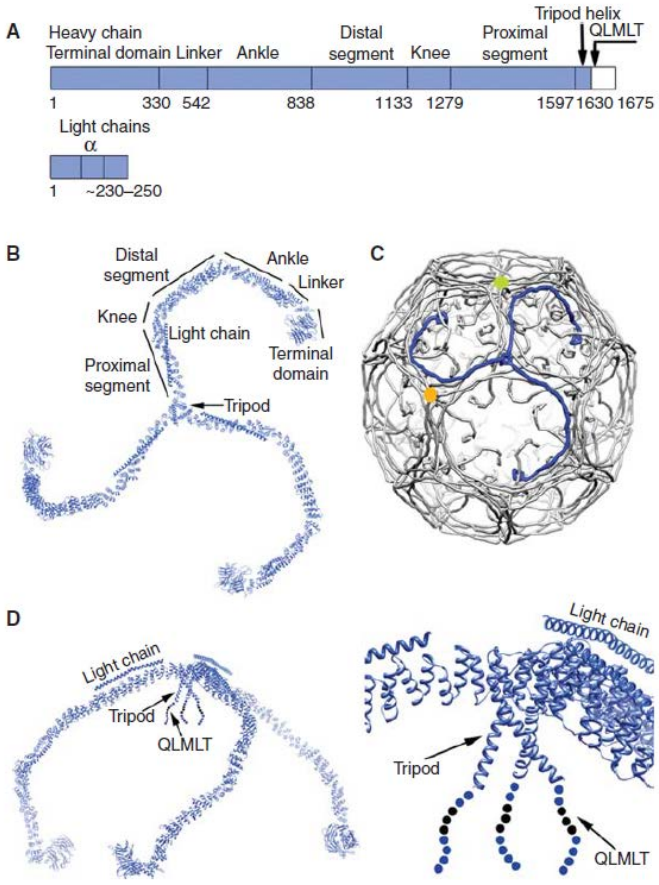

Figure 1.1 Structure and domains of the Clathrin triskelia A) Schematic overview of the CHC and CLC domains. **B)** Assembly of clathrin triskelia **C)** Position of triskelia within a CCV **D)** Side view of the triskelia pucker with attached light chains as well as the trimerization domain with the QLMLT motif that mediates auxilin binding. Figure from Fotin et al 2004.

1.2.1 Clathrin heavy chain

The clathrin heavy chains (CHCs) make up the largest part of the triskelia and are made up of 1675 amino acid residues which can be divided into seven functional domains (Kirchhausen, Owen, & Harrison, 2014. Fig.1 a) which shall be discussed in detail. From N- to C-terminus they are the: Terminal domain (aa 1-330), Linker domain (aa 330-542), Ankle domain (542-838), Distal segment (838-1133), Knee (1133-1279), Proximal segment (aa 1279-1597) and the Tripod domain containing the disorder carboxy-terminal segment (aa 1597-1675).

The terminal domain (TD) is made up out of the seven-bladed β-propeller, containing seven WD40 repeats (Fotin, Cheng, Sliz, *et al.*, 2004). These WD40 repeats are common folding patterns in proteins such as G-Proteins, transcription factors and ubiquitin ligase and are characterised by the position of Tryptophan (W) and aspartic acid (D) in the β sheets (Xu and Min, 2011). The β-propeller of the clathrin heavy chain is of particular significance since it mediates contact with a range of adaptor proteins that link cargo proteins to the clathrin lattice. Since clathrin is not able to bind membranes directly, binding to these adaptor proteins is required to initiate the formation of clathrin coated pits at the plasma membrane (Unanue, Ungewickell and Branton, 1981). These interactions take place at the terminal domain and currently four distinct binding sites are known which bind to a variety of adaptor proteins (Smith *et al.*, 2017). It is noteworthy, that these interactions are comparatively weak and show a high level of promiscuity, allowing for the interactions with a range of different adaptor proteins during the lifetime of a clathrin coated pit. This flexibility of the TD to bind to different adaptor proteins is key for the adaptability of CME during the uptake of a range of different cargo proteins. This is supported by the observation of redundancies of the four different binding sites. Even if three of these sites are mutated to block adaptor binding, binding of the remaining site(s) is still sufficient to progress through CME (Willox and Royle, 2012).

The terminal domain is followed by the 42 α-helical linker domain composed of opposing α-helixes in a “zigzag” of ~30 residues each (ter Haar *et al.*, 1998; Fotin, Cheng, Sliz, *et al.*, 2004). This linker domain is crucial for the formation of the clathrin lattices because it allows for different orientations of the terminal domain with the following ankle segment which is immobilized and reinforced through contacts with neighbouring triskelia in the lattice. Therefore, the flexibility of the linker region allows for the adaptation of different shapes in the clathrin lattice during formation of pentagons and hexagons.

The linker region is followed by the “ankle” segment which connects to the distal segment of the heavy chain. During auxilin and Hsc70 mediated uncoating of the clathrin lattice the terminal domains twist outward which is attributed to a change in the position of the ankle (Fotin, Cheng, Grigorieff, *et al.*,

2004). Therefore, the ankle region is important to mediate the long range changes in the clathrin lattice, which are initiated in the proximal domains, down to the terminal domain. This distal segment of the heavy chain is an important structural feature, as it connects with the proximal legs of neighbouring triskelia, giving rise to a spherical clathrin lattice (Fotin, Cheng, Sliz, *et al.*, 2004). The distal segment is followed by the "knee" region, which is crucial during lattice assembly and disassembly. The knee region controls the orientation of the distal segment and can adopt a bent or straight configuration. It is believed that under conditions where assembly is disfavoured, the knee adopts a straight configuration which is incompatible with lattice assembly. Additionally, it could be shown that auxilin mediated uncoating of CCVs also leads to a straightening of the knee angle which would lead to the exclusion of the triskelia from the clathrin lattice (Musacchio *et al.*, 1999; Wilbur *et al.*, 2010).

The proximal segment of the heavy chains is also in close contact with the distal segments of neighbouring triskelia in CCVs. In addition to its structural role in connecting neighbouring triskelia with each other, it is also the main binding site of the clathrin light chains (Kirchhausen *et al.*, 2008). This interaction with the light chains occurs along the whole proximal segment with the formation of three critical salt bridges through the basic residues (R1161KKAR1165 or KR loop) of the heavy chains with the three acidic residues E20ED22 at the n-terminus of the light chains (Ybe *et al.*, 1998). The interaction of the light chains with the heavy chains through these three salt bridges were shown to regulate the aforementioned change in the knee angle to regulate lattice (dis)assembly (Wilbur *et al.*, 2010).

The final segment of the CHC is the trimerization (or Tripod) domain which connects the three CHCs and their associated CLCs into the complete clathrin triskelion. It is mediated through the tripod helix domain and followed by a short unstructured region. This site joins three individual CHCs together by forming a distinct pucker with the short unstructured region pointing inwards (towards the membrane). This pucker is a crucial feature of the triskelia and determines the curvature of the assembled lattice (Kirchhausen, Harrison and Heuser, 1986). Some data suggest that the CLCs reach all the way from the proximal segment into the trimerization domain, although this interaction could not be verified thus far it could be an important factor in understanding how the CLCs modify lattice assembly (Ybe *et al.*, 2003). The internal site of the trimerization domain is an important hub for adjacent triskelia in a clathrin lattice and is associated with three terminal domains of the "nearest neighbour" triskelias. It is also the binding site for Auxilin and Hsc70, mediating lattice disassembly and uncoating (Rapoport *et al.*, 2008).

It is important to note, that the above section only describes one of the two isoforms of the CHCs. In many vertebrates, two isoforms of the CHC exists, CHC17 and CHC22. While CHC17 is the classical isoform discussed above and mediates CME, and the functions of CHC22 are very distinct of those of CHC17. Its expression is tissue specific and, while it also forms triskelia, it does not associate with CLCs and does not participate in receptor mediated uptake from the plasma membrane. Rather it is specialised for the intracellular transport of GLUT4 in muscle cells and adipocytes and is implicated in type 2 diabetes (Vassilopoulos *et al.*, 2009; Dannhauser *et al.*, 2017).

1.2.2 Clathrin light chains

The CLCs are a crucial feature of the clathrin triskelia, however their role during CME has remained elusive thus far, with some receptors requiring the contributions of the CLCs for their uptake while others do not. Since this thesis is focused on their role in cargo specific uptake of receptors from the plasma membrane, they will be discussed in detail below.

The clathrin light chains are 25kD small accessory proteins that bind to each of the CHCs in the triskelia, spanning from the knee segment into the trimerization domain (Fig. 1 A and D). In most mammalian cells, two different isoforms (CLCa and CLCb) are expressed with varying expression patterns in different tissues, as well as neuronal splice variants of both CLCa and CLCb (Jackson *et al.*, 1987; Kirchhausen *et al.*, 1987). The sequence of both isoforms are highly conserved, ~60% identical in protein sequence and with conservation of key residues, mediating interaction with the huntingtin-interacting proteins (mammalian Hip1 and Hip1R), in both CLCa and CLCb (Brodsky, 1988; Chen and Brodsky, 2005). Even though CLCb has a slightly higher affinity for binding to CHCs *in vitro*, most triskelia *in vivo* have a random distribution of both CLCa and CLCb bound, depending on the local expression level of the isoforms (Brodsky *et al.*, 1991). Whether CLCa or CLCb differentially modify the process of CME is an ongoing topic of research and it was shown that high expression of CLCb correlates with cells and tissues that maintain a regulated pathway of secretion, suggesting a role of CLCb in post Golgi trafficking (Acton and Brodsky, 1990). However, in mice deficient in CLCa, the expression of CLCb is upregulated in some tissues, suggesting a compensatory role and functional redundancies between these two isoforms (Wu *et al.*, 2016). Intriguingly it was recently shown that CLCb is specifically upregulated in non-small-cell lung cancer cell and that genome edited cells that only express CLCb (at a high level) show a migratory phenotype and altered CME dynamics (Chen *et al.*, 2017). This regulation of CME by the CLCb was termed “adaptive Clathrin-mediated endocytosis” through altered interactions of CLCb with Dynamin 1, leading to changes in Epidermal Growth Factor

Receptor (EGFR) trafficking with subsequent implications for cancer prognosis. Additionally, it was shown that CLCb is preferentially phosphorylated at multiple residues at its N-terminus (Hill *et al.*, 1988) and that phosphorylation of CLCb is a crucial regulatory role, controlling the uptake of multiple GPCRs from the cell surface and will be discussed in detail below (Ferreira *et al.*, 2012). Therefore, it seems the two different isoforms of the CLCs might finely regulate specific aspects of CME, however the mechanism(s) by which this occurs is still somewhat unclear.

The role of the CLCs in CME has been a challenging topic of research over the last four decades. The depletion of both CLC isoforms does not seem to have any significant effect on the uptake of classical receptor cargoes and does not seem to effect the structure of assembled clathrin cages *in vitro* either (Hinrichsen *et al.*, 2003; Fotin, Cheng, Sliz, *et al.*, 2004) . Therefore, it was long thought that they serve as accessory proteins that mainly modify some aspects of CME by interacting with different interaction partners on the cytosolic face of the clathrin lattice. Indeed, their position at the vertices of the triskelia would place them at the ideal position to interact with a range of different effector proteins (such as Hip1R, GAK and Auxilin) that modify lattice dynamics. In agreement with this, early studies have implied the CLCs to be crucial for the uncoating of the clathrin coat from clathrin cages after internalization (Schmid *et al.*, 1984; DeLuca-Flaherty *et al.*, 1990). However, these findings where challenged in 1995 when Ungewickell and Eisenberg demonstrate that the CLCs are not required for Auxilin mediated uncoating of clathrin cages (Ungewickell *et al.*, 1995). These contradictory results could be rectified recently by demonstrating that the CLCs modify the dynamics of vesicle uncoating, depending on the concentration of Auxillin (Young *et al.*, 2013). Therefore, it is possible that the contradictory results from earlier studies could be due to differences in the experimental setups, including the concentrations of Auxillin used in the different assays.

This role of the CLCs in the process of CCV uncoating is in line with the hypothesis that the light chains modify the stability and assembly of the clathrin lattice. This idea goes back to early observations that demonstrated that the CLCs regulate lattice assembly in a pH dependent manner (Ungewickell and Ungewickell, 1991; Ybe *et al.*, 1998). *In vitro*, lattice formation occurs spontaneously at low pH (6.5) but is inhibited by the presence of light chains. This pH sensitive self-assembly is regulated by the formation of the three critical salt bridges of the CLCs with the heavy chains. Intriguingly, these three salt bridges are also implicated in the uncoating process after Hsc70 binding, by inducing a conformational change of the knee segment in the CHC (Wilbur *et al.*, 2010). It is therefore feasible that the same mechanism that controls the pH sensitive assembly of the clathrin lattice is also important in the disassembly of the lattice during vesicle uncoating. Thus, it is likely that the CLCs act as important regulators of lattice dynamics.

In a seminal paper from 2012 Dannhauser and Ungewickell demonstrated that the formation of CCVs from model membranes in cell free systems does not require the presence of CLCs and only relies on adaptor proteins that recruit the CHCs to membranes, followed by dynamin for the scission of the neck from the deeply invaginated bud (Dannhauser and Ungewickell, 2012). Therefore, in these minimal systems, the CHCs are sufficient to deform the membrane from a flat plane into an invaginated bud, without the assistance of any other curvature inducing proteins (such as the BAR proteins CALM and Epsin2). However, in a follow up study in 2015 it was shown that when the model membranes were cooled down to 15˚C, the CHCs alone were not sufficient to deform the membranes but formed large, flat lattices and which could only be deformed into spherical buds in the presence of the CLCs (Dannhauser *et al.*, 2015). This effect was shown to be due decreased tensile strength of the triskelia in absence of the CLCs which is required to deform model membranes with higher rigidity due to the decreased temperature. The effect of the CLCs on the mechanical properties of the clathrin lattice is also apparent in their requirement for the uptake of large particles, such as bacteria, as well as under conditions of increased membrane tension (Bonazzi *et al.*, 2011; Boulant *et al.*, 2011). Therefore, the CLCs are crucial for the stability of the clathrin lattice and its correct (dis)assembly, as well as giving it enough tensile strength for the deformation of membranes that are difficult to deform due to high rigidity or tension.

The requirement of the CLCs for the deformation of the plasma membrane for uptake of these "difficult" cargoes is further supported by the observation that they serve as adaptors to link the actin cytoskeleton to the clathrin lattice (Chen and Brodsky, 2005; Wilbur *et al.*, 2008). This is mediated through binding of Hip1R to the CLCs, which in turn acts as local organiser of the actin cytoskeleton at the site of CME. This is supported by the observation that, in cells depleted of the CLCs, the actin cytoskeleton appears to be disorganized into local aggregates and is not connected to the clathrin lattice (Poupon *et al.*, 2008). The role of actin polymerization on CME is a complex topic of ongoing research. However, in general it is believed that the additional force of actin polymerization is required for CME to occur under conditions of increased membrane tension, and for large cargoes such as bacteria (Bonazzi *et al.*, 2011; Boulant *et al.*, 2011). In yeast actin is a crucial factor during CME to overcome the high turgor pressure (Aghamohammadzadeh and Ayscough, 2009), but in mammalian cells actin polymerization is only required under some circumstances and results differ between cell types (Fujimoto *et al.*, 2000). The factors that determine whether actin is required for CME to progress in mammalian cells are still somewhat unclear but most evidence points towards actin recruitment being crucial for the generation of additional force to push invaginated CCPs away from the plasma membrane and into the cytoplasm (Collins *et al.*, 2011; Picco *et al.*, 2015; Almeida-Souza *et al.*, 2018). Therefore, the initial deformation of the plasma membrane from flat into U- and Ω-shape seems to be

independent of actin polymerization. The observation that the CLCs are required for the initial deformation of rigid membrane *in vitro* into spherical buds, as well as for the recruitment of actin at late stages of vesicle formation, suggests multiple roles of the CLCs during the deformation of the plasma membrane under increased tension and/or rigidity.

Given these important regulatory roles of the CLCs, it is somewhat surprising that their depletion did not seem to affect the uptake of classical receptor cargoes such as the Transferrin or EGF receptor. However, work in our lab could show that the phosphorylation of CLCb at point specific residues is required for the uptake of certain GPCRs from the plasma membrane (Ferreira *et al.*, 2012). In detail, it was shown that overexpression of a CLCb version where all 19 serines where exchanged for alanine (CLCb-SallA) and could therefore not be phosphorylated, resulted in a complete block in the ligand stimulated uptake of the two purinergic receptors $P2Y_1$ and $P2Y_{12}$, as well as the mu-opioid receptor (*MOPr*), while only mildly affecting transferrin uptake. Furthermore, overexpression of a CLCb construct in which only a single serine at position 204 was exchanged for alanine (CLCb-S204A) led to a specific block for the uptake of the $P2Y_{12}$ receptor but not the $P2Y_1$ receptor. The phosphorylation of serine 204 was shown to be mediated by the G-protein coupled receptor kinase 2 (GRK2) which is recruited by $P2Y_{12}$ but not $P2Y_1$. Therefore, the site specific phosphorylation of serine 204, mediated by GRK2, controls uptake of the $P2Y_{12}$ receptor, while the phosphorylation site required for uptake of $P2Y_1$ is some other serine(s) that is phosphorylated by a different kinase and has not been characterized thus far. The mechanism(s) by which phosphorylation of CLCb can control cargo selectivity uptake has remained elusive. However, the data presented by Ferreira et al in 2012 suggested an altered interaction of the clathrin rearranging and uncoating protein GAK with phosphorylation deficient CLCb. Suggesting that GAK might be implied in the uptake of these CLC dependent GPCRs.

Importantly, the requirement of the CLCs for the uptake of a subset of GPCRs was subsequently verified *in vivo* by the generation of KO mice, deficient in CLCa (Wu et al., 2016). As stated previously, the different isoforms of the CLCs are capable of compensating for the loss of the other; however, B-Lymphocytes do not produce any CLCb and therefore cannot compensate for the loss of CLCa. These knockout mice displayed a deficiency in the formation and organization of germinal centres in the gut as well as an increased isotype switching of B lymphocytes towards IgG-A production. These alterations were shown to be due to a deficiency in the uptake of a subset of GPCRs, leading to increased signalling of transforming growth factor β receptor 2 (TGFβR2) at the cell surface due to defective endocytosis. Additionally, the uptake of the of C-X-C chemokine receptor 4 (CXCR4), but not CXCR5, was reduced and in cell lines depleted of both CLCa and CLCb. As well as the uptake of the δ-opioid receptor, but not the β2-adrenergic receptor. Taken together, these results clearly

demonstrated a role of the CLCs in cargo selective uptake, something that has previously only been attributed to adaptor proteins.

One of the main aims of this thesis was to define the mechanism by which the CLCs can control the uptake of a subset of receptors. As discussed above, the CLCs do not directly interact with cargo proteins, but are a crucial feature of the clathrin lattice and regulate the kinetics of both, its assembly as well as disassembly. Therefore, the next part of the introduction will briefly introduce the different forms of clathrin lattices that can be observed at the cell surface and how they might serve as distinct entry points for a subset of surface receptors.

1.3 THE CLATHRIN LATTICE

Ever since the pioneering work from John Heuser in the 1980s depicted the presence of different forms of clathrin lattices at the plasma membrane of unroofed cells, it was realised that they are remarkably heterogeneous and can adopt various different shapes and conformations (Heuser, 1980). Next to the already established clathrin coated vesicles, generated from brain homogenate (Crowther, Pinch and Pearse, 1976), a variety of different clathrin lattices were observed at the plasma membrane. These ranged from shallow, circular indentations to deeply invaginated CPPs, but also a large amount of flat clathrin lattices that were predominantly composed of hexagonal arrays. Strikingly, a lot of these large flat clathrin lattices displayed small circular CCPs, budding at their edges. These observations first suggested that curvature could be generated from initially flat lattices, however the mechanism(s) of curvature generation during CME will be discussed in detail in later sections of the introduction. Importantly, these early studies set the foundations for the studies of flat clathrin lattices which have gained a lot of attention in recent years.

Before focusing on the emerging roles of flat clathrin lattices, the different structures of the spherical clathrin coated vesicles shall briefly be discussed. As mentioned in the short review article at the beginning of the introduction, CCVs were first observed as coated vesicles just below the plasma membrane and were generated from pig brain homogenate on large scale. Early studies using electron microscopy demonstrated the formation of three different vesicles types made out of 12 pentagons with a variable number of hexagons, purified from these brain homogenates (Crowther, Pinch and Pearse, 1976). Later work was able to characterize these three types of CCVs in great detail using cryo EM and termed them “Mini-coat” for CCVs containing 28 triskelia, “Hexagonal (or D6) barrel” with 36 triskelia and the “Soccer ball” with 60 triskelia (Fotin, Cheng, Sliz, *et al.*, 2004) (Fig.2a). These differences in cage geometry highlights the ability of the clathrin lattice to adapt to different shapes.

Indeed the size of CCVs *in vivo,* as well as *in vitro,* is greatly modified by the presence of adaptor and cargo proteins (Ehrlich *et al.*, 2004; Miller *et al.*, 2015). When polymerization of clathrin into vesicles is initiated without the presence of adaptor proteins mainly mini-coats are formed. However, in the presence of the adaptor protein AP2, the larger hexagonal barrel is favoured (Fotin, Cheng, Sliz, *et al.*, 2004). In fact, the presence of the adaptor protein CALM (or AP180 in neuronal cells) also greatly influences the geometry of CCVs formed during CME (Miller *et al.*, 2015). In cells depleted of this adaptor, CCPs and CCVs appear to be almost twice as large. Highlighting the role of adaptor proteins in the generation of CCVs of different geometries. For these different geometries to occur, the clathrin triskelia has to be somewhat flexible regarding its arrangement in the vesicle. The curvature of differently sized vesicles is highly variable, with smaller vesicles requiring a higher curvature of the lattice than larger ones. The differences in curvature can be attributed to a change in the pucker angle as well as the "straightening" of the knee segment of each individual triskelion. How the growth of differently sized CCVs is regulated *in vivo* is still somewhat unclear but the current understanding is that the size and geometry of the cargo as well as the presence of different adaptor proteins during CCP formation are among the deciding factors for the generation of CCVs of different geometries. This is also the case for the uptake of large virus particles, which leads to the formation of unusually large CCVs encompassing the whole viral particle (Cossart and Helenius, 2014). Therefore, the clathrin lattice is a highly adaptable polymer that is able to change its geometry depending on the cellular function that is required.

It is important to note, that all of these structures described above are the result of clathrin polymerisation *in vitro* and that formation of these small clathrin cages is independent of the presence of the CLCs (Fotin, Cheng, Sliz, *et al.*, 2004). However, it is also important to state that these vesicles are unlikely to represent the actual structures of CCVs formed *in vivo*. This becomes apparent in the fact that these cages often do not contain any lipid vesicles inside of them and are often too small to enclose vesicles as well as cargo proteins. The development of new tomography cryo EM has enabled researchers to visualise actual CCVs isolated from cells, containing a lipid vesicles and cargo. Interestingly, these cargo containing CCVs had a much more irregular shape and geometry, including heptagons, and multiple asymmetries in their lattices (Cheng *et al.*, 2007) (Fig 2b). How the clathrin lattice is able to adapt to such different geometries will be an interesting topic of research as the development of cryo EM microscopy techniques improves.

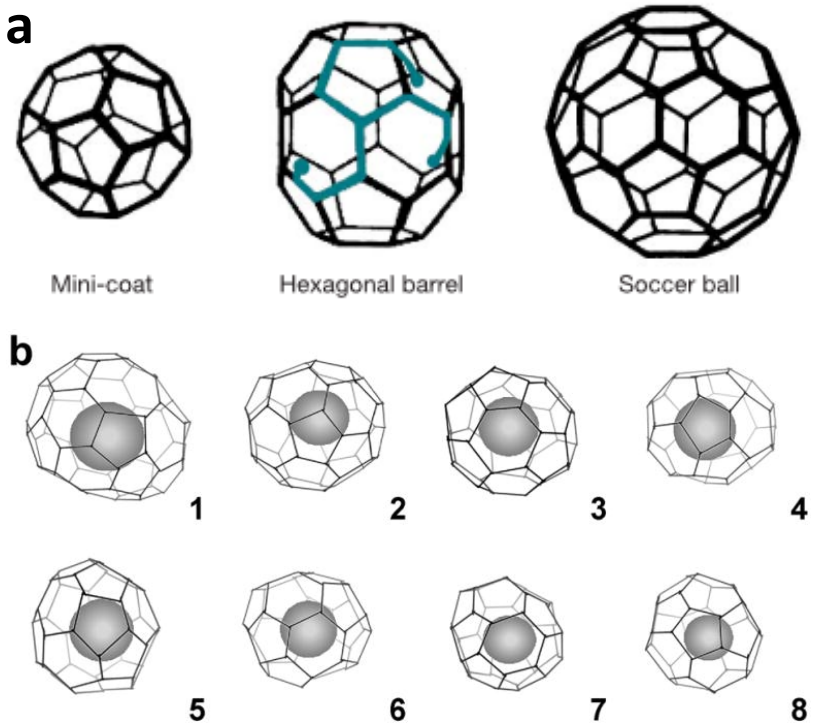

Figure 1.2 Geometries of CCVs: a) The regular structures of *in vitro* generated CCVs (Fotin et al.) varies significantly from those isolated from cells **(b)**, containing whole vesicles (Cheng et al. 2006)

The existence of flat clathrin lattices at the plasma membrane of cultured cells has been a controversial topic of debate within the community since their description by John Heuser in the 1980. Their formation was long thought to be an artefact due to growing cells on the stiff surfaces of tissue culture plastic and were therefore termed “clathrin coated plaques” to distinguish them from the canonical and “well behaved” clathrin coated pits (Kirchhausen, 2009; Saffarian, Cocucci and Kirchhausen, 2009) (Fig 3 a and b). This distinction, however, was largely arbitrary and mainly due to the fact that these large flat lattices did not fit well with the canonical model of CCP maturation which argued that they would assemble directly into spherical vesicles, starting as shallow invaginations. However, a vast amount of evidence throughout the last decades was able to demonstrate that these flat lattices are important features of the plasma membrane, incorporate cargo, are important for adhesion and migration and are unlikely to be a mere artefact of cultured cells. (Aggeler and Werb, 1982; Akisaka *et al.*, 2008; Maupin and Pollard, 1983; Miller *et al.*, 1991; Nicol and Nermut, 1987; Pumplin and Bloch, 1990; Sanan and Anderson, 1991; Signoret *et al.*, 2005; Grove *et al.*, 2014; Elkhatib *et al.*, 2017; Leyton-Puig *et al.*, 2017; Baschieri *et al.*, 2018)

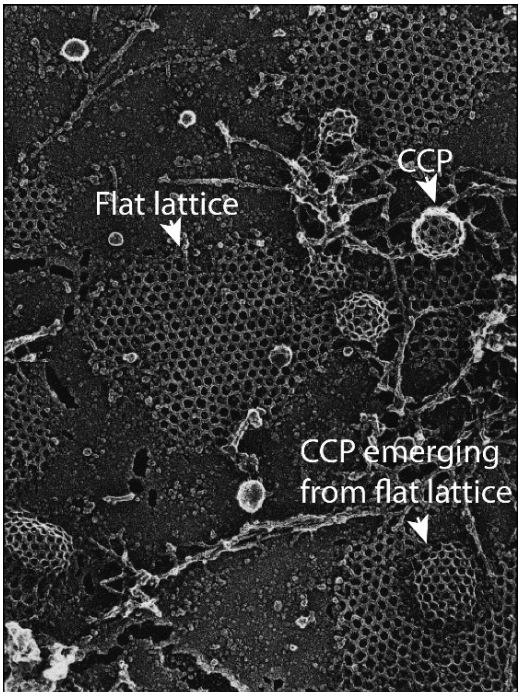

Figure 1.3: Different forms of clathrin lattices at the basal membrane of unroofed fibroblast as shown by unroofing and metal replica EM. (Jennifer Hirst and Margaret Robinson 1998)

The mechanism(s) behind the formation of flat clathrin lattices is still somewhat unclear, however a recent study argues that they form as a consequence of "frustrated" endocytosis, when ligands are immobilized on the extracellular substrate and cannot be taken up into the cell (Baschieri *et al.*, 2018). In this model, clathrin lattices serve as mechanism to detect substrate stiffness. Especially the interaction of transmembrane receptors (such as β5-Integrin) with the surrounding extracellular matrix would lead to tight connections of the receptors with the substrate and thereby inhibit membrane deformation, leading to the formation of a clathrin flat lattice. However, when the connections of these transmembrane receptors with the extracellular substrate are broken, these flat lattices start to internalize again. This notion of flat clathrin lattices as mechano-sensors and transducers is well in line with another study by Franck et al. (Franck *et al.*, 2018) demonstrating their role in the anchoring of desmin intermediate filaments in skeletal muscle as well as acting as signalling platforms, promoting translocation of YAP into the nucleus after mechanical stress. In agreement with this, actin filaments are often associated with these flat clathrin lattices and they are also present in podosomes highlighting their role in adhesion (Akisaka *et al.*, 2003, 2008). Alternatively to classical podosomes, clathrin and integrin αvβ5 dependent adhesions (termed "reticular" adhesions in this recent publication) were also shown to mediate the connection of cells with the extracellular matrix during cell division, independently of actin (Lock *et al.*, 2018). In agreement with this, integrin αVβ5 was shown to readily cluster into flat clathrin lattices in a tension dependent manner (Zuidema *et al.*, 2018).

These reported roles for flat clathrin lattices in adhesion and organization of actin at the plasma membrane seem to be in stark contrast to its canonical role in CME described initially. However, it is important to understand, that these flat lattices are also endocytically active and are crucial for the uptake of a range of cargo proteins (Grove *et al.*, 2014; Lampe, Vassilopoulos and Merrifield, 2016; Leyton-Puig *et al.*, 2017). It was first observed using electron microscopy that cargo proteins, such as Transferrin Receptor and LDL Receptor are concentrated in these structures and cluster at their edges (Sanan and Anderson, 1991; Keyel *et al.*, 2006). Through the development of live cell fluorescent imaging it was also shown that all the adaptor proteins that are recruited during canonical CME are also present at these flat clathrin lattices. Indeed, recruitment of the GTPase dynamin and GAK to these flat clathrin lattices is followed by a sudden decrease in the fluorescent intensity of the clathrin signal from these structures, indicating that parts of the larger lattices are internalized (Lampe, Vassilopoulos and Merrifield, 2016). This was further verified using an elegant technique developed by the late Christian Merriefield, which utilizes pulsing of different pH solutions to visualize the budding of freshly formed CCVs containing cargo proteins. Using this pulsed pH assay, it was shown that multiple CCVs bud consecutively from larger clathrin lattices (Lampe, Vassilopoulos and Merrifield, 2016). This is very much in line with the early observations from John Heuser, that multiple spherical CCPs and CCVs appeared at the edges of large flat clathrin lattices and clearly demonstrates that these structures actively take up cargo proteins by continuous budding of CCVs from their edges (Lampe, Vassilopoulos and Merrifield, 2016). This observation is in direct contrast to another study from the Kirchausen lab that argues for the complete uptake of these flat lattices into the cell through actin polymerization (Saffarian, Cocucci and Kirchhausen, 2009). However, several recent studies could show that most of these flat lattices stay immobile at the plasma membrane for several hours and their complete uptake seems to be a rare event.

These different roles of flat clathrin lattices places them at the perfect position for the interplay of membrane dynamics with signalling. Indeed, it was shown that flat lattices were crucial for uptake and signalling of different G-protein coupled receptors, such as the LPA receptor and CXCR5 (Grove *et al.*, 2014; Leyton-Puig *et al.*, 2017). In the case of the LPA receptor, its uptake from these flat lattices was shown to be dependent on local actin polymerization, driven by the Arp2/3 complex. Interestingly, it was also shown that recruitment of β-arrestin into CCPs leads to MAP kinase signalling from these clathrin structures even after the GPCR has disassociated from its β-arrestin (Ranjan, Gupta and Shukla, 2016). Flat clathrin lattices are therefore also signalling platforms that facilitate interactions of a range of different transmembrane receptors with intracellular interaction partners. This is also the case for the vast family of receptor tyrosine kinases that signal from clathrin coated structures at the plasma membrane (Miaczynska, 2013). How the signalling from these long lived flat clathrin

lattices is controlled and differs from that of the canonical short lived CCPs will be an exciting topic of future research.

1.4 Maturation of Clathrin coated pits

As stated in the short review article in the beginning of the introduction, clathrin is not able to bind to membranes directly and requires adaptor proteins to connect the growing clathrin lattice to the plasma membrane. The mechanism by which CCPs mature and grow after their initiation at the plasma membrane has been the topic of extensive research throughout the last four decades and has led to passionate discussions in the research community. Generally speaking, two distinct models of CCP growth and curvature generation have been postulated with compelling evidence for both models. A major aim of the work conducted in this thesis was to evaluate how cargo identity influences the mode of curvature generation of the clathrin lattice. Therefore, both models will be discussed in detail below, before focusing on how cargo proteins modulate the process of clathrin mediated endocytosis.

1.4.1 Constant curvature model

The constant curvature model of CCP initiation and curvature generation argues that formation of nascent CCPs is initiated by the chance encounter of the adaptor protein complex AP-2 with phosphatidylinositol-2-bisphosphate (PIP2) at the plasma membrane. After binding of this signalling lipid, as well as the cargo recognition sequence within cargo proteins, a conformational change occurs within the AP-2 complex that allows the terminal domains of the clathrin triskelia to bind (reviewed in: Kirchhausen, Owen and Harrison, 2014). Indeed, a lot of structural work has shown nicely that these structural changes, as well as phosphorylation of the AP-2 complex, lead to initiation of CCPs. The minimal components believed to be sufficient for the nucleation of CCPs consist of one clathrin triskelia, binding to two AP-2 complexes (Cocucci *et al.*, 2012). The contribution of additional adaptor proteins in the initiation of CCPs is somewhat unclear but it could be shown that a complex of Eps15 together with the F-BAR domain proteins FCHO1 and FCHO2 are also implicated in AP2 activation and CCP nucleation (Ma *et al.*, 2016). Their role in this process is still unresolved but it could be shown that there are functional redundancies for CCP initiation between Esp15 and FCHO1/2 (Wang *et al.*, 2016), which might explain why no severe effect on CCP initiation was observed upon FCHO1 knockdown (Cocucci *et al.*, 2012) as well as the mild effects of FCHO1 knockout in zebrafish (Umasankar *et al.*, 2012).

Once these minimal components nucleate a CCP, additional adaptor proteins and clathrin triskelia are recruited to form a clathrin lattice. In the constant curvature model of CCP maturation, the generation of curvature is intrinsic to the clathrin triskelia and occurs throughout the polymerization process with the same curvature. Therefore, the clathrin lattice directly adopts the shape of a spherical bud as the CCP grows and new triskelia are incorporated into the lattice. In this process, pentagons are directly formed as the lattice grows, circumventing the need of clathrin exchange and lattice rearrangements. This model of CCP maturation is certainly very elegant since it does not require the complex bonds and interactions of neighbouring triskelia to be broken and reformed throughout maturation. Indeed, in *in vitro* systems, model membranes can readily be deformed by the direct polymerization of clathrin into spherical buds without the need of lattice rearrangements (Dannhauser and Ungewickell, 2012). In these systems, the physical properties of the model membranes directly counteract their deformation by clathrin polymerization. This becomes apparent by the observations that increases in membrane tension or rigidity, lead to the formation of shallow invaginations that are unable to progress into deep buds (Saleem *et al.*, 2015). This is consistent with the model that the polymerization energy of the clathrin triskelia directly drives invagination of the membrane and, that in cases where the counteracting forces are higher than the inbuilt polymerization energy of the clathrin lattice, invagination is stalled. Interestingly, flat lattices were not observed under these conditions (Saleem *et al.*, 2015).

The fluorescent intensity signals from lifetime data of CCP initiation, growth and scission have been used to argue for this model (Kirchhausen, 2009). Indeed, the intensity traces of fluorescently labelled clathrin light chain, using TIRF microscopy, show and gradual increase in intensity as the CCP grows, followed by a plateau phase and terminate in their sudden disappearance from the TIRF field. This growth phase was argued to represent the polymerization of the clathrin lattice, directly into curved vesicles. Additionally the “dimming” of fluorescently labelled AP2 as well as Epsin during the growth phase was argued to represent gradual displacement of these adaptor proteins into the cell as the coat matures (Saffarian and Kirchhausen, 2008; Saffarian, Cocucci and Kirchhausen, 2009). However, fluorescence intensity traces alone are unable to provide any information about curvature generation and it was shown in great detail that a range of adaptor proteins are excluded from the growing clathrin lattice during coat invagination, explaining their dimming during CCP maturation (Sochacki *et al.*, 2017). In agreement with this, recent advances in microscopy enabled Scott *et al.* to simultaneously determine the Z-displacement as well as the fluorescent intensity traces of the growing clathrin coat. In their landmark study, they were able to demonstrate that some CCPs indeed gained curvature directly as the CCP assembles but that at the same time other CCPs first assembled as flat lattices before gaining curvature (Scott *et al.*, 2018). Therefore, the constant curvature model

of CCP assembly can only partially explain the data obtained from studies in cells. The most compelling argument in favour of the constant curvature model for membrane deformation lies in its simplicity and from the observations that clathrin is sufficient to drive curvature generation *in vitro*. However, a lot of cell biological processes are too complex to be faithfully represented by *in vitro* systems and the simplest answer is not necessarily the correct one.

1.4.2 Constant area model

As an alternative to the canonical pathway of constant curvature described above, the model of constant area for CCP maturation and curvature generation has been proposed. This model has been around since the first electron microscopy images of differently shaped clathrin lattices have been published by John Heuser in the 1980s. In this model, a CCP assembles initially as a flat, hexagonal lattice and subsequently gains curvature through incorporation of pentagons into the array (Kanaseki and Kadota, 1969). Importantly, this model is also able to explain how CCPs can bud off the edges of the large flat clathrin lattices described above. The debate about which of these two models best describes CCP maturation *in vivo* has long been going on but due to its elegance and simplicity, the model of constant curvature has been adapted as the canonical pathway. However, due to recent advances in both electron and fluorescent microscopy, the debate has been reignited, with ever more data supporting the constant area mode of curvature generation.

The seminal study that sparked new life into this old debate was performed by Avinoam *et al.* in 2015 (Avinoam *et al.*, 2015). In this study, the authors used fluorescence microscopy combined with electron tomography to show convincingly that in SK-MEL-2 cells, CCPs start as initially flat lattices that subsequently gain curvature while keeping a constant area. By using fluorescently labelled clathrin light chain as well as dynamin2, they could additionally demonstrate that clathrin exchange occurs throughout the entire maturation process of CCPs. These findings were supported by a recent publication that used a combined approach of fluorescence microscopy with the established method of metal replica EM, to demonstrate that CCPs grow initially as flat lattices to approximately 70% of their final size before generation of curvature is initiated (Bucher *et al.*, 2018). Furthermore, this generation of curvature is inhibited by an increase in membrane tension as evident by large number of flat lattices after hypo-osmotic swelling of the cells. These findings both directly support the model of constant area for CCP maturation. However, using an imaging technique that combines TIRF imaging with polarized illumination, it is possible to simultaneously detect the fluorescence intensity traces of labelled clathrin light chain and it's Z-displacement over time with nanometre precision. Using this imaging setup it was shown that in SK-MEL-2 cells, both modes of curvature generation can be observed in CCPs in the same cell, with about ~50% following the constant curvature model and ~50% the constant area model (Scott *et al.*, 2018). The authors of this study suggest that the local

energy landscape of the plasma membrane could be the determining factor for which model of membrane deformation is followed. Intriguingly, they were also able to show that CCPs following the constant area pathway of membrane bending tended towards longer lifetimes than those following the constant curvature model. Therefore, it seems that both models of CCP maturation can occur in parallel; however, the deciding factors for which mode is followed are still unclear.

1.4.3 Clathrin lattice rearrangement

For flat lattices to gain curvature, complex rearrangements of the hexagonal array are required to convert hexagons into pentagons. This rearrangement requires multiple bonds between neighbouring triskelia to be broken and reformed. Due to the complex nature of these rearrangements it was long thought to be unlikely to occur in nature. In an influential review article by T Kirchhausen it was stated that: “Repeated suggestions in the literature that flat arrays can rearrange into curved lattices ignore the molecular properties of the clathrin trimer and the specificity of contacts between triskelions within a coat. (Kirchhausen, Owen and Harrison, 2014)”. However, in light of the recent data, clearly demonstrating that flat lattices can gain curvature, this statement has to be reconsidered. In fact, it has been known for a while that CCPs are very dynamic structures with extensive exchange between clathrin triskelia at endocytic sites and the cytosol (Wu *et al.*, 2001). This exchange is a prerequisite for complex lattice rearrangements to occur and demonstrates that bonds between triskelia in a clathrin lattice are constantly broken and reformed. Otherwise an exchange of triskelia would not be possible. Computational modelling has been able to demonstrate that it is possible for curved lattices to arise from large flat structures by partial rupture of the lattice followed by lattice bending (den Otter and Briels, 2011). However, the problem behind lattice rearrangement and pentagon formation was not resolved in these simulations. A recent simulation performed by Sorokin et al. was able to demonstrate that lattice rearrangement and pentagon formation can occur within a lattice, if triskelia are allowed to associate and disassociate from the lattice (as seen in vivo). Under these conditions, the rate of 5-ring formation/dissociation and the 6-ring formation/dissociation are the determining factors whether curvature is generated or not (Sorokin *et al.*, 2018).

The mechanism by which lattice rearrangement occurs is still unclear, however the same factors that mediate uncoating of CCVs have shown to also mediate clathrin exchange. This process is energy dependent on requires the hydrolysis of ATP by Hsc70 as well as the molecular chaperon, auxilin (or GAK) (Yim *et al.*, 2005; Eisenberg and Greene, 2007). GAK is the ubiquitously expressed isoform of the neuronal Auxilin and differs from it in the expression of an N-terminal kinase domain. Both proteins have a PTEN lipid binding domain, a central domain that binds clathrin, AP2 and dynamin and J-domain

that recruits Hsc70 and mediates clathrin uncoating (Zhang *et al.*, 2005). Structural data from CCVs, bound with auxilin could show that it binds to the trimerization domain of the clathrin triskelia, just below the vertex of the clathrin basket and recruits Hsc70 which in turn mediates the ATP dependent release of the triskelia from the lattice (Rapoport *et al.*, 2008). Elegant experiments could show that they are key mediators of clathrin lattice dynamics and mediate both, the terminal removal of the clathrin coat from CCVs as well as the constant exchange of clathrin at clathrin coated structures at the plasma membrane (Ungewickell *et al.*, 1995; Yim *et al.*, 2005). Even though clathrin exchange is a prerequisite for the generation of curvature from a flat lattice, it is not a deterministic consequence of it. This becomes clear from experiments performed by Lois Greene that could show that in cholesterol depleted cells, clathrin is still freely exchange at endocytic sites (Wu *et al.*, 2003). However, under these conditions CCPs do not gain curvature but still exchange clathrin, therefore the clathrin lattice is a highly dynamic structure with high plasticity, able to adapt to (but not necessarily drive) changes in curvature through local rearrangements.

Depletion of both GAK and auxilin has been shown to abolish exchange of clathrin at the plasma membrane and also leads to the formation of clathrin microcages in the cytosol (Hirst *et al.*, 2008). Therefore, they are implied in both, the correct assembly of the clathrin lattice as well as its disassembly and rearrangement. How these different functions are controlled by the same proteins is still an ongoing topic of research, however the lipid binding domain of auxilin has a high affinity for both monophosphoinositol derivatives and phosphatidylinositol (4,5)-bisphosphate (PIP2) (He *et al.*, 2017). During the maturation of CCPs, the local lipid composition changes though conversion of PIP2 into both PI(3)P and PI(4)P, mediated by diverse lipid kinases and phosphatases such as synaptojanin1 and OCRL. During the end of the lifetime of CCPs, they become enriched in monophosphoinositol with the highest levels present in closed CCVs. It is argued that this change in the local PIP levels led to a burst in auxilin recruitment and to the complete removal of the clathrin coat from the vesicles (He *et al.*, 2017). It is therefore possible that the local lipid composition of CCPs could be a deciding factor in regulating the balance between clathrin exchange at CCPs and complete uncoating of CCVs.

1.5 CARGO SPECIFIC MODULATION OF CLATHRIN MEDIATED ENDOCYTOSIS

As discussed in previous sections of the introduction, a great variety of different receptor proteins are present at the plasma membrane and CME is an important pathway for their uptake into the cell. However, most research has focused on the trafficking of a small subset of these different cargo proteins with the LDL, EGF and Transferrin receptors being among the most widely researched. The trafficking of GPCRs has also gained a lot of attention over the last few decades and it has been established that the uptake of these receptor cargoes differs in many aspects to those of other cargoes such as Transferrin or EGF receptor. A major focus of this Thesis was to delineate how the nature of the cargo incorporated into CCPs dictate their dynamics and assembly. Therefore, the differences between the constitutive uptake of the Transferrin receptor and the ligand stimulated uptake of GPCRs shall briefly be outlined below.

1.5.1 Constitutive uptake of Transferrin receptor

The transferrin receptor (TfR) has long been used as model cargo to study general mechanisms of CME and has been a valuable tool for researchers. Iron homeostasis is a key physiological trait for all cell types and transferrin is the main route that facilitates its uptake. After binding of iron in the extracellular media, transferrin binds to the transferrin receptor on the cell surface, gets internalized through CME and is then recycled back to the cell surface where it is released back into the extracellular space to undergo constant cycling and iron uptake (Gkouvatsos, Papanikolaou and Pantopoulos, 2012). The robustness of this cycling as well as the ease of biochemical modifications of transferrin and its receptor have led to many key discoveries in the field of CME. Internalization of the TfR is initiated by the four amino acids YXRF at the N-Terminus binding to the AP-2 complex to initiate formation of nascent CCPs (Collawn *et al.*, 1990). This internalization sequence follows the classical Yxxϕ type (ϕ= bulky hydrophobic side chain) motif that is often found in cargo proteins to initiate CME (Ohno *et al.*, 1995). Artificial clustering of the TfR has also been shown to increase formation of CCPs and incorporation of TfR into nascent CCPs stabilizes their assembly and increase the amount of productive CCPs that mature into complete CCVs (Liu *et al.*, 2010). Due to the high abundance and constant cycling of the TfR, it is incorporated into most (if not all) CCPs during their lifetime (Keyel *et al.*, 2006) and has therefore been a valuable tool for researchers to investigate the steady state dynamics of CME. Importantly, the TfR is taken up almost exclusively through clathrin dependent pathways and is trafficked independently of binding to its ligand (Watts, 1985).

1.5.2 Ligand stimulated uptake of GPCRs

The ligand stimulated uptake of GPCRs through CME differs in many ways from that of the constitutive cycling of the TfR. GPCRs are very important signalling molecules at the plasma membrane with 7 transmembrane domains that signal though activation of G-Proteins at their cytosolic domains. The detailed signalling of GPCRs is a highly complex and important topic of research but has not been the focus of this thesis. Therefore, it will only be described in brief: GPCRs are able to bind to a range of extracellular ligands which leads to their activation and conformational changes. These changes lead to the activation of the G-Proteins through exchange of GDP to GTP. The activated G-Protein is than able to induce a unique signalling cascade depending on the GPCR and its ligand. The signalling is terminated by hydrolysis of the GTP and reassociation with the GPCR (Tuteja, 2009). Endocytic uptake of GPCRs has long thought to be the main pathway to terminate signalling but recent evidence suggests that GPCRs continue to signal along the endocytic pathway and that their uptake leads to a modified signalling response (see (Irannejad and von Zastrow, 2014) for an excellent review on the details of this process). Importantly, after ligand stimulated activation, the intracellular domain of GPCRs are phosphorylated though the family of G-protein coupled receptor kinase (GRK) which leads to the recruitment of arrestins. The arrestins are a small family of scaffolding proteins that that bind to activated GPCRs and regulate their uptake through CME as well as acting as signalling molecules themselves (Ebisuya, Kondoh and Nishida, 2005). Uptake of activated GPCRs is then facilitated by the terminal domain of the clathrin heavy chain binding to the arrestins as well as AP2 to initiate CME.

The GPCR superfamily is one of the major targets of pharmaceutical treatment with over 800 different genomic sequences encoding different GPCRs (Kochman, 2014). Due to the complexity of this vast family of receptors, the research conducted in this thesis focused on the trafficking of the purinergic $P2Y_{12}$ receptor due to the availability of previous studies as well as reagents and cell lines. The $P2Y_{12}$ receptor belongs to the family of purinergic receptors, that respond to extracellular nucleotides and specifically binds to ADP as extracellular ligand (review in: Erb and Weisman, 2012). It is most well known for its role in platelet aggregation during wound healing but is also expressed in astrocytes and microglia in the brain (Mamedova, Gao and Jacobson, 2006; Moore *et al.*, 2015). After binding of ADP the receptor becomes activated, undergoes conformational changes, binds to cholesterol and forms high order oligomers. Consistent with this, it has been found to be present in “detergent resistant membranes” and to be partitioned into so called “lipid rafts” (Savi *et al.*, 2006). Even though the nature of “lipid rafts” is still a controversial topic, the formation of high order oligomers as well as binding of cholesterol will lead to a change in the local lipid composition of oligomeric complex, compared to the surrounding plasma membrane. After activation though binding of ADP, the $P2Y_{12}$ receptor is

phosphorylated by GRK2 and signals though the specific G(i)-protein complex. Signalling of activated $P2Y_{12}$ is terminated by recruitment of either Arrestin2 or Arrestin3 and uptake though CME (Mundell *et al.*, 2006).

Importantly, the mechanisms of CME of the $P2Y_{12}$ (and other GPCRs) receptor differs in many aspects to that of the Transferrin receptor (TfR). While the TfR is continuously taken up into the cell and recycled back to the cell surface, internalization of the $P2Y_{12}$ receptor only occurs after receptor activation through ligand binding. Data obtained from investigation of other GPCRs has established that that the lifetime dynamics of CCPs trafficking either the TfR or ligand stimulated GPCRs are also different, with CCPs trafficking GPCRs having a significantly longer lifetime than those trafficking TfR (Henry *et al.*, 2012; Soohoo and Puthenveedu, 2013). These differences in CCPs dynamics were proposed to be due to receptor ubiquitination, however if the $P2Y_{12}$ receptor also undergoes ubiquitination is unclear (Nisar *et al.*, 2011). Additionally, many GPCRs (but not the TfR) contain PDZ domains in their C-Terminal parts that mediate interactions with the cytoskeleton and it could be shown that the PDZ domain in the C-Terminus of the $P2Y_{12}$ receptor is essential for its clathrin mediated uptake after ligand stimulation (Nisar *et al.*, 2011). Most importantly for this Thesis, the uptake of the $P2Y_{12}$ receptor is dependent on the capacity of clathrin light chain B to be phosphorylated while this is dispensable for CME of the TfR (Ferreira *et al.*, 2012). Since the focus of this thesis was to investigate the mechanism(s), by which CLCs control the uptake of specific cargo proteins, the Transferrin and $P2Y_{12}$ receptors were used as model systems to study this phenomenon.

2 MATERIALS AND METHODS

Most of the materials and methods performed in this thesis are already described in the methods section of the published article. However, due to the concise nature of the manuscript, some of the methods will be described in more detail as well as the methods of the experiments that were not part of the manuscript.

2.1 TRANSFECTION USING ELECTROPORATION

Transient transfection of HeLa cells expressing CLCb, WT, and mutants with constructs encoding dynamin2-mCherry, GAK-mCherry, eps15-mCherry, CALM-mCherry, and epsin2-mCherry was performed using electroporation with the NeonR system as follows: $3*10^6$ cells were resuspended in 125 µl of "R electroporation buffer" from the Neon® transfection system to which 5µg plasmid DNA was added. Cells were taken up with a Neon® pipette tip and the tip inserted into an electroporation tube filled with 3ml electrolytic E2 buffer connected to the transfection device. Electroporation was carried out using one 1200V pulse of 50ms. The electroporated cells were added to 3 ml equilibrated growth medium without antibiotics and 500 µl of the cell suspension was seeded as a meniscus on top of a poly-L-lysine coated cover slip. Cells were allowed to attach to the coated cover slip surface for 30 to 60 minutes at 37°C before an additional 1,5ml growth medium with antibiotics was added.

2.2 COATING OF COVERSLIPS WITH POLY-L-LYSINE

Coating of cover slips with Poly-L lysine Glass cover slips (radius 25 mm, Marienfeld, Germany) were gently rocked for 1h in 1 M HCl, and washed 3x with ddH2O. Afterwards, they were gently rocked for 1 h with 1 M NaOH. The coverslips were then washed again 3x with ddH2O. Finally, they were rocked for 2 h in 100 % EtOH and after discarding the EtOH, baked at 100°C for 1h. The clean cover slips were then dispersed in 6-well plates and coated with 500 µl of a 1x poly-L-lysine solution. After 20 min of incubation, the solution was aspirated and coverslips were washed 3x with ddH2O, dried and exposed to ultraviolet light for 20min under the sterile hood. The 6-wells were stored at 4 °C until needed for experiments.

2.3 WESTERN BLOT

Cells were washed and detached from the flask with trypsin/EDTA at 37°C for 5 min and centrifuged (1000 x g, 3 min), the pellet was washed twice with 1x PBS. Then, the pellet was resuspended in 80 µl RIPA buffer (1mM EDTA, 1% TritonX-100, 0.1% Sodium Deoxycholate, 0.1% SDS, 140mM NaCl, 1 mM Phenylmethylsulfonyl fluoride) and kept on ice for 30 min. After lysis, the sample was centrifuged at 10min 4 °C at 14000 x g and the supernatant was transferred into a new tube.4X Laemmli buffer (4% SDS, 20% glycerol, 0.004% bromphenol blue, 0.125M Tris-CL pH 6.8, 10% 2-mercaptoethanol added immediately before use) was added to 30µg of the protein lysate in a 3:1 ratio boiled for 10min at 95°C and loaded onto an 8% SDS gel. Gels were immersed in SDS running buffer and run at 70 V until the running front had left the stacking gel, then the voltage was increased to 100 V and the gels were run until the running front left the end of the gel. The proteins from the gel were then transferred onto a Roti-NC nitrocellulose membrane using the "wet-blot" method. Briefly, the membrane was placed on top of the gel, between two Whatman papers in transfer buffer and an electric field of 100V as applied for 1h at RT. The membrane was then blocked with 10% milk powder in PBS solution for 1h and incubated with α-Auxilin (abcam: ab103321) and α-GAK antibody [1C2] (abcam: ab115179) and antibodies 10% milk powder in PBS overnight. After this, the membrane was washed 3x15 min with PBS-T and incubated with the corresponding secondary antibodies conjugated to IRDye® 800 and IRDye® 680 for 1h and again washed 3x15min with PBS with 2% Tween-20. The fluorescent signal was detected with the Odyssey Infrared Imaging System.

2.4 BRADFORD ASSAY

Protein concentration was determined using Bio-Rad Protein Assay Reagent based on the Bradford method (1976). The cell lysate was diluted in 800 µl ddH_2O with 200µl Bradford Reagent and absorbance was measured at 595nm using a spectrometer and compared to known BSA standard curve.

2.5 GENERATION OF BIOTINYLATED TRANSFERRIN

200 µl of 10mg/ml solution of holo transferrin (Sigma-Aldrich T0665) was desalted at 14000g for 5 min in a Vivaspin 20, 10kDa MWCO column (GE healthcare) and absorbance was measured at 208nm to determine final protein concentration. From the solution, 1mg was biotinylated using a 20-fold molar excess of EZ-Link SulfoNHS-LC-Biotin (Thermo Scientific™) at 30˚C for 30min. The reaction was

quenched by addition of Tris (pH 6.5) and free biotin was removed by centrifugation at 14000g for 5min in a Vivaspin 20, 10kDa MWCO column (GE healthcare). The solution was diluted to 1mg/ml in PBS with 0.2%BSA, aliquoted, snap frozen in liquid nitrogen and stored at -20˚C.

2.6 TRANSFORMATION OF E COLI

In-house chemically competent DH5α E. coli were thawed on ice and ~10ng of plasmid DNA was added and cells were incubated on ice for 20min followed by a heat shock at 42˚C for 45 seconds and returned back on ice for 2min. 500 µl of pre warmed LB media (950ml ddH_2O, 10g Tryptone, 10g NaCl, 5g Yeast extract) without antibiotics was added and cells were grown at 37˚C for 1h. Different amounts of this cell solution were spread onto LB agar plates containing the appropriate selection antibiotics and incubated for 24-48h at 37°C.

2.7 PLASMID PURIFICATION

Plasmids from transformed E. coli were purified by picking single colonies of transformed E.coli using either the Miniprep Kit (Qiagen #27104), for small scale purifications or the Maxiprep Kit (Invitogen #K210017) for large scale purifications according to the manufacturer's instructions.

2.8 ATOMIC FORCE MICROSCOPY

Expression of the CLCb-WT-GFP construct in HeLa cells was by addition of 10ug/ml Doxycycline overnight and fixed with 4% PFA (Paraformaldehyde) in PBS for 20min followed by washing and quenching of PFA with 50mM NH_4Cl in PBS for 20min and sent to JPK Berlin via mail. Cells were grown in µ-Dishes 35 mm, low (ibidi #80136), to allow the AFM head to fit into the dish. Images were acquired using a Nanowizard 4 (JPK Berlin) mounted onto an Epifluorescence microscope (Zeiss) with filter set for GFP. For AFM measurements a qp-BioAC-50 scanning probe tip for soft measurements (Nanosensors™) was used and the spring constant was calibrated using the thermal tune method, based on Measuring Thermal Noise (Butt et al. 1995). Once the spring constant was determined, measurements in QI mode were taken using the following settings:

- Z-length: 800nm
- Setpoint: 600pN
- Data Rate: 25k Hertz

- Scan speed: 66.67 µm/s
- Duration 12ms

For an overview a 20x20 µm area was imaged followed by higher resolution measurements in 10x10 µm and 5x5 µm areas. A fluorescent imaged was taken before each round of AFM measurements and correlated using the "Direct Overlay" settings in the imaging software.

The Young's modulus was calculated for each force curve after setting the baseline update to 70% of the slope, correcting for the vertical tip position due to bending of the cantilever and fitting an elasticity fit according to the hertz model.

2.9 SAMPLE PREPARATION THIN SECTION ELECTRON MICROSCOPY

HeLa cells expressing either CLCb-WT-GFP or CLCb-SallA-GFP were grown in 60mm dishes to ~80% confluence and 10µg/ml Doxycycline was added to full growth media containing 10% FCS overnight to induce expression of the CLCb constructs. The next morning cells were fixed with EM grade 2%PFA mixed with 0.25% EM grade Glutaraldehyde for 1-2h in PBS. Cells were detached with cell scraper and pelleted at 500g for 5min. 1% EM grade Osmium in 0.2M Cacodylate buffer (pH 7.4) was added for 1h on ice in the dark and washed 3x with Cacodylate buffer followed by three washes with ddH20. Afterwards, 0.5% freshly prepared Uranyl Acetate in ddH_2O was added at 4°C O.N. in the dark. On the next day, 10% Gelatine (weight/Volume) was prepared in PBS at 37C, centrifuged at 5000g for 5min and the supernatant was used. The stained pellet was resuspended in 1ml of Gelatine and spun down again at 5000g and left to harden for ~1h at 4˚C. The pellet was cut out of the Eppendorf and depending on the size of the pellet, it was cut into smaller fragments to make it more permeable in the following steps. The pellets was transferred into cold 50% EtOH for 10min, followed by 70%, 80%, 90% and 100% EtOH for 10min each. Fresh Epoxy Resin (EMbed 812 20 ml, DDSA 16ml, NMA 8ml, DMP-30, BDMA 1.1ml) was prepared and the pellet was transferred into Epoxy Resin in EtOH (1:1) for 1-2h, exchanged for pure Epon after 1-2h and exchanged again for pure Epon for 2h at RT, followed by a final exchange into Epon and cured at 60°C for 24h in a dry capsule.

The sample were sectioned into 70nm slices and mount on EM grids. Washed 3x10 min with ddH_2O and stained with 5% freshly prepared Uranyl Acetate for 10min followed by 3x10 min washes with ddH_2O. Grids were stained with Lead citrate for 10min and washed 3x10min with ddH_2O. The lead citrate was prepared as follows: 1.33 g lead nitrate, 1.76 g sodium citrate was added to 30 ml CO_2-free

double-distilled water giving rise to a milky solution of lead precipitate, 5 to 7 ml of 1 N NaOH was added dropwise to the suspension while stirring until it turned clear and free of precipitates at pH 12.

2.10 Fluorescence activated *cell sorting* (FACS) of live cells

1321N1 cells, isolated in 1972 from human brain (astrocytoma), were genetically modified to stably overexpress the $P2Y_{12}$ receptor with N-Terminal HA tag and are described in (Mundell et al. 2006) were a kind gift of S. Mundell (University of Bristol). However, visual inspection revealed that only a small proportion of cells we received still expressed the receptor. To increase the amount of $P2Y_{12}$ expressing cells, FACS sorting was as performed as follows:

Anti HA antibody (rat; clone 3F10; Roche) was directly conjugated with Alexa 555 fluorophore using the APEX® Antibody Labeling Kits (ThermoFisher A10494) according to the manufactures instructions. Cells were grown in 60mm dishes, chilled at 4˚C in PBS and stained with the directly conjugated anti HA antibody (1:1000) for 45min on ice. Cells were washed 3X with ice cold PBS and transferred back to 37˚C for 10min to allow for internalization of surface bound antibodies. Cells were detached with Trypsin and transferred into ice cold PBS and FACS sorting was performed by the Flow Cytometry Core. Photo multiplier tube (PMT3) measuring the intensities of the Alexa 555 signal. After two rounds of cell sorting, two distinct populations of $P2Y_{12}$ expressing and non-expressing cells were detected and cells positive for $P2Y_{12}$ (Fig 2.1) were sorted into a fresh flask, grown in the presence of Gentamicin and frozen for future use.

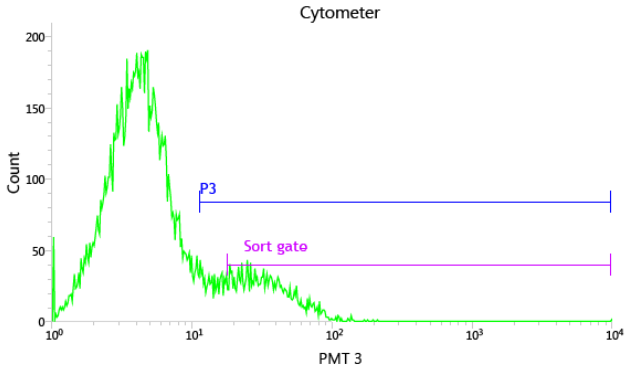

Statistics: Cytometer

Populations	Events	% Total	% Parent	PMT 3 Geo Mean
All Events	20,000	100.00%	####	6.26
P1	14,464	72.32%	72.32%	5.76
P2	14,368	71.84%	99.34%	5.75
P3	2,762	13.81%	19.22%	27.34
Sort gate	2,088	10.44%	14.53%	34.16

Figure 2.1 FACS sorting of $P2Y_{12}$ positive 1321N1 cells: 1321N1 cells stably overexpressing HA-tagged P2Y12 receptor were stained against the HA epitope and sorted by flow cytometry. 10.44% of the total cell population were positive for the $P2Y_{12}$ receptor and used for further experiments.

3 MAIB ET AL. 2018 "CARGO REGULATES CLATHRIN-COATED PIT INVAGINATION VIA CLATHRIN LIGHT CHAIN PHOSPHORYLATION" JCB, VOL. 217 NO. 12.

As stated throughout the Introduction section, the main aim of this study was to decipher the differential requirements for CLCb phosphorylation in the uptake of GPCRs vs. TfR. The main results of this research have been published in the Journal of Cell Biology on September 18, 2018 and went through a peer review process. I apologize to the reader for repetitions of some parts of the introduction in the article. However, in this format of the Thesis, some repetitions are inevitable due to the word limit and concise nature of the article.

All of the experiments in the article were performed be me (Hannes Maib) with the exception of the metal replica EM of unroofed HeLa cells. These experiments were performed by our collaborator Stéphane Vassilopoulos at the Sorbonne Université in Paris after receiving the cell lines by mail. The stable cell lines as well as the constructs encoding CLCb-WT-GFP, CLC-S204A-GFP and CLCb-SallA-GFP were produced by Felipe Ferreira who left the lab shortly after I arrived. The 1321N1 cells stably expressing the HA-Tagged $P2Y_{12}$ receptor were a kind gift of S Mundell from Bristol. The construct encoding Arrestin3-GFP was a kind gift of Mark von Zastrow and the other constructs for, Dynamin2-GFP, GAK-GFP, Eps15-GFP, Epsin2-GFP and CALM-GFP were purchased from Addgene. Elizabeth Smythe and I devised the experiments and wrote the manuscript together.

_____ _____

Hannes Maib Elizabeth Smythe

JCB Journal of Cell Biology

ARTICLE

Cargo regulates clathrin-coated pit invagination via clathrin light chain phosphorylation

Hannes Maib[1], Filipe Ferreira[1], Stéphane Vassilopoulos[2], and Elizabeth Smythe[1]

Clathrin light chains (CLCs) control selective uptake of a range of G protein–coupled receptors (GPCRs), although the mechanism by which this occurs has remained elusive thus far. In particular, site-specific phosphorylation of CLCb controls the uptake of the purinergic GPCR $P2Y_{12}$, but it is dispensable for the constitutive uptake of the transferrin receptor (TfR). We demonstrate that phosphorylation of CLCb is required for the maturation of clathrin-coated pits (CCPs) through the transition of flat lattices into invaginated buds. This transition is dependent on efficient clathrin exchange regulated by CLCb phosphorylation and mediated through auxilin. Strikingly, this rearrangement is required for the uptake of $P2Y_{12}$ but not TfR. These findings link auxilin-mediated clathrin exchange to early stages of CCP invagination in a cargo-specific manner. This supports a model in which CCPs invaginate with variable modes of curvature depending on the cargo they incorporate.

Introduction

Clathrin-mediated endocytosis (CME) is a major pathway that controls receptor uptake from the plasma membrane and is essential for physiological processes including synaptic vesicle recycling, developmental signaling, and immune responses (McMahon and Boucrot, 2011; Mettlen et al., 2018). A triskelion is composed of three units of clathrin heavy chain, each associated with a clathrin light chain (CLC; Brodsky, 2012; Maib et al., 2017). Clathrin triskelia assemble onto the plasma membrane to form clathrin-coated pits (CCPs), which trap receptor cargoes and invaginate, becoming spherical clathrin-coated vesicles (CCVs) that are pinched off and deliver their cargoes into the cell (Lampe et al., 2016; Kaksonen and Roux, 2018).

How the clathrin coat deforms the membrane from a flat patch into a spherical vesicle has long been a matter of debate. Currently, two distinct models have been proposed to explain this process. In the first, the constant curvature model, the clathrin coat directly polymerizes into curved lattices driving invagination, while in the second model, clathrin initially assembles as a flat lattice and is continuously rearranged into a spherical bud while keeping its area constant. In vitro data (Kirchhausen and Harrison, 1981; Dannhauser and Ungewickell, 2012; Kirchhausen et al., 2014) largely support the first model, while cellular data favor the second (Heuser, 2000; Avinoam et al., 2015). Most recently, however, it was shown that both modes of curvature can happen in the same cell, suggesting that cooperating and competing forces will define which model of invagination is followed (Scott et al., 2018). Such forces will include the local protein and lipid content of the CCP and how they contribute to the energetic costs of membrane deformation (Stachowiak et al., 2013; Sorokin et al., 2018).

Flat clathrin lattices are hexagonal arrays, and to gain curvature, rearrangement is needed to convert hexagons into pentagons (Kanaseki and Kadota, 1969), and this in turn requires clathrin exchange (den Otter and Briels, 2011). FRAP experiments have shown that there is extensive exchange between membrane-associated and cytoplasmic clathrin (Wu et al., 2001). This is mediated by cyclin G–associated kinase (GAK; Lee et al., 2006), which is the ubiquitously expressed form of the neuronal protein, auxilin, both of which also act as cofactors for clathrin disassembly during CCV uncoating (Ungewickell et al., 1995; Eisenberg and Greene, 2007). Consistent with this, these proteins have been implicated functionally in early stages of CCP formation (Newmyer et al., 2003).

The energy of clathrin polymerization contributes to membrane deformation (Dannhauser and Ungewickell, 2012; Saleem et al., 2015), and in vitro research showed that CLCs contribute to the tensile strength of the lattice and are required for the deformation of artificial membranes with high bending rigidity (Dannhauser et al., 2015). This impact of the CLCs on the mechanical properties of the clathrin lattice is also reflected in their requirement for CME of large particles such as bacteria (Bonazzi et al., 2011) as well as at sites of increased membrane tension (Boulant et al., 2011). Our recent research revealed that CLCs and specific phosphorylation sites are required for the ligand-stimulated uptake of a subset of G protein–coupled receptors (GPCRs; Ferreira et al., 2012), which contrasted with their dispensable

[1]Centre for Membrane Interactions and Dynamics, Department of Biomedical Science, University of Sheffield, Sheffield, UK; [2]Sorbonne Université, INSERM, Institute of Myology, Centre for Research in Myology, UMRS 974, Paris, France.

Correspondence to Elizabeth Smythe: e.smythe@sheffield.ac.uk.

role for uptake of single-pass transmembrane proteins such as transferrin receptor (TfR) and epidermal growth factor receptor in some (Hinrichsen et al., 2003; Huang et al., 2004) but not all cases (Chen et al., 2017). The requirement for CLCs for the uptake of some GPCRs was subsequently verified in vivo (Wu et al., 2016). Importantly, CME of ligand-stimulated GPCRs differs in certain respects from that of constitutive uptake of cargoes such as TfR (Irannejad and von Zastrow, 2014). However, the mechanism or mechanisms by which CLCs contribute to cargo-selective uptake have remained elusive thus far.

In this study, we provide evidence that clustering of cargoes such as the multimembrane-spanning GPCR $P2Y_{12}$ can influence the mode of curvature generation by the clathrin lattice. For CCPs with high amounts of $P2Y_{12}$, this process is dependent on the transition of flat clathrin lattices into spherical CCVs though clathrin rearrangement regulated by phosphorylation of CLCb and is mediated though auxilin in neuronal cells. However, this process is not required for the uptake of TfR, leading us to propose that CCPs invaginate using variable modes of curvature depending on the composition of the cargo that they incorporate.

Results

CLCb phosphorylation controls cargo uptake from CCPs

Our previous research (Ferreira et al., 2012) using an ELISA-based assay showed that expression of a nonphosphorylatable mutant CLCb where all 19 serines had been mutated to alanines, $CLCb^{SallA}$, inhibited internalization of both the GPCR purinergic receptors $P2Y_1$ and $P2Y_{12}$ in 1321N1 astrocytoma cell lines, which stably expressed HA-tagged receptors. By contrast, expression of a mutant with a single point mutation converting $serine_{204}$ to alanine, $CLCb^{S204A}$, inhibited $P2Y_{12}$ uptake but did not affect $P2Y_1$ uptake (Ferreira et al., 2012). This indicated that although CLCb phosphorylation is important for the uptake of $P2Y_1$, the relevant site is not $serine_{204}$ but some other site or sites. HeLa cells are a well-established model for exploring general mechanisms of endocytosis applicable to multiple cargoes, while 1321N1 cells, because of their neuronal origin, are likely to have specialized machinery required for $P2Y_{12}$ uptake. For this reason, in the experiments described below, we compared $CLCb^{SallA}$ with $CLCb^{WT}$ in HeLa cells when we tested effects on endocytosis that were likely to affect a range of cargoes, and $CLCb^{S204A}$ with $CLCb^{WT}$ when we were specifically measuring $P2Y_{12}$ uptake in 1321N1 astrocytoma cells. It is of note that we see similar results with $CLCb^{SallA}$ and $CLCb^{S204A}$ when we measure uptake of $P2Y_{12}$, further indicating that phosphorylation of $serine_{204}$ is the key residue in phosphorylation-mediated regulation of uptake of this receptor (Fig. 1; Ferreira et al., 2012).

To more precisely define the requirement for CLCb phosphorylation in $P2Y_{12}$ uptake, we expressed CLCb WT and phosphorylation-deficient mutants in 1321N1 astrocytoma cells that stably express HA-tagged $P2Y_{12}$. Following incubation in serum-free medium and stimulation with 10 mM ADP, the agonist for the $P2Y_{12}$ receptor, cells expressing $CLCb^{WT}$-GFP internalized $P2Y_{12}$ from the plasma membrane into EEA1-positive endosomes (Fig. 1, a–c). In contrast, expression of $CLCb^{SallA}$-GFP led to a decreased colocalization of $P2Y_{12}$ with EEA1 after 10 min ligand stimulation. Consistent with our previous research (Ferreira et al., 2012), expression of $CLCb^{S204A}$-GFP resulted in the same phenotype. Expression of phosphorylation-deficient mutants caused increased colocalization with clathrin at the plasma membrane compared with expression of $CLCb^{WT}$ (Fig. 1, a–c). The increased colocalization of $P2Y_{12}$ with clathrin at the plasma membrane indicates that reduced internalization in the presence of phosphorylation-deficient mutants is likely due to defects in CCP dynamics.

Ligand-stimulated CME of GPCRs differs in certain aspects from that of housekeeping cargoes such as TfR. Arrestins are specialized adaptor proteins that facilitate GPCR uptake, and arrestin3 is specifically required for $P2Y_{12}$ internalization (Kelly et al., 2008). To address whether CLCb phosphorylation affected arrestin3 recruitment, we expressed arrestin3 fused to mApple (mApple-arrestin3) in 1321N1 cells expressing either $CLCb^{WT}$-GFP or $CLCb^{S204A}$-GFP and assessed its ligand-dependent clustering into CCPs. In the absence of ligand, mApple-arrestin3 localized diffusely in the cytoplasm, and it was recruited into CCPs immediately after stimulation regardless of the phosphorylation state of CLCb (Fig. 1 d). Therefore, the receptor is able to enter into CCPs and recruit an essential adaptor protein but is not endocytosed if CLCb cannot be phosphorylated at $serine_{204}$.

Previous studies (Hinrichsen et al., 2003; Huang et al., 2004) have established that CLCs are dispensable for TfR uptake in contrast with their essential role for GPCR uptake (Ferreira et al., 2012; Wu et al., 2016). In our previous work, expression of phosphorylation-deficient mutants resulted in a mild effect on transferrin internalization when measured at 31°C (Ferreira et al., 2012). However, when measured at 37°C, expression of phosphorylation-deficient mutants in HeLa cells did not affect internalization of biotinylated transferrin compared with cells expressing $CLCb^{WT}$-GFP (Fig. 2 a). In this experiment, we first serum starved the cells, and then we measured internalization of biotinylated transferrin in serum-free medium. This is usual for such assays (Smythe et al., 1992, 1994) because it allows the uptake of a single cargo to be measured in the absence of other cargo molecules. However, cells grown in the presence of serum are exposed to a range of molecules, including GPCR agonists and growth factors, that could stimulate uptake of their cognate cell surface receptors. We were curious as to whether the presence of such cargo molecules might affect TfR uptake in HeLa cells expressing $CLCb^{SallA}$-GFP compared with those expressing $CLCb^{WT}$-GFP. To test this, we measured uptake of biotinylated transferrin in the presence of media containing 10% FCS. Under these conditions, we observed a decrease in the rate of biotinylated transferrin uptake in cells expressing phosphorylation-deficient CLCb (Fig. 2 b). This indicated that in the presence of other cargoes, efficient TfR internalization becomes dependent on CLCb phosphorylation.

This raised the question as to whether TfR and $P2Y_{12}$ are copackaged in the same CCPs. When we analyzed the colocalization of the $P2Y_{12}$ receptor with TfR in CCPs, after short ligand stimulation with ADP, we found that they partially colocalize into the same clathrin-coated structures (CCSs), albeit to different extents (Figs. 2 c and S1 a; ~22% of TfR was present in structures positive for $P2Y_{12}$). This suggests that TfR is stochastically packed into most, if not all, CCPs but also that it may be outcompeted

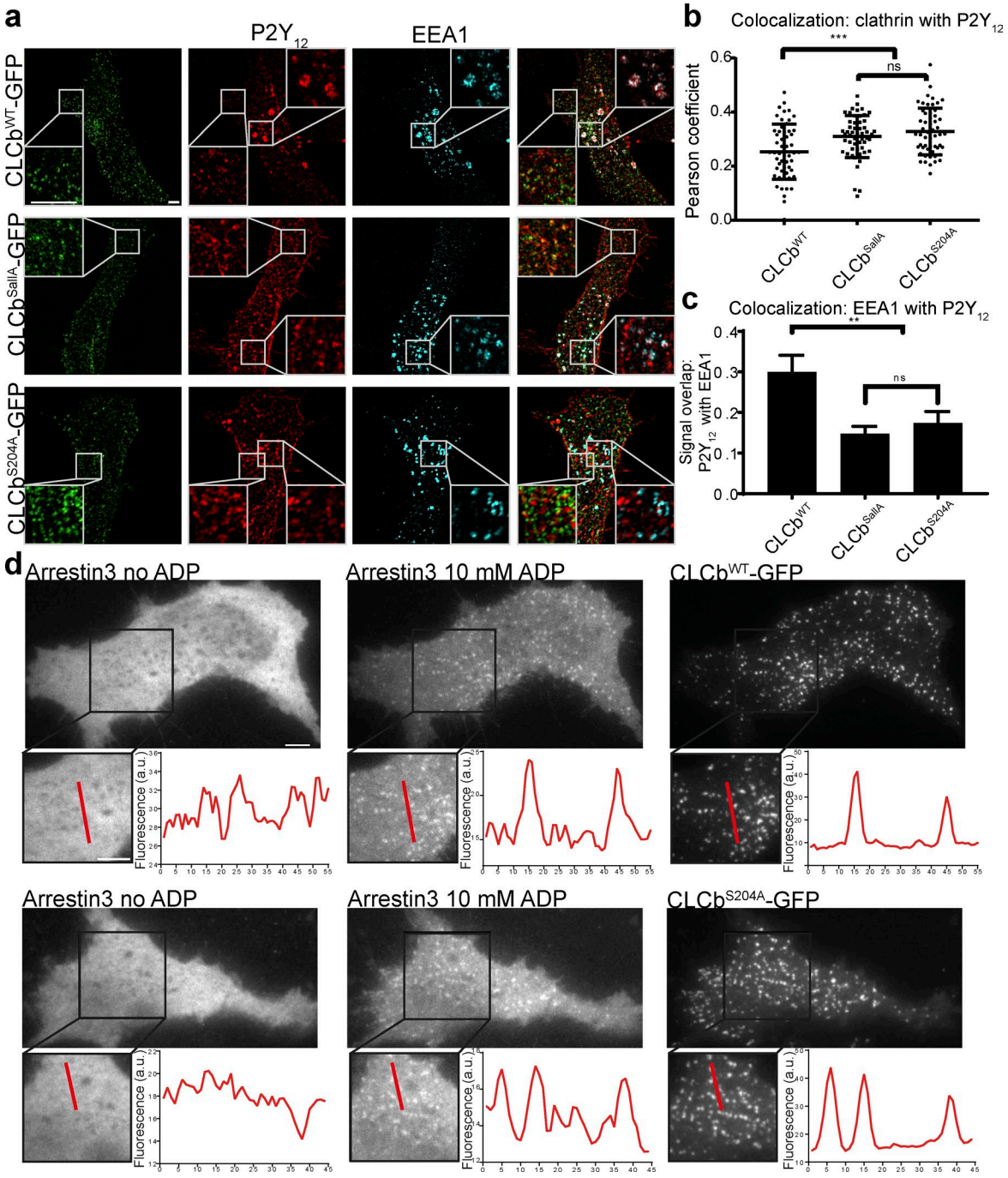

Figure 1. **CLCs control $P2Y_{12}$ uptake. (a)** 1321N1 cells stably expressing HA-tagged $P2Y_{12}$ receptor were transfected with $CLCb^{WT}$-GFP, $CLCb^{SallA}$-GFP, or $CLCb^{S204A}$-GFP, and following incubation in serum-free medium for 1 h and treatment with 10 mM ADP for 10 min, stained with antibodies against the HA tag and EEA1. White boxes show the indicated area at higher magnification. Bars, 5 µm. **(b)** Colocalization measured by Pearson's coefficient of $P2Y_{12}$ with $CLCb^{WT}$-GFP, $CLCb^{SallA}$-GFP, and $CLCb^{S204A}$-GFP at the plasma membrane. *n* = 50–55 from 24–27 cells. Error bars are mean ± SD. ***, P < 0.001. **(c)** Percent signal overlap between $P2Y_{12}$ with EEA1 from whole *Z* stacks using image segmentation. *n* = 24–27 cells. Error bars are mean ± SEM. **, P < 0.01. **(d)** 1321N1 cells were transfected with arrestin3-mApple together with $CLCb^{WT}$-GFP or $CLCb^{S204A}$-GFP and imaged with TIRF microscopy before and after treatment with 10 mM ADP; fluorescence was analyzed using line scans. Bars, 5 µm.

by high levels of $P2Y_{12}$. Therefore, stimulation of $P2Y_{12}$ uptake should make TfR uptake sensitive to CLCb phosphorylation at $serine_{204}$ (the site specific for $P2Y_{12}$ uptake). To test this, we measured the uptake of transferrin–Alexa Fluor 568 following costimulation of 1321N1 cells with ADP to stimulate $P2Y_{12}$ uptake. We found that there was a decrease in transferrin–Alexa Fluor 568 uptake in 1321N1 cells expressing $CLCb^{S204A}$-GFP compared with those expressing $CLCb^{WT}$-GFP (Fig. 2 c). Together, these data indicate that TfR and $P2Y_{12}$ receptors can be copackaged in the same CCPs following stimulation with ADP, and when this happens, uptake of these endocytic structures becomes dependent on CLCb phosphorylation.

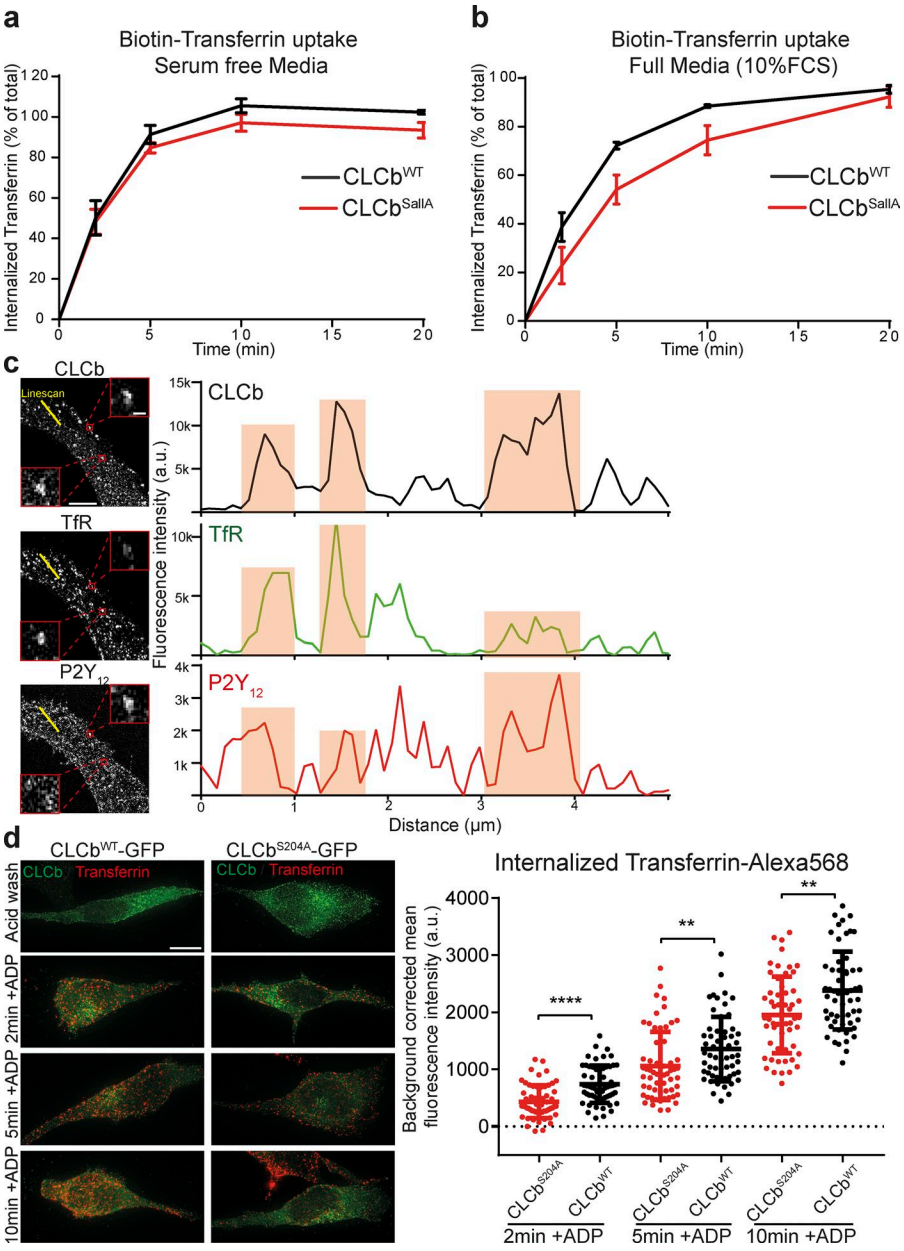

Figure 2. **Transferrin uptake becomes dependent on CLCb phosphorylation in the presence of other cargoes. (a)** HeLa cells expressing $CLCb^{WT}$ and $CLCb^{SallA}$ were serum starved for 1 h, and uptake of biotinylated transferrin in serum-free media was measured using an ELISA assay. Numbers represent mean ± SEM. $n = 3$. **(b)** Uptake of biotinylated transferrin in HeLa cells expressing $CLCb^{WT}$ or $CLCb^{SallA}$ without prior serum starvation and in the presence of full growth media containing 10% FCS. Numbers represent mean ± SEM. $n = 3$. **(c)** 1321N1 cells stably expressing HA-tagged $P2Y_{12}$ receptor were stimulated with ADP for 3 min and stained with antibodies against HA, TfR, and CLCb. Yellow line represents the intensity profiles in the right panels. Boxed areas show examples of CCPs with different amount of cargo packing. Bars: 5 µm (overview); 400 nm (boxed areas). **(d)** 1321N1 cells stably expressing the $P2Y_{12}$ receptor were transfected with either $CLCb^{WT}$-GFP or $CLCb^{S204A}$-GFP, and uptake of fluorescently labeled transferrin in the presence of ADP was determined by fluorescence microscopy. Error bars are mean ± SD. $n = 75–80$ cells for each time point pooled from three independent repeats. **, $P < 0.01$; ****, $P < 0.0001$. Bar, 10 µm.

CLCb phosphorylation and cargo influences lifetime dynamics of CCPs

Total internal reflection fluorescence (TIRF) microscopy is a well-established technique to measure the dynamics of CCP initiation and growth. The lifetime of CCPs is indicative of their functionality, and it has been shown that bona fide CCPs that recruit cargo, grow, invaginate, and pinch off to form CCVs have a broad lifetime distribution (20–60 s). By contrast, short-lived CCPs with a lifetime of 10–20 s are predominately abortive events that disassemble rapidly before they can capture cargo, gain curvature, or recruit dynamin (Merrifield et al., 2002; Ehrlich et al., 2004; Loerke et al., 2011; Taylor et al., 2012; Aguet et al., 2013). We compared the lifetime dynamics of CCPs in the absence and presence of arrestin3 (as a measure of $P2Y_{12}$ recruitment to CCPs) and transferrin. As observed previously (Aguet et al., 2013), the incorporation of transferrin stabilized nascent CCPs as evidenced by their broad lifetime distribution, while CCPs that failed to take up this housekeeping cargo displayed a predominately short lifetime of <20 s (Fig. S1 b). Stimulation with ADP resulted in recruitment of arrestin3 to ∼50% of CCPs, which showed a similar broad lifetime distribution (Fig. S1 c). It is noteworthy that the productive CCP population containing arrestin3 was almost twice as long lived as the population containing transferrin (63.09 s versus 31.52 s). Therefore, CCPs that mainly internalize TfR have a higher turnover rate and could compensate for the decreased uptake of TfR that is copackaged with the $P2Y_{12}$ receptor and is slower to internalize. It was recently shown that CCPs with longer lifetimes tend to gain curvature using the constant area mode, while CCPs with shorter lifetimes tend more toward the constant curvature pathway (Scott et al., 2018). Therefore, the difference in the lifetime dynamics of CCPs trafficking transferrin or arrestin3 suggests different modes of CCP assembly.

Previous studies have implicated the CLCs in the stability of the clathrin lattice (Schmid et al., 1982; Ungewickell, 1983; Ybe

et al., 1998, 2007; Wilbur et al., 2010), and their depletion was shown to affect the lifetime dynamics of CCPs (Mettlen et al., 2009; Boulant et al., 2011). We confirmed that CLCs affect lattice stability in 1321N1 cells by depleting both CLCa and CLCb using siRNA and analyzing the lifetime dynamics of CCPs after addition of fluorescently labeled transferrin. Depletion of both CLCs caused an increase in those short-lived events that fail to incorporate transferrin (Fig. S2 a). There was also an increased number of short-lived CCPs in HeLa cells expressing $CLCb^{SallA}$ or 1321N1 cells expressing $CLCb^{S204A}$ under ligand-stimulated conditions compared with cells expressing $CLCb^{WT}$-GFP (Fig. S2, b and c). Consistent with previous results (Loerke et al., 2009; Aguet et al., 2013), these short-lived events failed to recruit dynamin, cargo, and adaptor proteins including eps15, epsin2, and CALM, all of which have been shown to have important roles in CCP maturation (Figs. S2 and S3; Chen et al., 1998; Benmerah et al., 1999; Tebar et al., 1999; Meyerholz et al., 2005; Boucrot et al., 2012; Sahlender et al., 2013; Messa et al., 2014; Holkar et al., 2015; Miller et al., 2015; Ma et al., 2016). Additionally, the short-lived events also failed to recruit arrestin3 when $P2Y_{12}$ uptake was stimulated in 1321N1 cells (Fig. S2 c). Strikingly, when we investigated the recruitment of the ubiquitously expressed GAK, we found that it was recruited to short-lived events (Fig. S2 d). GAK regulates clathrin lattice rearrangement as well as uncoating, and its presence at these short-lived events could indicate that they are either abortive CCPs that fail to mature and get actively disassembled or that they are CCVs that have recruited GAK but fail to uncoat and transiently visit the TIRF field. Together, these data show that phosphorylation of CLCb is required for the maturation of a population of CCPs when cells are stimulated with ligand and that inability to phosphorylate CLCb increases the number of short-lived clathrin structures that recruit GAK.

CLCb phosphorylation controls invagination

To gain a better understanding of how CLCb phosphorylation controls maturation of a proportion of CCPs, we wanted to investigate whether there was a correlation between CLCb phosphorylation and CCP invagination. HeLa cells expressing $CLCb^{WT}$ and $CLCb^{SallA}$ were grown in media containing 10% FCS, processed for thin-section EM, and the morphology of CCPs was assessed. As expected, CCPs from cells expressing $CLCb^{WT}$ showed a broad distribution of morphologies ranging from shallow to U shaped and constricted (Fig. 3 a). Conversely, CCPs in cells expressing $CLCb^{SallA}$ showed a shift in distribution toward shallow CCPs compared with $CLCb^{WT}$ (Fig. 3 b). Failure to phosphorylate CLCb is thus reflected in an increased population of CCPs that fail to invaginate in the presence of FCS, where uptake of a range of cargoes is stimulated, some of which are dependent on CLCb phosphorylation.

Thin-section EM is a powerful tool to investigate CCP morphologies, but it is unable to detect flat clathrin lattices. The latter are larger and longer lived than classical CCPs and have been shown to control the uptake of lysophosphatidic acid (LPA; Leyton-Puig et al., 2017) and CCR5 receptors (Grove et al., 2014). It is noteworthy that LPA is a major constituent of serum (Eichholtz et al., 1993) and might contribute to the effect of serum on TfR uptake in the presence of phosphorylation-deficient CLCb. To investigate flat clathrin lattices, we employed metal replica EM of the plasma membrane from unroofed HeLa cells grown in the presence of FCS and expressing either $CLCb^{WT}$ or $CLCb^{SallA}$. We found that flat lattices as well as deeply invaginated CCPs were present in both $CLCb^{WT}$- and $CLCb^{SallA}$-expressing cells (Fig. 3, c and d). In cells expressing $CLCb^{SallA}$, there was an increase in the percentage of the plasma membrane that is covered by flat lattices (Fig. 3 e). Interestingly, although there was no significant difference in the mean area of flat lattices in either $CLCb^{WT}$- or $CLCb^{SallA}$-expressing cells (Fig. 3 f), the lattices formed in the presence of the phosphorylation-deficient CLCb mutant had a more irregular shape, which is apparent in a significant decrease in their circularity (Fig. 3 g). The increase in shallow CCPs is therefore also reflected in an increase in flat clathrin lattices of more irregular shapes. These flat lattices are unlikely to represent the short-lived events observed by TIRF microscopy but rather point to defects in lattice rearrangement and curvature generation likely due to altered interactions of GAK with phosphorylation-deficient CLCb.

CLCb phosphorylation is required for rapid clathrin exchange

To convert a flat lattice to a more invaginated CCP, clathrin needs to be rearranged to allow the incorporation of pentagons, which increases curvature (Kanaseki and Kadota, 1969; den Otter and Briels, 2011). To address whether the decrease in receptor uptake and curvature generation might be due to a defect in clathrin rearrangement, FRAP experiments were performed on individual CCSs at the plasma membrane of HeLa cells expressing either $CLCb^{WT}$-GFP or $CLCb^{SallA}$-GFP in the presence of 10% FCS (Fig. 4, a and b). In HeLa cells expressing $CLCb^{WT}$-GFP, the fluorescence signal recovered rapidly with a $t_{1/2}$ of 3.83 s, in agreement with previous research (Avinoam et al., 2015). However, this rapid recovery was greatly reduced in HeLa cells expressing $CLCb^{SallA}$-GFP as evident by the increased $t_{1/2}$ of 10.45 s with no significant effect on the mobile fraction (MF; Fig. 4, c and d), indicating a defect in clathrin exchange and lattice rearrangement.

We have previously shown that phosphorylation of $serine_{204}$, mediated by GPCR kinase 2 (GRK2), is a specific requirement for the uptake of the $P2Y_{12}$ receptor (Ferreira et al., 2012). We therefore wanted to address whether defects in clathrin rearrangement in the presence of $CLCb^{S204A}$ could be responsible for the reduction in $P2Y_{12}$ uptake. In the absence of ligand, the $P2Y_{12}$ receptor is retained at the plasma membrane and is only endocytosed upon ADP stimulation. We therefore treated 1321N1 cells expressing the $P2Y_{12}$ receptor with ADP and performed FRAP experiments before and directly after ligand stimulation. In 1321N1 cells expressing $CLCb^{WT}$-GFP, ADP stimulation only mildly affected the recovery half-time, with a change in the $t_{1/2}$ from 7.46 s to 9.33 s and no apparent change in the MF (Fig. 4, e and g). In the absence of ADP, the $t_{1/2}$ in cells expressing CLC^{S204A}-GFP was similar to that of cells expressing CLC^{WT}-GFP, with a $t_{1/2}$ of 8.27 s (Fig. 4, f and g). The difference in the half-time of recovery in HeLa cells expressing $CLCb^{WT}$-GFP (3.83 s) and 1321N1 cells expressing $CLCb^{WT}$-GFP (7.46 s) is likely due to differences in the expression of endocytic factors such as auxilin and GAK, which have both been implicated in clathrin exchange (Wu et al., 2001; Yim et al., 2005; Lee et al., 2006). Strikingly, however, upon

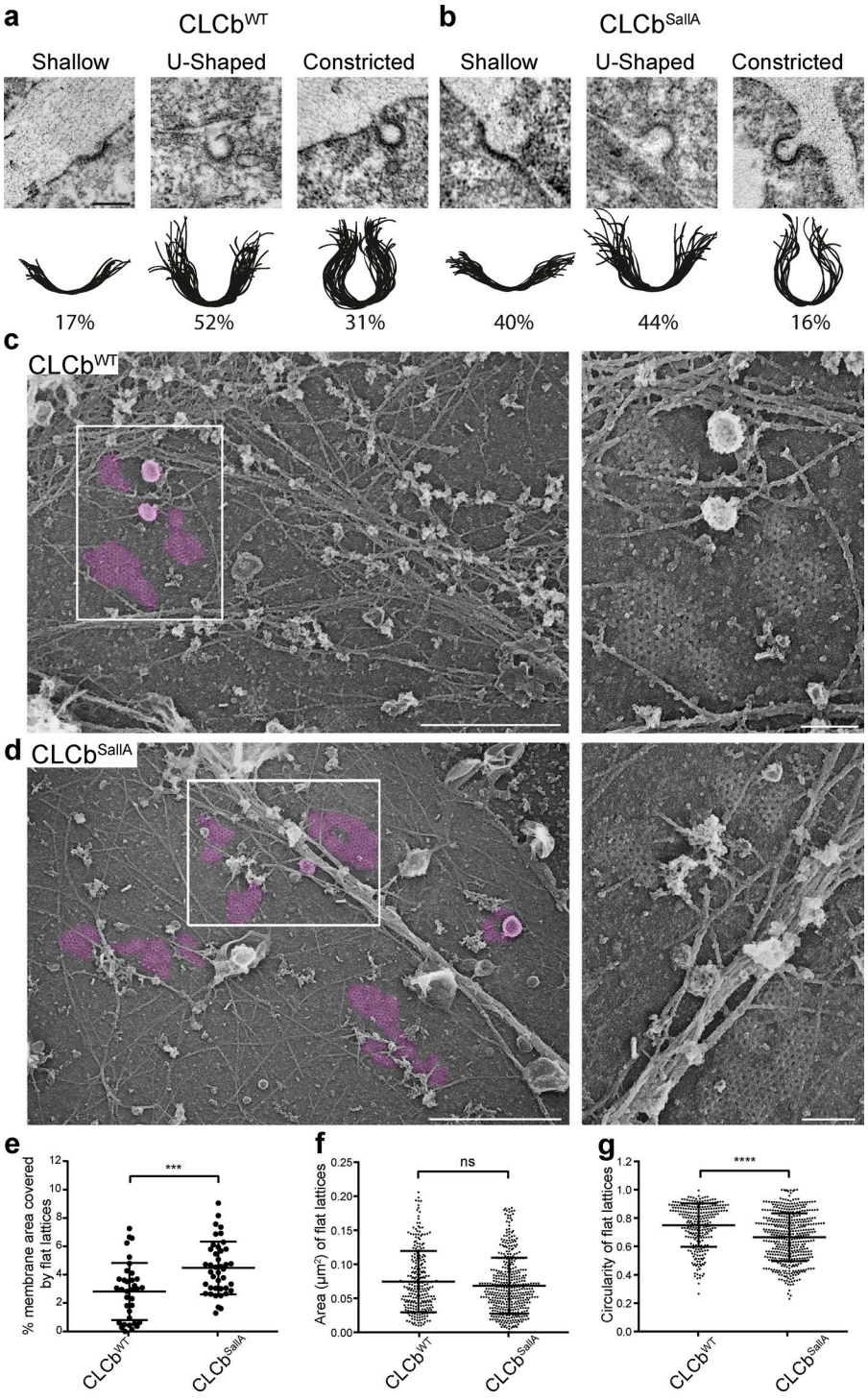

Figure 3. **CLCb phosphorylation regulates CCP invagination. (a and b)** HeLa cells expressing either $CLCb^{WT}$-GFP (a) or $CLCb^{SallA}$-GFP (b) were prepared for standard resin-embedded thin-section transmission EM, and individual CCPs were traced by hand using Illustrator and binned into shallow, U-shaped, or constricted. Bar, 200 nm. *n* = 67–88. **(c and d)** Survey view of the cytoplasmic surface of the plasma membrane in unroofed HeLa cells expressing either $CLCb^{WT}$-GFP or $CLCb^{SallA}$-GFP. Clathrin lattices are pseudocolored in purple. Insets corresponding with boxed regions in c and d show high-magnification views. Bars: 1 µm (main images); 200 nm (insets). **(e)** Percent membrane area covered by flat lattices. *n* = 35–41. ***, P < 0.001. **(f)** Area of all individual flat lattices from 35–41 different membranes. *n* = 278–461. **(g)** Circularity of all individual flat lattices as defined by Circularity = $4\pi \times \left(\frac{Area}{Perimeter^2}\right)$, with a value of 1.0 indicating a perfect circle. *n* = 278–461. ****, P < 0.0001. Values represent mean ± SD.

ligand stimulation in cells expressing $CLCb^{S204A}$-GFP, the $t_{1/2}$ increased significantly to 16.23 s, while the MF remained unaffected (Fig. 4, f and g). The effect on clathrin rearrangement is thus ligand dependent in cells expressing $CLCb^{S204A}$-GFP and is only manifest once uptake of the $P2Y_{12}$ receptor is stimulated.

Auxilin is required for $P2Y_{12}$ uptake

Since auxilin and GAK are required for efficient clathrin rearrangement and since auxilin expression is high in neuronal cells (Fig. 5 b), a prediction of these results is that auxilin and/or GAK should also be required for $P2Y_{12}$ uptake in 1321N1 astrocytoma cells. To test this, we depleted 1321N1 cells of auxilin using siRNA (Fig. 5 b), and $P2Y_{12}$ uptake was stimulated by addition of ADP for 10 min. In cells treated with nontargeting (NT) control siRNA, the receptor was readily taken up into EEA1-positive endosomes, while in cells depleted of auxilin, the $P2Y_{12}$ receptor was mainly localized at the plasma membrane (Fig. 5, a and c), similar to cells expressing either $CLCb^{SallA}$-GFP or $CLCb^{S204A}$-GFP (Fig. 1 c). To verify these results biochemically, we used an ELISA assay to determine the level of receptor uptake after ADP stimulation. In

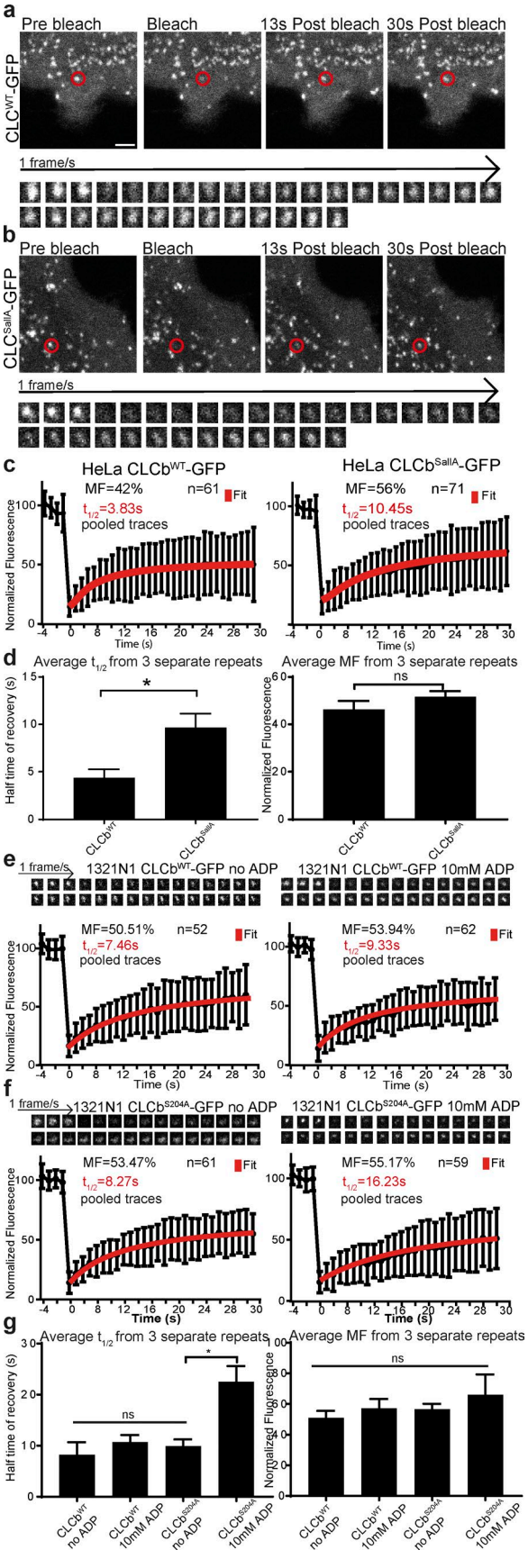

agreement with the microscopy data, cells treated with NT siRNA readily internalized the $P2Y_{12}$ receptor from the plasma membrane, while receptor uptake was almost completely abolished in cells depleted of auxilin (Fig. 5 f). By contrast, depletion of auxilin had only a very mild effect (evident in an ELISA assay after 5 min only) on transferrin uptake when measured under serum-free conditions (Fig. 5, d, e, and g). This indicates that auxilin-mediated clathrin rearrangement is a requirement for the uptake of the $P2Y_{12}$ receptor but not for the classical CME cargo transferrin in this cell line. Interestingly, in 1321N1 cells, GAK is expressed at levels comparable with those found in HeLa cells, where auxilin is expressed at almost undetectable levels (Fig. 5 b). However, GAK does not appear to be capable of compensating for loss of auxilin in the astrocytoma cells. This is consistent with in vivo research, which supports independent and overlapping functions of GAK and auxilin (Yim et al., 2010).

Discussion

Cargo regulates CCP invagination

The aim of our study was to understand the underlying mechanism for the differential requirement for CLCs and their phosphorylation in the uptake of the GPCR $P2Y_{12}$ versus TfR. It has been well established that CLCs are not generally required for the uptake of transferrin (Hinrichsen et al., 2003; Huang et al., 2004), which is often used as a canonical measure of CME because the route followed by receptor and ligand has been so well defined (Hopkins and Trowbridge, 1983; Watts, 1985). However, we show that uptake of transferrin is sensitive to the presence of other cargoes when they are copackaged into the same endocytic structures. Stimulation of 1321N1 cells with ADP results in the clustering of $P2Y_{12}$ in CCPs, and we have shown that TfR can be copackaged with $P2Y_{12}$. In line with our previous research (Ferreira et al., 2012), we show that uptake of $P2Y_{12}$ is regulated by CLCb phosphorylation at $serine_{204}$. When $P2Y_{12}$ uptake is stimulated, transferrin uptake is also decreased in cells expressing $CLCb^{S204A}$. A similar result is observed in HeLa cells expressing $CLCb^{SallA}$, where all 19 serine residues are mutated to alanine. Cells expressing this phosphorylation-deficient CLCb mutant show a delay in transferrin uptake in the presence of FCS, which contains ligands for other transmembrane receptors. While the

Figure 4. **CLCb phosphorylation regulates clathrin lattice rearrangements. (a and b)** Fluorescence from individual CCSs at the plasma membrane of HeLa cells grown in the presence of 10% FCS and expressing either $CLCb^{WT}$-GFP (a) or $CLCb^{SallA}$-GFP (b) was photobleached, and recovery of the signal was measured for 30 s at one frame per second. Bar, 2 µm. **(c)** Normalized recovery traces were fitted to cumulative data from three repeats with a hyperbola function of $y(t) = offset + MF * t/(t + t_{1/2})$ with Offset = bleaching efficiency and $t_{1/2}$ = halftime of recovery. Error bars are mean ± SD. **(d)** Average values from each of the three separate repeats from c. $n = 3$ with 16–23 traces from each repeat. Error bars are mean ± SEM. **(e and f)** 1321N1 cells were transfected with either $CLCb^{WT}$-GFP or $CLCb^{S204A}$-GFP, and fluorescence recovery of a single CCS was measured following incubation in serum-free medium before and directly after addition of 10 mM ADP. Top: Typical traces with the cumulative data from three independent repeats. Error bars are mean ± SD. **(g)** Average values from each of the repeats shown in e and f. Error bars show mean ± SEM. $n = 3$ with 16–26 traces from each repeat. *, $P < 0.05$.

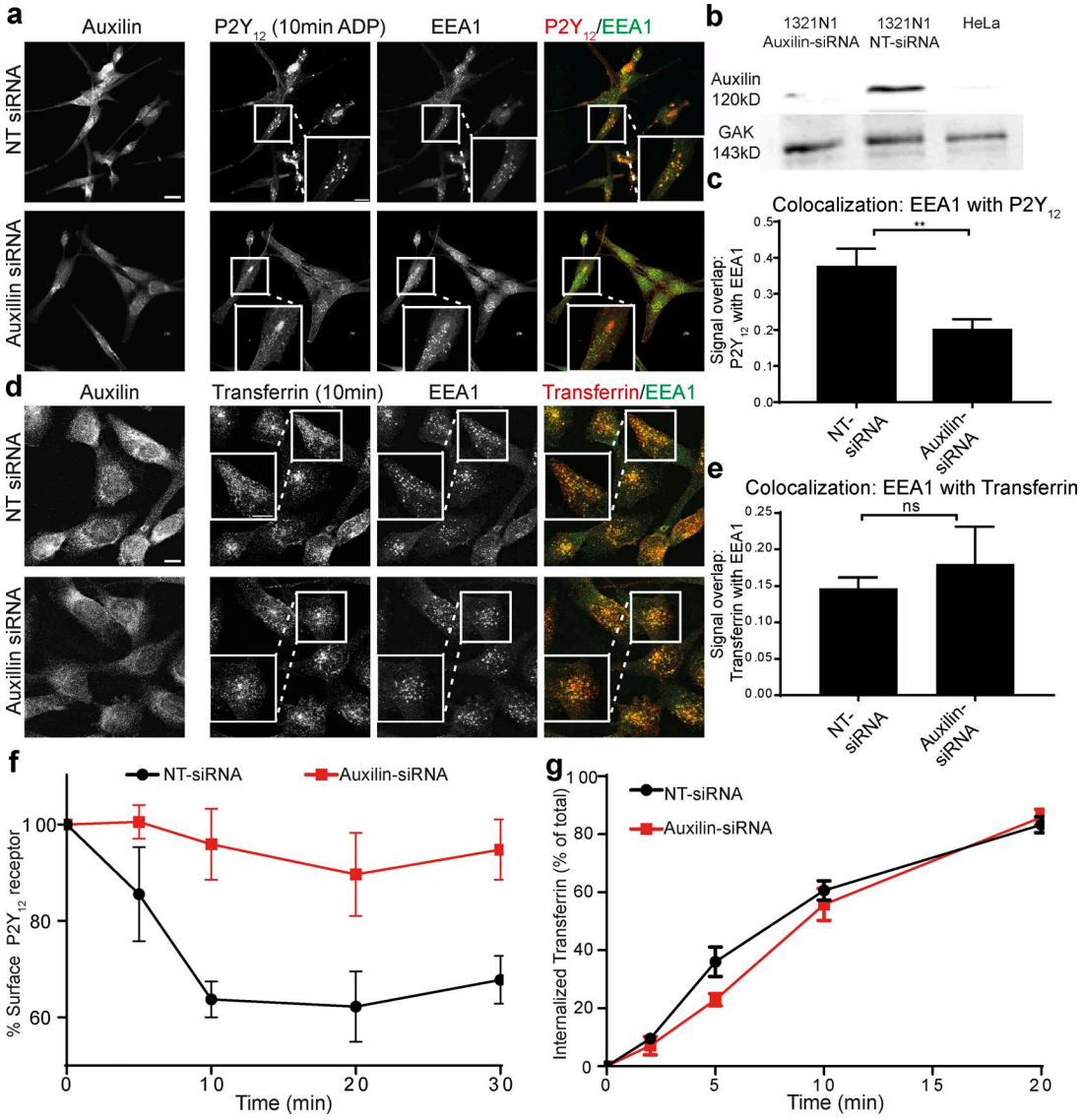

Figure 5. **Auxilin is required for efficient $P2Y_{12}$ uptake. (a)** 1321N1 cells were treated with control NT siRNA or siRNA targeting auxilin, treated with 10 mM ADP for 10 min to stimulate $P2Y_{12}$ uptake, and stained with antibodies against auxilin, $P2Y_{12}$, and EEA1. White boxes show an enlarged area. **(b)** Western blots showing levels of auxilin and GAK in HeLa cells and in 1321N1 cells following treatment with NT siRNA and siRNA targeting auxilin. Equal amounts of protein were loaded in each lane. **(c)** Quantification of the percent signal overlap between $P2Y_{12}$ with EEA1 from whole Z stacks using the image segmentation tool SQUASSH. **, $P < 0.01$. **(d)** 1321N1 cells were treated with control NT siRNA or siRNA targeting auxilin, treated with Alexa Fluor 568 transferrin (5 µg/ml) for 10 min, and stained with antibodies against auxilin and EEA1. White boxes show an enlarged area. Bars, 10 µm. **(e)** Quantification of the percent signal overlap between Alexa Fluor 568 transferrin with EEA1 from whole Z stacks using the image segmentation tool SQUASSH. **(f)** ADP-induced (10 mM) loss of surface $P2Y_{12}$ receptor was measured by ELISA in 1321N1 cells treated with NT siRNA or auxilin siRNA. $n = 3$. **(g)** Uptake of biotinylated transferrin was measured by ELISA in 1321N1 cells treated with NT siRNA or auxilin siRNA. Numbers represent mean ± SEM. $n = 3$.

phosphorylation sites required for uptake of other cargoes are not yet defined, our data show that transferrin uptake can become more dependent on phosphorylation of CLCb when the local cargo composition of CCPs is changed (e.g., by clustering of GPCRs that are dependent on CLCs).

The sorting of cargo proteins into distinct CCPs has been a matter of debate (Keyel et al., 2006). In this study, we show that TfR and $P2Y_{12}$ partially colocalize into the same CCPs, albeit to different extents. This is consistent with previous studies that showed that receptors are stochastically recruited into CCPs (Keyel et al., 2006; Lampe et al., 2014). However, high levels of $P2Y_{12}$ are likely to outcompete TfR from CCPs due to their oligomeric nature (Fig. 6). Under ligand-stimulated conditions, ∼50% of productive CCPs recruited arrestin3 with a lifetime of ∼60 s, while CCPs trafficking TfR had a mean lifetime of ∼30 s. Therefore, it is possible that TfR uptake "catches up" through CCPs that do not recruit $P2Y_{12}$ or arrestin3 and have a higher turnover rate. This may explain why TfR uptake is reduced and not abolished in cells expressing phosphorylation-deficient CLCb mutants.

Our study has revealed that CLC phosphorylation plays an essential role in CCP invagination, leading to efficient internalization of CCS containing high amounts of $P2Y_{12}$. The two models of membrane curvature generation during CCP invagination, constant area versus constant curvature, are conceptually quite different,

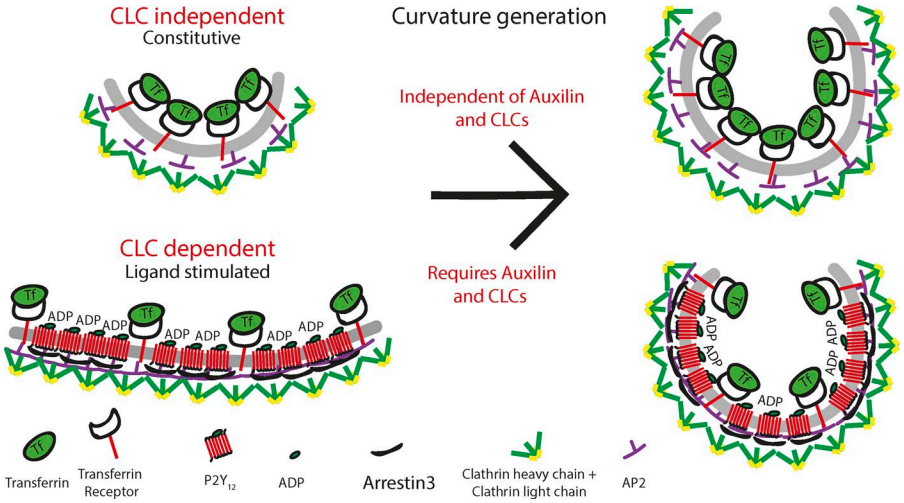

Figure 6. **Model for cargo regulation of CCP assembly mode regulated by CLC phosphorylation and auxilin.** CME of single-pass transmembrane proteins such as TfR that are constitutively internalized is independent of CLCs and lattice rearrangement when measured in the absence of other cargo. Following ligand stimulation, cargo such as $P2Y_{12}$ will recruit specialized adaptor proteins and oligomerize, packing tightly into CCPs, which will result in some exclusion of other cargo. Maturation of these CCPs then becomes dependent on CLCs and their ability to be phosphorylated as well as auxilin-mediated clathrin exchange, likely by contributing to the flat-to-curved transition of CCPs containing high amounts of $P2Y_{12}$.

requiring different mechanisms of lattice assembly. Both behaviors have however been observed in CCPs in SK-MEL-2 cells (Scott et al., 2018). Furthermore, a recent study argues for the assembly of flat lattices to ∼70% of their final size before curvature is initiated (Bucher et al., 2018). Curvature generation during CME is likely to be a complex process with different modes of membrane bending occurring in parallel, reflecting the energetics of coat assembly relative to competing forces. It has been shown in vitro that high membrane tension as well as rigidity directly opposes polymerization of clathrin into curved vesicles (Saleem et al., 2015). However, increased membrane tension in cellular systems is overcome by the actin cytoskeleton and requires CLCs to allow CME to occur (Boulant et al., 2011). It is reasonable to propose that in cases where the polymerization energy of the clathrin triskelia is not sufficient to deform the membrane directly, it will initially assemble as a flat lattice, whereas membranes that are easier to deform might follow the path of constant curvature, directly polymerizing into spherical vesicles. This is consistent with results from a recent study showing that increased tension of the plasma membrane inhibits its deformation and leads to an increase in flat clathrin lattices that fail to generate curvature (Bucher et al., 2018).

The two main factors that oppose local membrane deformation are its lateral tension as well as its rigidity. Membrane rigidity will depend on the local lipid and protein composition, and thus, cargo composition inside a CCP will have a significant impact on the biophysical properties of the membrane (Stachowiak et al., 2013). It is therefore possible that ligand-stimulated clustering of multimembrane-spanning GPCRs alters the local properties of the plasma membrane and biases the mechanism of invagination of CCPs toward the constant area mode. Rearrangement of the lattice is then driven by auxilin (in neuronal cells) and is dependent on the capacity of CLCb to be phosphorylated. CLCs could be needed to increase lattice rigidity, similar to the role of Sec13 in the incorporation of GPI-linked cargoes, predicted to drive opposing curvature, into COPII vesicles on the secretory pathway (Copic et al., 2012). An alternative, although not mutually exclusive, role for CLCb phosphorylation would be to efficiently recruit GAK for lattice rearrangement (see below).

It is also possible that recruitment of specialized endocytic effector proteins influences which mode of invagination is followed. Ligand-stimulated uptake of GPCRs requires the recruitment of the adaptor family of arrestins as well as ubiquitination and interactions of PDZ domains with the cytoskeleton (Hanyaloglu and von Zastrow, 2008). Notably, ligand-stimulated endocytosis of GPCRs results in altered CCP dynamics, with an increased lifetime of CCPs positive for arrestin3 compared with those that are positive for TfR as demonstrated in this study and in previous ones (Henry et al., 2012; Soohoo and Puthenveedu, 2013). Strikingly, a recent study has shown that even though both modes of curvature coexist in SK-MEL-2 cells, CCPs with longer lifetimes tend to gain curvature using the constant area mode, while CCPs with shorter lifetimes tend more toward the constant-curvature pathway (Scott et al., 2018). This further supports the notion that cargo proteins influence the mode of curvature generation of CCPs.

Phosphorylation of CLCb alters interaction with GAK and lattice rearrangement

How does CLCb phosphorylation control cargo uptake? The recruitment of cargo into CCPs as well as the recruitment of a wide range of adaptor proteins is unaffected by CLCb phosphorylation. Therefore, the defect in receptor uptake is likely to occur during CCP maturation. Lifetime analysis of CCPs revealed an increase in short-lived events with a lifetime of 10–20 s in the background of phosphorylation-deficient CLCb. The nature of these events is somewhat unclear, and they could either be abortive CCPs that fail to mature or they could be CCVs that transiently visit the TIRF field and have not yet uncoated. Importantly, these short-lived events were positive for the clathrin rearranging and uncoating protein GAK but did not recruit the GTPase dynamin2 or a wide array of adaptor proteins (such as eps15, CALM, arrestin3, or epsin2). Their increased appearance in the CLCb mutant could be due to altered interactions with GAK, leading to a delay in uncoating. This is in agreement with previous results showing that CLCb phosphorylation modulates GAK binding to clathrin cages (Ferreira et al., 2012) as well as studies that have implicated CLCs in the uncoating of CCVs (Schmid et al., 1984; Young et al., 2013). However, it is also possible that these short-lived events are abortive events and recruit GAK in its capacity as clathrin chaperone and/or to promote rapid disassembly in the absence

of cargo and dynamin. In support of this, depletion of GAK increases the turnover of abortive CCPs (Mettlen et al., 2009). Depletion of both GAK and auxilin in HeLa M cells, where both are expressed, reduces CCP formation at the cell surface by 50% and increases nonproductive cage assembly in the cytoplasm (Hirst et al., 2008), further supporting a role for GAK and auxilin in chaperoning clathrin to the cell surface. Both possibilities point toward an altered interaction of GAK with short-lived CCPs that are increased when CLCb cannot be phosphorylated.

The altered interaction of phosphorylation-deficient CLCb mutants with GAK appears to have a profound effect on clathrin rearrangements during the invagination of maturing pits. This rearrangement is crucial for flat lattices to gain curvature, and in line with this, cells expressing phosphorylation-defective CLCb mutants have an increased number of shallow CCPs as well as an increased number of flat clathrin lattices of more irregular shape. Flat lattices have been shown to be active sites of endocytosis by continuous budding of CCVs from their edges (Lampe et al., 2016) and to be important for the uptake of GPCRs (Grove et al., 2014; Leyton-Puig et al., 2017). For these lattices to invaginate, pentagons have to be incorporated into the flat hexagonal array, and this requires clathrin rearrangement mediated by GAK and auxilin (Lee et al., 2006). Our FRAP data indicate that the half-time of recovery of $CLCb^{SallA}$-GFP is significantly slower than that of $CLCb^{WT}$-GFP. Cells expressing $CLCb^{S204A}$ reveal a similar delay in FRAP but, strikingly, only after stimulation of $P2Y_{12}$ internalization, indicating that CLCs are important for clathrin exchange and that following ligand-induced clustering, lattice rearrangement is required for receptor uptake. Auxilin and GAK are crucial factors for clathrin exchange, and their depletion has been shown to drastically reduce exchange of clathrin at endocytic sites (Greener et al., 2001; Lee et al., 2006). The reduction in $P2Y_{12}$ uptake after auxilin depletion in 1321N1 cells further reinforces the requirement for clathrin exchange for the maturation of these endocytic sites. It also links auxilin-mediated clathrin exchange to early stages of CCP maturation in a cargo-specific manner.

By defining a molecular mechanism by which CLCb phosphorylation and GAK can regulate cargo-specific invagination, our data support a model whereby cargo can determine the mode of CCP assembly. Additionally, the recruitment of adaptor proteins during ligand-stimulated CME could also influence the mode of CCP assembly (Keyel et al., 2006). This idea is supported by a recent study showing that high levels of AP2µ2 lead to the formation of flat lattices (Dambournet et al., 2018). High concentrations of cargo within CCPs would also lead to an increased recruitment of AP2 and bias curvature toward the constant area model compared with CCPs with lower amounts of cargo loading. The assembly of flat lattices followed by lattice rearrangement, regulated by CLCb phosphorylation, would then be required for invagination. This is further supported by the specific effect of auxilin knockdown on $P2Y_{12}$ uptake in 132N1 cells compared with a very mild effect on transferrin and explains why previous studies may not have detected significant effects of auxilin or GAK knockdown on transferrin uptake in other cell types (Zhang et al., 2005; Hirst et al., 2008).

Taken together, these data support a model in which the local concentration and composition of cargo inside a CCP modulates the way it can be deformed (Fig. 6). For cargo such as the $P2Y_{12}$ receptor, CCPs would assemble as flat lattices that require clathrin rearrangement and CLCb phosphorylation. However, for cargo such as transferrin, CCPs could invaginate independently of lattice rearrangement and the CLCs. Importantly, we did not observe separation of cargoes into specialized CCPs, as evidenced by the decrease in transferrin uptake under ligand-stimulated conditions in the background of phosphorylation-deficient CLCb. This suggests that depending on the environment in which the cell finds itself, CCPs will form by variable curvature (Scott et al., 2018), which would be defined, at least in part, by the nature of the cargo incorporated by CCPs.

Materials and methods

Cell culture and transfection

HeLa cells and 1321N1 cells were cultured in DMEM supplemented with 10% FCS, glutamine, and penicillin/streptomycin. 1321N1 cells stably expressing the $P2Y_{12}$ receptor with N-terminal HA tag were a gift from S. Mundell and were grown in the presence of G418 as described by Mundell et al. (2006). HeLa cells stably expressing $CLCb^{WT}$-GFP and $CLCb^{SallA}$-GFP were cultured as described previously (Ferreira et al., 2012), and expression of CLCb was induced by addition of 1 mg/ml doxycycline overnight before each experiment. The construct encoding arrestin3-mApple was a gift from M. von Zastrow (University of California, San Francisco, San Francisco, CA). Constructs encoding dynamin2-mCherry, GAK-mCherry, eps15-mCherry, CALM-mCherry, and epsin2-mCherry were gifts from C. Merrifield and acquired from Addgene as described by Taylor et al. (2011). Transient transfection of HeLa cells expressing CLCb, WT, and mutants with constructs encoding dynamin2-mCherry, GAK-mCherry, eps15-mCherry, CALM-mCherry, and epsin2-mCherry was performed using electroporation with the NeonR system the day before imaging. Transfection of 1321N1 cells with constructs encoding $CLCb^{WT}$-GFP, $CLCb^{SallA}$-GFP, $CLCb^{S204A}$-GFP, AP2-GFP, or arrestin3-mApple was performed using Polyfect according to the manufacturer's guidelines.

For CLC siRNA experiments, 1321N1 cells were split into 6-cm dishes, and the next day, when ∼50% confluent, they were transfected with CLC or NT siRNA (final concentration, 200 nM) using Lipofectamine 2000 and left overnight. The next day, the cells were transfected again with siRNA as before, together with plasmid DNA encoding AP2-GFP. Cells were left for two more days before TIRF imaging. For knockdown of auxilin, 1321N1 cells were grown in 10-cm dishes, and the following day, at ∼30% confluency, cells were transfected with auxilin or NT siRNA at 200 nM final concentration using oligofectamine. Cells were left for 48 h and transfected again with the same siRNAs and used for ELISA assays the following day. Auxilin was detected by immunofluorescence and Western blotting using anti-auxilin antibodies (rabbit; anti-DNAJC6; ab103321; Abcam). EEA1 was detected using mouse anti-EEA1 antibodies (ab70521; Abcam). GAK was detected on Western blots using rabbit antibody from Abcam (ab115179).

The siRNAs had following sequences and were characterized previously: siRNA CLCa, 5′-AAAGACAGUUAUGCAGCUAUU-3′ (Ferreira et al., 2012); siRNA CLCb, 5′-AAGCGCCAGAGUGAACAA

GUA-3′ (Ferreira et al., 2012); and siRNA auxilin, 5′-UAUGUUACC UCCAGAAUUA-3′ (Hirst et al., 2008).

Confocal immunofluorescence and colocalization

1321N1 cells were grown on coverslips and transfected with either $CLCb^{WT}$-GFP, $CLCb^{SallA}$-GFP, or $CLCb^{S204A}$-GFP as described above. On the following day, cells were serum starved for 1 h in the presence of 0.1 U/ml apyrase, stimulated with 10 mM ADP for 10 min, and immediately fixed with 4% PFA. The PFA was quenched using 50 mM NH_4Cl in PBS, and nonspecific binding was blocked with 1% BSA. Cells were permeabilized using 0.1% Triton X-100. Cells were treated with antibodies against HA (rat; clone 3F10; Roche) and EEA1 (rabbit; clone 1G11; Abcam), and then they were stained using the corresponding secondary antibodies conjugated to Alexa Fluor 561 or Alexa Fluor 647 (Thermo Fisher Scientific). Coverslips were mounted onto microscopy slides and imaged using a Zeiss LSM880 AiryScan confocal microscope with a Plan Apochromat 63× 1.4 NA oil lens. Whole Z stacks were taken at 200-nm intervals.

Colocalization of the HA signal with the CLCb signal was analyzed at the plane of the plasma membrane by choosing three to five random regions (depending on cell size) of 250 × 250 pixels in each channel and determining the Pearson's correlation coefficient between them using ImageJ (National Institutes of Health). Overlap of the HA signal with EEA1 was determined by image segmentation using the ImageJ plugin SQUASSH (Rizk et al., 2014) on maximum-intensity projections of collapsed Z stacks.

For colocalization of $P2Y_{12}$ and TfR with 1321N1, cells were stimulated with 10 mM ADP for 3 min and stained against the HA (rat; clone 3F10; Roche), TfR (mouse; B3/25; ATCC), and CLCb (rabbit; sc-28277; Santa Cruz Biotechnology, Inc.) with the corresponding secondary antibodies conjugated to Alexa Fluor 488, Alexa Fluor 561, or Alexa Fluor 647. Coverslips were mounted onto microscopy slides and imaged using an LSM880 AiryScan confocal microscope with a Plan Apochromat 63× 1.4 NA oil lens at the plane of the plasma membrane. Colocalization of $P2Y_{12}$ with TfR was determined by image segmentation using the ImageJ plugin SQUASSH (Rizk et al., 2014).

Live-cell TIRF imaging and data analysis

For live-cell imaging, cells were transfected as described above and split into an eight-well microscopy chamber on the day before imaging. Cells were imaged in an environmental controlled chamber at 37°C in the presence of CO_2-independent media. Cells were imaged using a Zeiss Cell Observer with TIRF3 fitted with an α Plan Apochromat 100× 1.46 NA lens controlled by Axiovision. To reduce phototoxicity, cells were imaged at low laser power of ≤1% in two channels by sequential excitation at 1 Hz and were detected with a charge-coupled device camera with a pixel size of 16 µm. The depth of the evanescent field was 60–70 nm. For arrestin3 clustering, 1321N1 cells were serum starved for 1 h in the presence of 0.1 U/ml apyrase and imaged directly before and after addition of 10 mM ADP into the imaging media. Lifetime dynamics of CCPs and recruitment of adaptor proteins was determined using the MATLAB script cmeAnalysis (Aguet et al., 2013). Multiple cells from different repeats were pooled to account for cell to cell variability, and outliers were removed according to the criteria of the program.

FRAP imaging

For FRAP measurements, 1321N1 cells were transfected with $CLCb^{WT}$-GFP or $CLCb^{S204A}$-GFP as described above, while HeLa cells stably expressing $CLCb^{WT}$-GFP or $CLCb^{SallA}$-GFP were treated with 10 mM doxycycline and transferred into Ibidi glass-bottomed 35-mm dishes the day before imaging. For 1321N1 cells, recovery traces were determined without the presence of ADP in serum-free media and again directly after addition of 10 mM ADP within a 10-min window. Cells were imaged in an environmentally controlled chamber at 37°C in the presence of CO_2-independent media using a Nikon A1 confocal system with a CFI Plan Apochromat VC 60× 1.4 NA oil lens. An area of 256 × 256 pixels at the plasma membrane of transfected cells was imaged at 0.1-µm pixel size. Single CCSs were identified and imaged for 3 s at 1 Hz before bleaching the GFP signal for 1 s at 100% laser power using the 403 nm and 488 nm laser lines. Recovery of the signal was recorded over 30 s at 1 Hz at laser powers <1% to reduce photobleaching. Recovery traces were determined in two regions of interest (ROIs) of 7 × 7 pixels containing a single CCS and a control ROI devoid of CCS to determine the background signal. Background signal was subtracted from each CCS trace. The first three background-corrected frames were averaged and set to 100% for normalization, while the signal from the background ROI at the time of bleaching was set to 0% to account for recovery from out-of-focus GFP signal, unrelated to the signal from the CCS. The background-corrected signal directly after photobleaching was defined as bleaching efficiency and represents $t = 0$ of the recovery trace. Only traces with a bleaching efficiency of ≥80% were used for further analysis. All normalized recovery traces were averaged, the SD was determined, and a hyperbola curve of $y(t) = offset + MF^* t/(t + t_{1/2})$ was fitted based on the minimal squared difference. The offset was determined as the average bleaching efficiency from all traces, with $t_{1/2}$ being the halftime of recovery.

EM

Resin-embedded sections

HeLa cells expressing $CLCb^{WT}$-GFP or $CLCb^{SallA}$-GFP were grown in media containing 10% FCS and embedded in resin according to standard protocols (Smythe et al., 1989). In brief, cells were grown on 60-mm dishes, fixed with 4% PFA, pelleted, and postfixed with 1% glutaraldehyde and 4% tannic acid. Pellets were staining with 1% osmium for 1 h and 0.5% uranyl acetate overnight, embedded in epon resin, cut into 70-nm sections, and stained en bloc with uranyl acetate and lead citrate before imaging using an FEI Tecnai T12 Spirit at 80 kV. Samples were processed blind, and CCPs were analyzed by determining the width of the neck and the depth of each CCP using ImageJ as well as tracing around their contours manually using Adobe Illustrator.

Unroofed cells

Adherent plasma membrane from HeLa cells plated on glass coverslips were grown in DMEM containing 10% FCS and disrupted by sonication as described previously (Heuser, 2000). Glutaraldehyde/PFA-fixed cells were further sequentially treated with OsO_4, tannic acid, and uranyl acetate before dehydration and hexamethyldisilazane drying (Sigma-Aldrich). Dried samples were then rotary shadowed with platinum and carbon with a

high-vacuum sputter coater (Leica Microsystems). Platinum replicas were floated off the glass by angled immersion into hydrofluoric acid, washed several times by flotation on distilled water, and picked up on 200 mesh formvar/carbon-coated EM grids. The grids were mounted in a eucentric side-entry goniometer stage of a transmission electron microscope operated at 80 kV (CM120; Philips), and images were recorded with a Morada digital camera (Olympus). Images were processed in Adobe Photoshop to adjust brightness and contrast and presented in inverted contrast.

Endocytosis assays

Endocytosis of the $P2Y_{12}$ receptor was determined as described by Ferreira et al. (2012). In brief, the extracellular HA tag on the $P2Y_{12}$ receptor was used in an ELISA to determine the surface receptor level after various time points following stimulation with 10 mM ADP. The level of surface receptor without stimulation was set to 100%. Endocytosis of biotinylated transferrin was measured by its loss of accessibility to exogenously added avidin following internalization as previously described (Smythe et al., 1992). Briefly, cells were incubated with 1 µg/ml biotinylated transferrin either in serum-free media following serum starvation for 1 h before the experiment or in media containing 10% FCS without prior serum starvation. At different times, as indicated in figure legends, cells were washed 2× with ice-cold PBS/0.2% BSA and incubated for 30 min with 50 µg/ml avidin dissolved in PBS/0.2% BSA. Cells were then washed and incubated in PBS/0.2% BSA containing 1 mg/ml biocytin for 10 min before solubilization in buffer A (20 mM Tris, pH 7.5, 100 mM NaCl, 1 mM $MgCl_2$, 1% Triton X-100, and 0.1% SDS). Lysates were applied to ELISA plates coated with antitransferrin antibody (a gift from the Scottish Antibody Production Unit) and incubated overnight at 4°C. ELISA plates were washed 3× with buffer A and incubated with streptavidin-HRP for 1 h. Following washing, 200 µl HRP substrate, o-phenylenediamine (Sigma-Aldrich; 25 mg in 25 ml assay buffer: 51 mM sodium citrate and 27 mM sodium phosphate, pH 5.0, plus 10 µl H_2O_2) was added to each well. The reaction was terminated by addition of 50 µl of 2 M sulphuric acid. Absorbance at 492 nm was read on an ELISA plate reader. The total amount of internalized biotinylated transferrin was determined from samples that were not treated with avidin.

For internalization of fluorescently labeled transferrin, 1321N1 cells were transfected with either CLC^{WT}-GFP or CLC^{SallA}-GFP using PolyFect and serum starved as well as ATP depleted with 0.1 U/ml apyrase for 1 h. 5 µg/ml transferrin conjugated to Alexa Fluor 568 was added in the presence of 10 mM ADP for the indicated time points and chilled on ice, and then surface-bound transferrin was stripped with acid wash (2 × 5–min washes with 50 mM glycine, 100 mM NaCl, and 2 M urea, pH 3, interspersed with 5-min washes with PBS/0.2% BSA). Coverslips were mounted onto microscopy slides, and whole Z stacks were imaged with a DeltaVision/GE OMX optical microscope with a 60× 1.42 NA oil Plan Apochromat lens in widefield mode with a step size of 400 nm with subsequent deconvolution. Mean fluorescent intensity of internalized transferrin in transfected cells was measured in ImageJ by using the GFP signal as mask on maximum-intensity projections of Z stacks.

Online supplemental material

Fig. S1 shows cargo influences the properties of CCPs. Fig. S2 shows lifetime dynamics of CCPs. Fig. S3 shows dynamics of eps15, CALM, and epsin2 recruitment to CCP cohorts.

Acknowledgments

EM was performed at the University of Sheffield Faculty of Science EM facility. We thank Aurelien Roux and Vincent Mercier for advice on EM and Kai Erdmann and Jason King for comments on the manuscript.

This work was supported by Medical Research Council grant MR/J001546/1 to E. Smythe. The project has received funding from the European Union's Horizon 2020 research and innovation program under the Marie Skłodowska-Curie grant agreement 641639. Imaging work was performed at the Wolfson Light Microscopy Facility at the University of Sheffield using the Nikon A1 confocal/TIRF microscope (Wellcome Trust grant WT093134AIA) and Nikon stochastic optical reconstruction microscope (Medical Research Council SHIMA award MR/K015753/1).

The authors declare no competing financial interests.

Author contributions: E. Smythe and H. Maib devised the experiments; H. Maib, F. Ferreira, and S. Vassilopoulos performed the experiments; E. Smythe and H. Maib wrote the manuscript.

Submitted: 2 May 2018
Revised: 20 July 2018
Accepted: 7 September 2018

References

Aguet, F., C.N. Antonescu, M. Mettlen, S.L. Schmid, and G. Danuser. 2013. Advances in analysis of low signal-to-noise images link dynamin and AP2 to the functions of an endocytic checkpoint. *Dev. Cell.* 26:279–291. https://doi.org/10.1016/j.devcel.2013.06.019

Avinoam, O., M. Schorb, C.J. Beese, J.A. Briggs, and M. Kaksonen. 2015. Endocytic sites mature by continuous bending and remodeling of the clathrin coat. *Science.* 348:1369–1372. https://doi.org/10.1126/science.aaa9555

Benmerah, A., M. Bayrou, N. Cerf-Bensussan, and A. Dautry-Varsat. 1999. Inhibition of clathrin-coated pit assembly by an Eps15 mutant. *J. Cell Sci.* 112:1303–1311.

Bonazzi, M., L. Vasudevan, A. Mallet, M. Sachse, A. Sartori, M.C. Prevost, A. Roberts, S.B. Taner, J.D. Wilbur, F.M. Brodsky, and P. Cossart. 2011. Clathrin phosphorylation is required for actin recruitment at sites of bacterial adhesion and internalization. *J. Cell Biol.* 195:525–536. https://doi.org/10.1083/jcb.201105152

Boucrot, E., A. Pick, G. Çamdere, N. Liska, E. Evergren, H.T. McMahon, and M.M. Kozlov. 2012. Membrane fission is promoted by insertion of amphipathic helices and is restricted by crescent BAR domains. *Cell.* 149:124–136. https://doi.org/10.1016/j.cell.2012.01.047

Boulant, S., C. Kural, J.C. Zeeh, F. Ubelmann, and T. Kirchhausen. 2011. Actin dynamics counteract membrane tension during clathrin-mediated endocytosis. *Nat. Cell Biol.* 13:1124–1131. https://doi.org/10.1038/ncb2307

Brodsky, F.M. 2012. Diversity of clathrin function: new tricks for an old protein. *Annu. Rev. Cell Dev. Biol.* 28:309–336. https://doi.org/10.1146/annurev-cellbio-101011-155716

Bucher, D., F. Frey, K.A. Sochacki, S. Kummer, J.P. Bergeest, W.J. Godinez, H.G. Kräusslich, K. Rohr, J.W. Taraska, U.S. Schwarz, and S. Boulant. 2018. Clathrin-adaptor ratio and membrane tension regulate the flat-to-curved transition of the clathrin coat during endocytosis. *Nat. Commun.* 9:1109. https://doi.org/10.1038/s41467-018-03533-0

Chen, H., S. Fre, V.I. Slepnev, M.R. Capua, K. Takei, M.H. Butler, P.P. Di Fiore, and P. De Camilli. 1998. Epsin is an EH-domain-binding protein impli-

cated in clathrin-mediated endocytosis. *Nature.* 394:793–797. https://doi.org/10.1038/29555

Chen, P.H., N. Bendris, Y.J. Hsiao, C.R. Reis, M. Mettlen, H.Y. Chen, S.L. Yu, and S.L. Schmid. 2017. Crosstalk between CLCb/Dyn1-Mediated Adaptive Clathrin-Mediated Endocytosis and Epidermal Growth Factor Receptor Signaling Increases Metastasis. *Dev. Cell.* 40:278–288.

Copic, A., C.F. Latham, M.A. Horlbeck, J.G. D'Arcangelo, and E.A. Miller. 2012. ER cargo properties specify a requirement for COPII coat rigidity mediated by Sec13p. *Science.* 335:1359–1362. https://doi.org/10.1126/science.1215909

Dambournet, D., K.A. Sochacki, A.T. Cheng, M. Akamatsu, J.W. Taraska, D. Hockemeyer, and D.G. Drubin. 2018. Genome-edited human stem cells expressing fluorescently labeled endocytic markers allow quantitative analysis of clathrin-mediated endocytosis during differentiation. *J. Cell Biol.* 217:3301–3311. https://doi.org/10.1083/jcb.201710084

Dannhauser, P.N., and E.J. Ungewickell. 2012. Reconstitution of clathrin-coated bud and vesicle formation with minimal components. *Nat. Cell Biol.* 14:634–639. https://doi.org/10.1038/ncb2478

Dannhauser, P.N., M. Platen, H. Böning, H. Ungewickell, I.A. Schaap, and E.J. Ungewickell. 2015. Effect of clathrin light chains on the stiffness of clathrin lattices and membrane budding. *Traffic.* 16:519–533. https://doi.org/10.1111/tra.12263

den Otter, W.K., and W.J. Briels. 2011. The generation of curved clathrin coats from flat plaques. *Traffic.* 12:1407–1416. https://doi.org/10.1111/j.1600-0854.2011.01241.x

Ehrlich, M., W. Boll, A. Van Oijen, R. Hariharan, K. Chandran, M.L. Nibert, and T. Kirchhausen. 2004. Endocytosis by random initiation and stabilization of clathrin-coated pits. *Cell.* 118:591–605. https://doi.org/10.1016/j.cell.2004.08.017

Eichholtz, T., K. Jalink, I. Fahrenfort, and W.H. Moolenaar. 1993. The bioactive phospholipid lysophosphatidic acid is released from activated platelets. *Biochem. J.* 291:677–680. https://doi.org/10.1042/bj2910677

Eisenberg, E., and L.E. Greene. 2007. Multiple roles of auxilin and hsc70 in clathrin-mediated endocytosis. *Traffic.* 8:640–646. https://doi.org/10.1111/j.1600-0854.2007.00568.x

Ferreira, F., M. Foley, A. Cooke, M. Cunningham, G. Smith, R. Woolley, G. Henderson, E. Kelly, S. Mundell, and E. Smythe. 2012. Endocytosis of G protein-coupled receptors is regulated by clathrin light chain phosphorylation. *Curr. Biol.* 22:1361–1370. https://doi.org/10.1016/j.cub.2012.05.034

Greener, T., B. Grant, Y. Zhang, X. Wu, L.E. Greene, D. Hirsh, and E. Eisenberg. 2001. Caenorhabditis elegans auxilin: a J-domain protein essential for clathrin-mediated endocytosis in vivo. *Nat. Cell Biol.* 3:215–219. https://doi.org/10.1038/35055137

Grove, J., D.J. Metcalf, A.E. Knight, S.T. Wavre-Shapton, T. Sun, E.D. Protonotarios, L.D. Griffin, J. Lippincott-Schwartz, and M. Marsh. 2014. Flat clathrin lattices: stable features of the plasma membrane. *Mol. Biol. Cell.* 25:3581–3594. https://doi.org/10.1091/mbc.e14-06-1154

Hanyaloglu, A.C., and M. von Zastrow. 2008. Regulation of GPCRs by endocytic membrane trafficking and its potential implications. *Annu. Rev. Pharmacol. Toxicol.* 48:537–568. https://doi.org/10.1146/annurev.pharmtox.48.113006.094830

Henry, A.G., J.N. Hislop, J. Grove, K. Thorn, M. Marsh, and M. von Zastrow. 2012. Regulation of endocytic clathrin dynamics by cargo ubiquitination. *Dev. Cell.* 23:519–532. https://doi.org/10.1016/j.devcel.2012.08.003

Heuser, J. 2000. The production of 'cell cortices' for light and electron microscopy. *Traffic.* 1:545–552. https://doi.org/10.1034/j.1600-0854.2000.010704.x

Hinrichsen, L., J. Harborth, L. Andrees, K. Weber, and E.J. Ungewickell. 2003. Effect of clathrin heavy chain- and alpha-adaptin-specific small inhibitory RNAs on endocytic accessory proteins and receptor trafficking in HeLa cells. *J. Biol. Chem.* 278:45160–45170. https://doi.org/10.1074/jbc.M307290200

Hirst, J., D.A. Sahlender, S. Li, N.B. Lubben, G.H. Borner, and M.S. Robinson. 2008. Auxilin depletion causes self-assembly of clathrin into membraneless cages in vivo. *Traffic.* 9:1354–1371. https://doi.org/10.1111/j.1600-0854.2008.00764.x

Holkar, S.S., S.C. Kamerkar, and T.J. Pucadyil. 2015. Spatial Control of Epsin-induced Clathrin Assembly by Membrane Curvature. *J. Biol. Chem.* 290:14267–14276. https://doi.org/10.1074/jbc.M115.653394

Hopkins, C.R., and I.S. Trowbridge. 1983. Internalization and processing of transferrin and the transferrin receptor in human carcinoma A431 cells. *J. Cell Biol.* 97:508–521. https://doi.org/10.1083/jcb.97.2.508

Huang, F., A. Khvorova, W. Marshall, and A. Sorkin. 2004. Analysis of clathrin-mediated endocytosis of epidermal growth factor receptor by RNA interference. *J. Biol. Chem.* 279:16657–16661. https://doi.org/10.1074/jbc.C400046200

Irannejad, R., and M. von Zastrow. 2014. GPCR signaling along the endocytic pathway. *Curr. Opin. Cell Biol.* 27:109–116. https://doi.org/10.1016/j.ceb.2013.10.003

Kaksonen, M., and A. Roux. 2018. Mechanisms of clathrin-mediated endocytosis. *Nat. Rev. Mol. Cell Biol.* 19:313–326. https://doi.org/10.1038/nrm.2017.132

Kanaseki, T., and K. Kadota. 1969. The "vesicle in a basket". A morphological study of the coated vesicle isolated from the nerve endings of the guinea pig brain, with special reference to the mechanism of membrane movements. *J. Cell Biol.* 42:202–220. https://doi.org/10.1083/jcb.42.1.202

Kelly, E., C.P. Bailey, and G. Henderson. 2008. Agonist-selective mechanisms of GPCR desensitization. *Br. J. Pharmacol.* 153(S1, Suppl 1):S379–S388. https://doi.org/10.1038/sj.bjp.0707604

Keyel, P.A., S.K. Mishra, R. Roth, J.E. Heuser, S.C. Watkins, and L.M. Traub. 2006. A single common portal for clathrin-mediated endocytosis of distinct cargo governed by cargo-selective adaptors. *Mol. Biol. Cell.* 17:4300–4317. https://doi.org/10.1091/mbc.e06-05-0421

Kirchhausen, T., and S.C. Harrison. 1981. Protein organization in clathrin trimers. *Cell.* 23:755–761. https://doi.org/10.1016/0092-8674(81)90439-6

Kirchhausen, T., D. Owen, and S.C. Harrison. 2014. Molecular structure, function, and dynamics of clathrin-mediated membrane traffic. *Cold Spring Harb. Perspect. Biol.* 6:a016725. https://doi.org/10.1101/cshperspect.a016725

Lampe, M., F. Pierre, S. Al-Sabah, C. Krasel, and C.J. Merrifield. 2014. Dual single-scission event analysis of constitutive transferrin receptor (TfR) endocytosis and ligand-triggered β2-adrenergic receptor (β2AR) or Mu-opioid receptor (MOR) endocytosis. *Mol. Biol. Cell.* 25:3070–3080. https://doi.org/10.1091/mbc.e14-06-1112

Lampe, M., S. Vassilopoulos, and C. Merrifield. 2016. Clathrin coated pits, plaques and adhesion. *J. Struct. Biol.* 196:48–56. https://doi.org/10.1016/j.jsb.2016.07.009

Lee, D.W., X. Wu, E. Eisenberg, and L.E. Greene. 2006. Recruitment dynamics of GAK and auxilin to clathrin-coated pits during endocytosis. *J. Cell Sci.* 119:3502–3512. https://doi.org/10.1242/jcs.03092

Leyton-Puig, D., T. Isogai, E. Argenzio, B. van den Broek, J. Klarenbeek, H. Janssen, K. Jalink, and M. Innocenti. 2017. Flat clathrin lattices are dynamic actin-controlled hubs for clathrin-mediated endocytosis and signalling of specific receptors. *Nat. Commun.* 8:16068. https://doi.org/10.1038/ncomms16068

Loerke, D., M. Mettlen, D. Yarar, K. Jaqaman, H. Jaqaman, G. Danuser, and S.L. Schmid. 2009. Cargo and dynamin regulate clathrin-coated pit maturation. *PLoS Biol.* 7:e1000057. https://doi.org/10.1371/journal.pbio.1000057

Loerke, D., M. Mettlen, S.L. Schmid, and G. Danuser. 2011. Measuring the hierarchy of molecular events during clathrin-mediated endocytosis. *Traffic.* 12:815–825. https://doi.org/10.1111/j.1600-0854.2011.01197.x

Ma, L., P.K. Umasankar, A.G. Wrobel, A. Lymar, A.J. McCoy, S.S. Holkar, A. Jha, T. Pradhan-Sundd, S.C. Watkins, D.J. Owen, and L.M. Traub. 2016. Transient Fcho1/2·Eps15/R·AP-2 Nanoclusters Prime the AP-2 Clathrin Adaptor for Cargo Binding. *Dev. Cell.* 37:428–443. https://doi.org/10.1016/j.devcel.2016.05.003

Maib, H., E. Smythe, and K. Ayscough. 2017. Forty years on: clathrin-coated pits continue to fascinate. *Mol. Biol. Cell.* 28:843–847. https://doi.org/10.1091/mbc.e16-04-0213

McMahon, H.T., and E. Boucrot. 2011. Molecular mechanism and physiological functions of clathrin-mediated endocytosis. *Nat. Rev. Mol. Cell Biol.* 12:517–533. https://doi.org/10.1038/nrm3151

Merrifield, C.J., M.E. Feldman, L. Wan, and W. Almers. 2002. Imaging actin and dynamin recruitment during invagination of single clathrin-coated pits. *Nat. Cell Biol.* 4:691–698. https://doi.org/10.1038/ncb837

Messa, M., R. Fernández-Busnadiego, E.W. Sun, H. Chen, H. Czapla, K. Wrasman, Y. Wu, G. Ko, T. Ross, B. Wendland, and P. De Camilli. 2014. Epsin deficiency impairs endocytosis by stalling the actin-dependent invagination of endocytic clathrin-coated pits. *eLife.* 3:e03311. https://doi.org/10.7554/eLife.03311

Mettlen, M., M. Stoeber, D. Loerke, C.N. Antonescu, G. Danuser, and S.L. Schmid. 2009. Endocytic accessory proteins are functionally distinguished by their differential effects on the maturation of clathrin-coated pits. *Mol. Biol. Cell.* 20:3251–3260. https://doi.org/10.1091/mbc.e09-03-0256

Mettlen, M., P.H. Chen, S. Srinivasan, G. Danuser, and S.L. Schmid. 2018. Regulation of Clathrin-Mediated Endocytosis. *Annu. Rev. Biochem.* 87:871–896. https://doi.org/10.1146/annurev-biochem-062917-012644

Meyerholz, A., L. Hinrichsen, S. Groos, P.C. Esk, G. Brandes, and E.J. Ungewickell. 2005. Effect of clathrin assembly lymphoid myeloid leukemia protein depletion on clathrin coat formation. *Traffic.* 6:1225–1234. https://doi.org/10.1111/j.1600-0854.2005.00355.x

Miller, S.E., S. Mathiasen, N.A. Bright, F. Pierre, B.T. Kelly, N. Kladt, A. Schauss, C.J. Merrifield, D. Stamou, S. Höning, and D.J. Owen. 2015. CALM regulates clathrin-coated vesicle size and maturation by directly sensing and driving membrane curvature. *Dev. Cell.* 33:163–175. https://doi.org/10.1016/j.devcel.2015.03.002

Mundell, S.J., J. Luo, J.L. Benovic, P.B. Conley, and A.W. Poole. 2006. Distinct clathrin-coated pits sort different G protein-coupled receptor cargo. *Traffic.* 7:1420–1431. https://doi.org/10.1111/j.1600-0854.2006.00469.x

Newmyer, S.L., A. Christensen, and S. Sever. 2003. Auxilin-dynamin interactions link the uncoating ATPase chaperone machinery with vesicle formation. *Dev. Cell.* 4:929–940. https://doi.org/10.1016/S1534-5807(03)00157-6

Rizk, A., G. Paul, P. Incardona, M. Bugarski, M. Mansouri, A. Niemann, U. Ziegler, P. Berger, and I.F. Sbalzarini. 2014. Segmentation and quantification of subcellular structures in fluorescence microscopy images using Squassh. *Nat. Protoc.* 9:586–596. https://doi.org/10.1038/nprot.2014.037

Sahlender, D.A., P. Kozik, S.E. Miller, A.A. Peden, and M.S. Robinson. 2013. Uncoupling the functions of CALM in VAMP sorting and clathrin-coated pit formation. *PLoS One.* 8:e64514. https://doi.org/10.1371/journal.pone.0064514

Saleem, M., S. Morlot, A. Hohendahl, J. Manzi, M. Lenz, and A. Roux. 2015. A balance between membrane elasticity and polymerization energy sets the shape of spherical clathrin coats. *Nat. Commun.* 6:6249. https://doi.org/10.1038/ncomms7249

Schmid, S.L., A.K. Matsumoto, and J.E. Rothman. 1982. A domain of clathrin that forms coats. *Proc. Natl. Acad. Sci. USA.* 79:91–95. https://doi.org/10.1073/pnas.79.1.91

Schmid, S.L., W.A. Braell, D.M. Schlossman, and J.E. Rothman. 1984. A role for clathrin light chains in the recognition of clathrin cages by 'uncoating ATPase'. *Nature.* 311:228–231. https://doi.org/10.1038/311228a0

Scott, B.L., K.A. Sochacki, S.T. Low-Nam, E.M. Bailey, Q. Luu, A. Hor, A.M. Dickey, S. Smith, J.G. Kerkvliet, J.W. Taraska, and A.D. Hoppe. 2018. Membrane bending occurs at all stages of clathrin-coat assembly and defines endocytic dynamics. *Nat. Commun.* 9:419. https://doi.org/10.1038/s41467-018-02818-8

Smythe, E., M. Pypaert, J. Lucocq, and G. Warren. 1989. Formation of coated vesicles from coated pits in broken A431 cells. *J. Cell Biol.* 108:843–853. https://doi.org/10.1083/jcb.108.3.843

Smythe, E., L.L. Carter, and S.L. Schmid. 1992. Cytosol- and clathrin-dependent stimulation of endocytosis in vitro by purified adaptors. *J. Cell Biol.* 119:1163–1171. https://doi.org/10.1083/jcb.119.5.1163

Smythe, E., P.D. Smith, S.M. Jacob, J. Theobald, and S.E. Moss. 1994. Endocytosis occurs independently of annexin VI in human A431 cells. *J. Cell Biol.* 124:301–306. https://doi.org/10.1083/jcb.124.3.301

Soohoo, A.L., and M.A. Puthenveedu. 2013. Divergent modes for cargo-mediated control of clathrin-coated pit dynamics. *Mol. Biol. Cell.* 24:1725–1734.

Sorokin, A., K.F. Heil, J.D. Armstrong, and O. Sorokina. 2018. Rule-based modelling provides an extendable framework for comparing candidate mechanisms underpinning clathrin polymerisation. *Sci. Rep.* 8:5658. https://doi.org/10.1038/s41598-018-23829-x

Stachowiak, J.C., F.M. Brodsky, and E.A. Miller. 2013. A cost-benefit analysis of the physical mechanisms of membrane curvature. *Nat. Cell Biol.* 15:1019–1027. https://doi.org/10.1038/ncb2832

Taylor, M.J., D. Perrais, and C.J. Merrifield. 2011. A high precision survey of the molecular dynamics of mammalian clathrin-mediated endocytosis. *PLoS Biol.* 9:e1000604. https://doi.org/10.1371/journal.pbio.1000604

Taylor, M.J., M. Lampe, and C.J. Merrifield. 2012. A feedback loop between dynamin and actin recruitment during clathrin-mediated endocytosis. *PLoS Biol.* 10:e1001302. https://doi.org/10.1371/journal.pbio.1001302

Tebar, F., S.K. Bohlander, and A. Sorkin. 1999. Clathrin assembly lymphoid myeloid leukemia (CALM) protein: localization in endocytic-coated pits, interactions with clathrin, and the impact of overexpression on clathrin-mediated traffic. *Mol. Biol. Cell.* 10:2687–2702. https://doi.org/10.1091/mbc.10.8.2687

Ungewickell, E. 1983. Biochemical and immunological studies on clathrin light chains and their binding sites on clathrin triskelions. *EMBO J.* 2:1401–1408. https://doi.org/10.1002/j.1460-2075.1983.tb01598.x

Ungewickell, E., H. Ungewickell, S.E. Holstein, R. Lindner, K. Prasad, W. Barouch, B. Martin, L.E. Greene, and E. Eisenberg. 1995. Role of auxilin in uncoating clathrin-coated vesicles. *Nature.* 378:632–635. https://doi.org/10.1038/378632a0

Watts, C. 1985. Rapid endocytosis of the transferrin receptor in the absence of bound transferrin. *J. Cell Biol.* 100:633–637. https://doi.org/10.1083/jcb.100.2.633

Wilbur, J.D., P.K. Hwang, J.A. Ybe, M. Lane, B.D. Sellers, M.P. Jacobson, R.J. Fletterick, and F.M. Brodsky. 2010. Conformation switching of clathrin light chain regulates clathrin lattice assembly. *Dev. Cell.* 18:854–861. https://doi.org/10.1016/j.devcel.2010.04.007

Wu, S., S.R. Majeed, T.M. Evans, M.D. Camus, N.M. Wong, Y. Schollmeier, M. Park, J.R. Muppidi, A. Reboldi, P. Parham, et al. 2016. Clathrin light chains' role in selective endocytosis influences antibody isotype switching. *Proc. Natl. Acad. Sci. USA.* 113:9816–9821. https://doi.org/10.1073/pnas.1611189113

Wu, X., X. Zhao, L. Baylor, S. Kaushal, E. Eisenberg, and L.E. Greene. 2001. Clathrin exchange during clathrin-mediated endocytosis. *J. Cell Biol.* 155:291–300. https://doi.org/10.1083/jcb.200104085

Ybe, J.A., B. Greene, S.H. Liu, U. Pley, P. Parham, and F.M. Brodsky. 1998. Clathrin self-assembly is regulated by three light-chain residues controlling the formation of critical salt bridges. *EMBO J.* 17:1297–1303. https://doi.org/10.1093/emboj/17.5.1297

Ybe, J.A., S. Perez-Miller, Q. Niu, D.A. Coates, M.W. Drazer, and M.E. Clegg. 2007. Light chain C-terminal region reinforces the stability of clathrin heavy chain trimers. *Traffic.* 8:1101–1110. https://doi.org/10.1111/j.1600-0854.2007.00597.x

Yim, Y.I., S. Scarselletta, F. Zang, X. Wu, D.W. Lee, Y.S. Kang, E. Eisenberg, and L.E. Greene. 2005. Exchange of clathrin, AP2 and epsin on clathrin-coated pits in permeabilized tissue culture cells. *J. Cell Sci.* 118:2405–2413. https://doi.org/10.1242/jcs.02356

Yim, Y.I., T. Sun, L.G. Wu, A. Raimondi, P. De Camilli, E. Eisenberg, and L.E. Greene. 2010. Endocytosis and clathrin-uncoating defects at synapses of auxilin knockout mice. *Proc. Natl. Acad. Sci. USA.* 107:4412–4417. https://doi.org/10.1073/pnas.1000738107

Young, A., S. Stoilova-McPhie, A. Rothnie, Y. Vallis, P. Harvey-Smith, N. Ranson, H. Kent, F.M. Brodsky, B.M. Pearse, A. Roseman, and C.J. Smith. 2013. Hsc70-induced changes in clathrin-auxilin cage structure suggest a role for clathrin light chains in cage disassembly. *Traffic.* 14:987–996. https://doi.org/10.1111/tra.12085

Zhang, C.X., A.E. Engqvist-Goldstein, S. Carreno, D.J. Owen, E. Smythe, and D.G. Drubin. 2005. Multiple roles for cyclin G-associated kinase in clathrin-mediated sorting events. *Traffic.* 6:1103–1113. https://doi.org/10.1111/j.1600-0854.2005.00346.x

Supplemental material

Maib et al., https://doi.org/10.1083/jcb.201805005

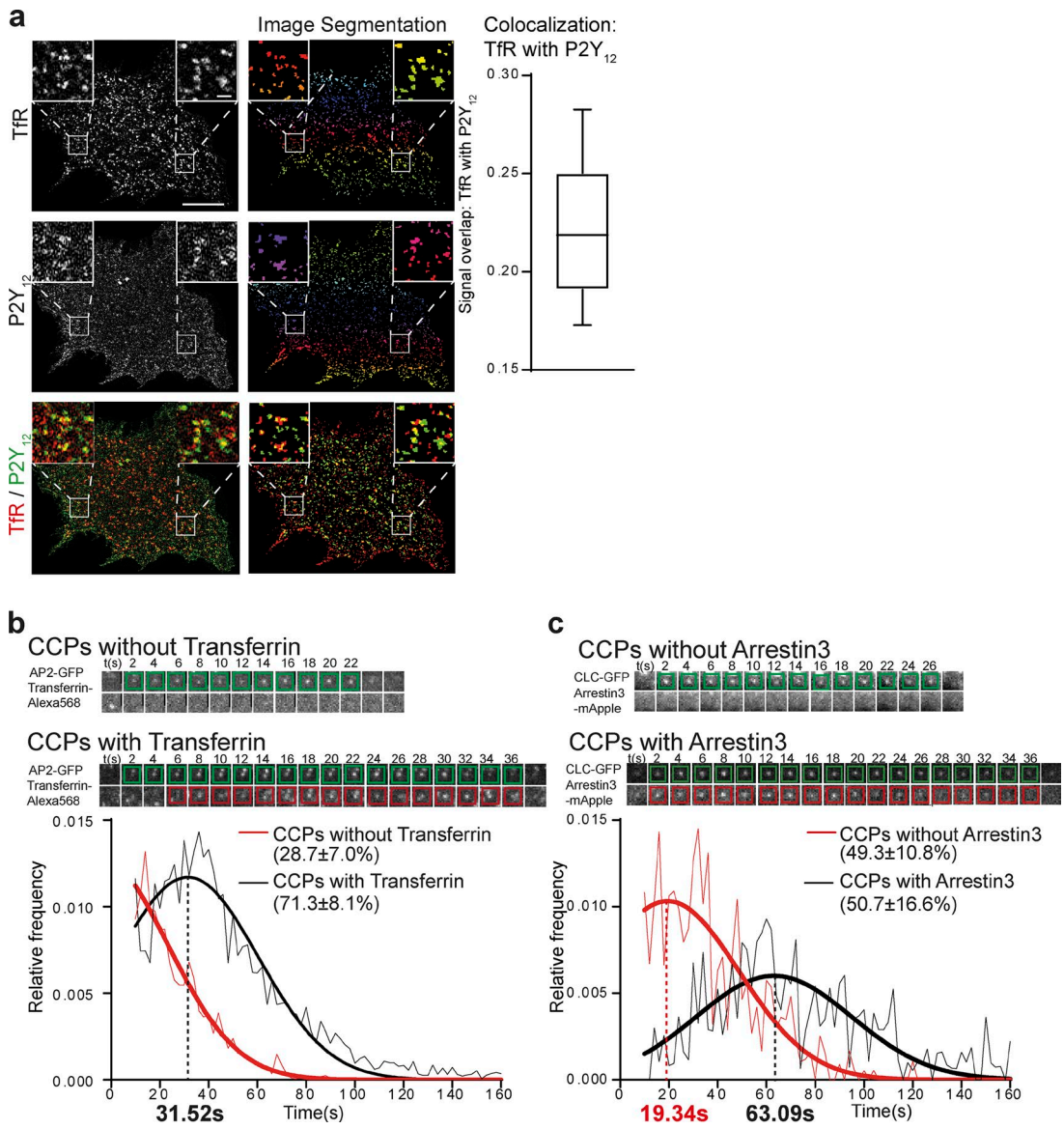

Figure S1. **Cargo packing influences the properties of CCPs. (a)** Colocalization at the plasma membrane of $P2Y_{12}$ with TfR after 3 min ligand stimulation. Images were quantified using the image segmentation tool SQUASSH. *n* = 22 cells. Box and whiskers plot with 25th to 75th percentiles and range. Bars: 10 µm (main images); 1 µm (insets). **(b)** 1321N1 cells were transfected with AP2-GFP, and the lifetime of CCPs was determined in the presence of Alexa Fluor 568–labeled transferrin and binned for traces with and without detection of transferrin using cmeAnalysis script (Aguet et al., 2013). *n* = 18,700 traces from 32 cells from three independent repeats. Mean lifetime of CCPs was determined by Gaussian fits. The dataset was reused in Fig. S2 a (left). **(c)** 1321N1 cells were transfected with $CLCb^{WT}$-GFP together with arrestin3-mApple, and the lifetime of CCPs was determined and binned for traces with and without detection of arrestin3 directly after 10 mM ADP stimulation. *n* = 3,040 traces from 18 cells from three independent experiments. Mean lifetime of CCPs was determined by Gaussian fits. The dataset was reused in Fig. S2 c (left).

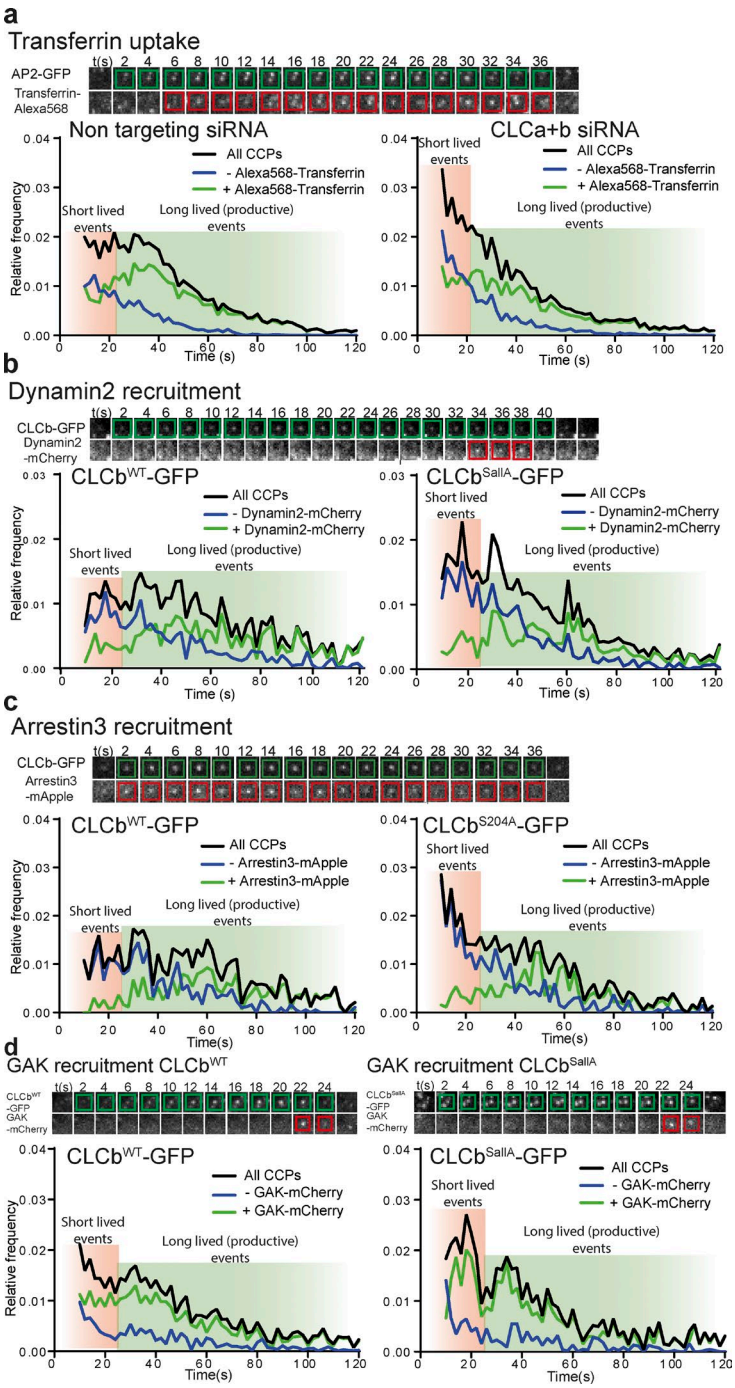

Figure S2. **Lifetime dynamics of CCPs. (a)** 1321N1 cells stably expressing HA-tagged $P2Y_{12}$ receptor were treated either with NT control siRNA or siRNA targeting both CLCa and CLCb and then transfected with AP2-GFP, and the lifetime of CCPs was determined in the presence of Alexa Fluor 568–transferrin and binned for traces with (+Alexa-568transferrin, NT siRNA = 71.3 ± 8.1%; CLCa+b siRNA = 65.1 ± 6.6%) and without (−Alexa568-transferrin, NT siRNA = 28.7 ± 7%; CLCa+b siRNA = 34.9 ± 6.8%) detection of transferrin using cmeAnalysis script (Aguet et al., 2013). *n* > 18,700–25,139 traces from 32 cells each from three independent experiments. The left panel reuses the dataset from Fig. S1 c. **(b)** HeLa cells stably expressing either $CLCb^{WT}$-GFP or $CLCb^{SallA}$-GFP were transfected with dynamin2-mCherry, and the lifetime of CCPs was measured and binned for traces with (+dynamin2-mCherry, $CLCb^{WT}$-GFP = 59.9 ± 11.7%; $CLCb^{SallA}$-GFP = 47.9 ± 13.5%) and without (−dynamin2-mCherry, $CLCb^{WT}$-GFP = 40.1 ± 9.7%; $CLCb^{SallA}$-GFP = 52.1 ± 9.5%) detection of dynamin2. *n* = 6,721–8,050 traces from 21 cells each from three independent experiments. **(c)** 1321N1 cells were transfected with either $CLCb^{WT}$-GFP or $CLCb^{S204A}$-GFP together with arrestin3-mApple, and the lifetime of CCPs was determined and binned for traces with (+arrestin3-mApple, $CLCb^{WT}$-GFP = 50.7 ± 16.6%; $CLCb^{S204A}$-GFP = 44.8 ± 14.6%) and without (−arrestin3-mApple, $CLCb^{WT}$-GFP = 49.3 ± 10.8%; $CLCb^{S204A}$-GFP = 55.2 ± 14.6%) detection of arrestin3 directly after 10 mM ADP stimulation. *n* = 3,040–3,069 traces from 18–24 cells from three independent experiments. The left panel reuses the dataset from Fig. S1 d. **(d)** HeLa cells expressing either $CLCb^{WT}$-GFP or $CLCb^{SallA}$-GFP were transfected with GAK-mCherry and imaged by TIRF microscopy, and detection of productive CCPs and GAK recruitment was determined using cmeAnalysis script (Aguet et al., 2013). Lifetime of CCPs was binned for traces with (+GAK-mCherry, $CLCb^{WT}$-GFP = 74.6 ± 12.9%; $CLCb^{SallA}$-GFP = 76.5 ± 12.9%) and without (−GAK-mCherry, $CLCb^{WT}$-GFP = 25.4 ± 8.3%; $CLCb^{SallA}$-GFP = 23.5 ± 7.9%) detection of GAK. *n* = 5,438–8,379 traces from 20–27 cells from three independent experiments.

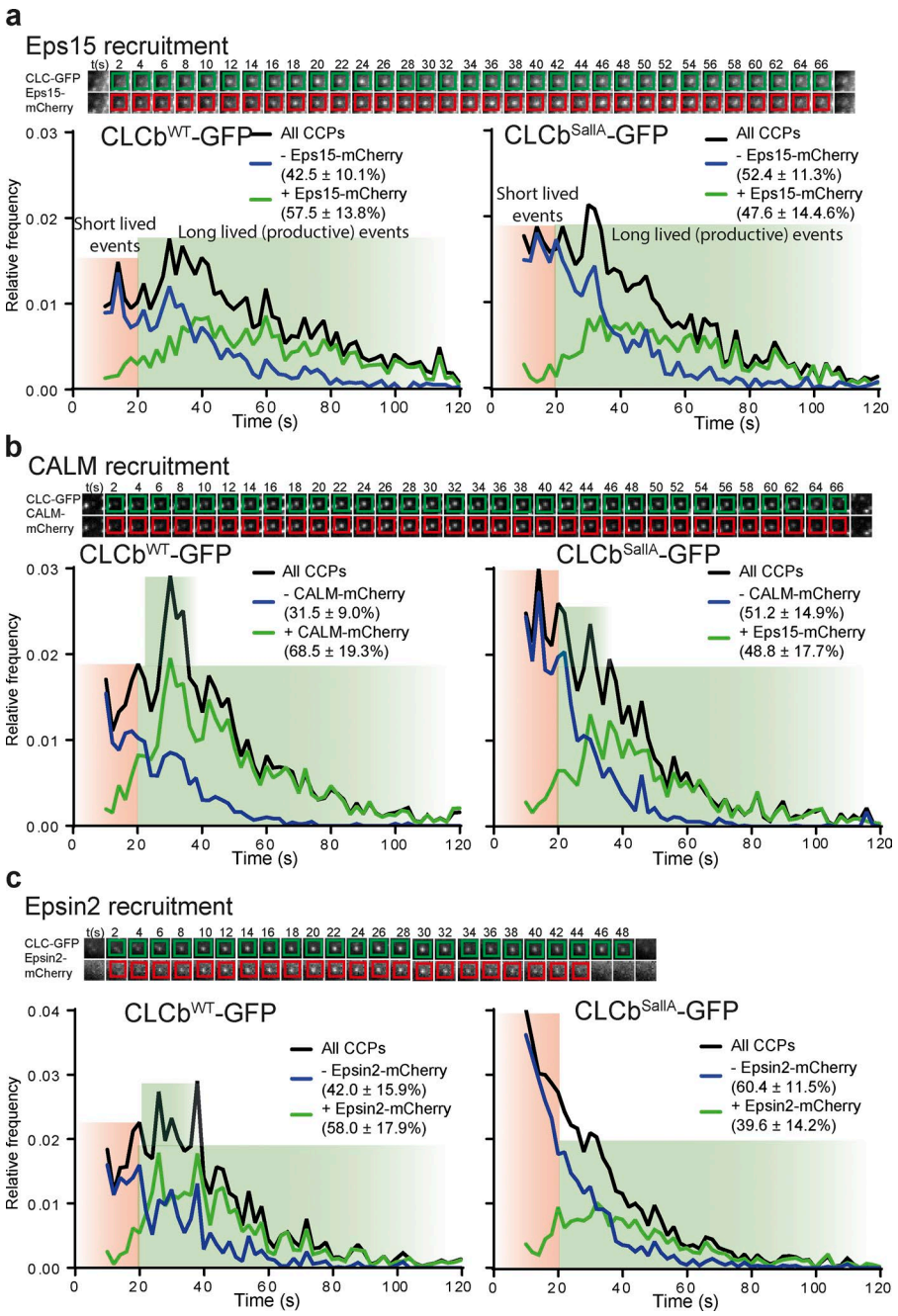

Figure S3. **Dynamics of eps15, CALM, and epsin2 recruitment to CCP cohorts. (a)** HeLa cells stably expressing either CLCb^{WT}-GFP or CLCb^{SallA}-GFP were transfected with eps15-mCherry, and the lifetime of CCPs was measured and binned for traces with (+eps15-mCherry) and without (−eps15-mCherry) detection of eps15. *n* = 9,397–11,848 traces from 31–34 cells from three independent experiments. **(b)** HeLa cells stably expressing either CLCb^{WT}-GFP or CLCb^{SallA}-GFP were transfected with CALM-mCherry, and the lifetime of CCPs was measured and binned for traces with (+CALM-mCherry) and without (−CALM-mCherry) detection of CALM. *n* = 7,211–8,605 traces from 29–31 cells from three independent experiments. **(c)** HeLa cells stably expressing either CLCb^{WT}-GFP or CLCb^{SallA}-GFP were transfected with epsin2-mCherry, and the lifetime of CCPs were measured and binned for traces with (+epsin2-mCherry) and without (−epsin2-mCherry) detection of epsin2. *n* = 5,656–7,351 traces from 22–24 cells from three independent experiments. Percentages refer to the traces in each binned cohort. Lifetimes were measured using cmeAnalysis script (Aguet et al., 2013).

Reference

Aguet, F., C.N. Antonescu, M. Mettlen, S.L. Schmid, and G. Danuser. 2013. Advances in analysis of low signal-to-noise images link dynamin and AP2 to the functions of an endocytic checkpoint. *Dev. Cell.* 26:279–291. https://doi.org/10.1016/j.devcel.2013.06.019

4 PHYSICAL PROPERTIES OF CCPS MIGHT INFLUENCE CLC DEPENDENCY

As discussed in the manuscript, the physical properties of the plasma membrane might be a major factor that influences the mode of curvature generation of CCPs. Additionally, the mechanisms by which the CLCs control clathrin exchange is still not known. Therefore, this experimental chapter will focus on attempts to investigate the effects of changing the physical properties of the plasma membrane on CME, as well as the addressing the molecular mechanism by which the CLCs control clathrin exchange. Finally, attempts to measure the physical properties of CCPs by atomic force microscopy will be presented.

4.1 LOW TEMPERATURES BUT NOT HYPOTONIC MEDIA MAKES TRANSFERRIN UPTAKE SENSITIVE TO CLCB PHOSPHORYLATION

One of the hypotheses that emerged from the results of our published work is that different cargo compositions might alter the physical properties of CCPs and lead to the formation of flat clathrin lattices. Since efficient clathrin exchange and therefore curvature generation from flat lattices seemed to be dependent on the capacity of CLCb to be phosphorylated, we asked whether changes to the physical properties of the plasma membrane might also make uptake of TfR sensitive to CLCb phosphorylation. As shown in the article, at 37˚C and in the absences of other cargo proteins, uptake, of TfR is not dependent on CLCb phosphorylation.

Hypotonic media has often been used in published studies to induce swelling of cells; this increases their surface area and is therefore argued to increase membrane tension (Bucher *et al.*, 2018). HeLa cells, overexpressing either CLCb-WT or CLCb-SallA were pre-incubated with serum free media diluted with 50% ddH2O for 10min. The uptake of biotinylated Transferrin was then measured over 2, 5, 10 and 20 min in the presence of diluted media at 37˚C (Fig 4.1a). No noticeable difference in the uptake of biotinylated Tf was observed for cells expressing either CLCb-WT or CLCb-SallA.

In a previous study by Ferreira et al. a slight decrease in the kinetics of Tf uptake was observed in HeLa cells overexpressing CLCb-SallA at 31˚C. Additionally, work by Dannhauser demonstrated that the CLCs are required for the deformation of *in vitro* membranes at low temperatures (Dannhauser *et al.*, 2015). Low temperatures increase the bending rigidity of the plasma membrane and we therefore wondered whether CLCb phosphorylation would be required for the uptake of Tf at lower temperatures. To test this, we repeated the experiments of Tf uptake in serum free media at 25˚C and 19˚C in cells overexpressing CLCb-WT or CLCb-SallA. At 25˚C there is a slight delay in Tf uptake in CLCb-

SallA expressing cells after 2 and 5min, but no difference after 10 or 20min (Fig 4.1b). This data indicates that there is an initial lag time in Tf uptake that "catches up" after longer timepoints. When measured at 19˚C, there is no difference in the initial rate of Tf uptake after 2 and 5min but a decrease after 10 and 20min (Fig 4.1c). Therefore, while at 25˚C the initial rate of Tf uptake is decreased but is compensated after longer timepoints, at 19˚C the difference is only apparent after longer timepoints and might need longer to reach the same level of receptor uptake. These differences in the kinetics at lower temperatures support the notion that CLCb phosphorylation is required for efficient ligand uptake under conditions of increased membrane rigidity.

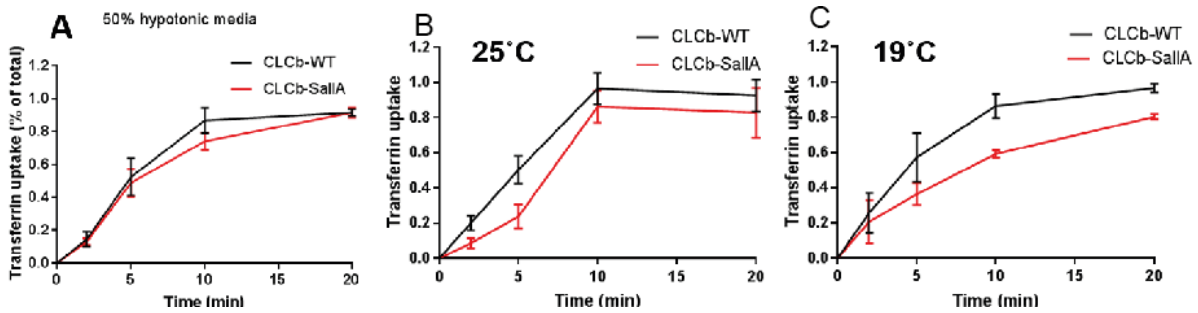

Figure 4.1 Low temperatures effect Transferrin uptake in HeLa cells overexpressing CLCb-SallA: Uptake of biotinylated Transferrin in HeLa cells overexpressing either CLCb-WT or CLCb-SallA was measured using an ELISA assay. **A)** Uptake was measured in the presence of serum free media diluted with 50% ddH_2O or in the presence of serum free media at 25˚C **(B)** or 19˚C **(C)**. n=3 independent repeats, error bars ± SEM

4.2 TRANSFERRIN UPTAKE AT LOW TEMPERATURES DOES NOT REQUIRE AUXILIN

The effect of lower temperature on the rate of Tf uptake in the background of phosphorylation deficient CLCb, suggests that there might be a dependence on clathrin exchange and lattice rearrangements for CME to occur under these conditions. Auxilin is one of the key proteins that regulate this process and should therefore also be required for efficient Tf uptake at low temperatures. To test this, we depleted 1321N1 cells of Auxilin as described before and measured Tf uptake at 19˚C (Fig. 4.2b). No difference in the rate of Tf uptake could be observed in 1321N1 cells depleted of Auxilin at either 37˚C or 19˚C. Therefore, Auxilin does not seem to be required for the efficient uptake of Tf at low temperatures. However, in 1321N1 cells GAK is expressed at similar levels to auxilin and might be able to compensate for its loss.

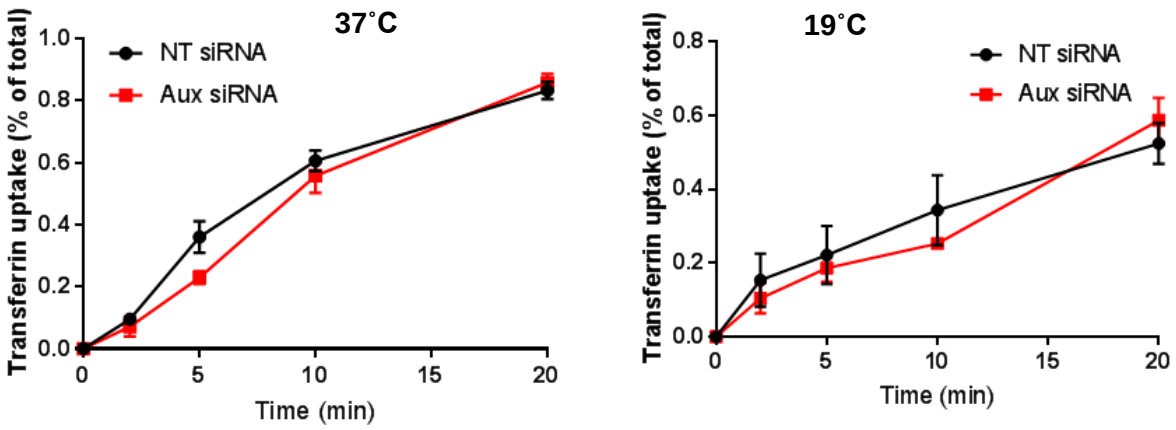

Figure 4.2 Auxilin is not required for Transferrin uptake at low temperatures: Uptake of biotinylated Transferrin was measured using an ELISA assays in 1321N1 cells treated with siRNA against Auxilin or non-Targeting control in Serum free media at 37˚C (left) or 19˚C (right). n=3 independent repeats, error bars ± SEM

4.3 THE PRESENCE OF EGF DOES NOT AFFECT EFFICIENT TRANSFERRIN UPTAKE

In our published work (Maib *et al.*, 2018), we were able to show that presence of a wide array of ligands in media containing full serum (with 10% FBS) leads to a decreased rate of Transferrin uptake in the background of cells overexpressing CLCb-SallA (Fig 4.3 a). We therefore wanted to investigate what ligands might be responsible for this phenotype and tested the effect of EGF on the rate of Tf uptake in HeLa cells overexpressing either CLCb-WT or CLCb-SallA (Fig. 4.3 B). EGF was added to serum free media at a concentration of 10ng/ml, which was shown to lead to uptake through CME. Under these conditions, no change in the rate of Tf uptake was observed in cells overexpressing CLCb-SallA compared to those expressing CLCb-WT. Therefore the presence of EGF does not seem to influence the uptake of Tf.

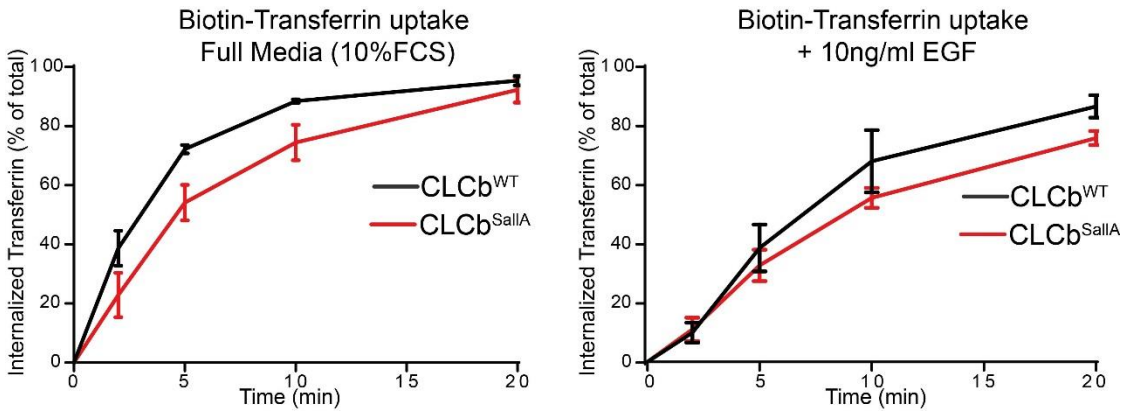

Figure 4.3 Full growth media but not EGF effects rate of transferrin uptake in CLCb-SallA expressing cells: Uptake of biotinylated Transferrin in HeLa cells overexpressing either CLCb-WT or CLCb-SallA was measured using an ELISA assay in the presence of full growth media containing 10% FBS (left) or serum free media supplemented with 10ng/ml EGF (right). n=3 independent repeats, error bars ± SEM

4.4 BURSTS OF GAK RECRUITMENT CAN BE DETECTED THROUGHOUT THE MATURATION OF *BONA FIDE* CCPS

One of the predictions of the published results is that GAK (or auxilin) is recruited at early stages throughout CCP maturation to mediate clathrin exchange and lattice rearrangements. To test for this, we reanalysed the lifetime data of GAK recruitment to CCPs and focused on the fluorescent intensity traces of GAK recruitment to *bona fide* CCPs. HeLa cells overexpressing CLCb-WT-GFP were transfected with GAK-mCherry, imaged by life cell TIRF microscopy and the traces were analysed using the MATLAB script cmeAnalysis as previously described.

When binned into three different lifetime cohorts of 20-40s, 40-60s and 60-80s, the fluorescent intensity traces of CLC-GFP are well in line with published data, showing an initial growth phase, followed by a plateau and terminating in the sudden disappearance from the TIRF field. Intriguingly, the fluorescent intensity traces of GAK-mCherry differ between the different lifetime cohorts, while it seems to be present at early stages in 20-40s cohort, it is mainly recruited at bursts at the end of the CLC traces in the 40-60s and 60-80s cohorts. However, in these longer lived cohorts, transient peaks of GAK recruitment can be detected throughout their lifetime (Fig 4.4 a). This becomes more apparent when single traces of GAK recruitment are observed. In one example trace, GAK is recruited in transient bursts through the lifetime of a single CCP, starting 28s after CCP initiation, before terminating in a strong burst of recruitment, just prior to scission (Fig 4.4 b and c). Importantly, Scott et al were able to demonstrate that generation of curvature of CCPs, along the constant area pathway, starts with a lag time of several seconds in which the clathrin assembles as a flat lattice. It is therefore

possible, that the transient peaks of GAK recruitment, starting after 28s, represent the curvature generation and lattice rearrangements of the CCP.

These transient peaks throughout CCP maturation have not been reported thus far. The interaction of GAK with the clathrin lattice during rearrangement is likely to be very transient and short lived and therefore difficult to detect. To reduce phototoxic effects, the cells were imaged at 0.5Hz with an acquisition time of 50-100ms, therefore these transient interactions are easily lost. The strong burst of GAK recruitment just prior to the disappearance of the CCP from the TIRF field is in agreement with previously published studies. This is similar to the recruitment of dynamin2 which is also present at early stages of coat maturation with a strong burst just prior to scission (Sochacki et al. 2017).

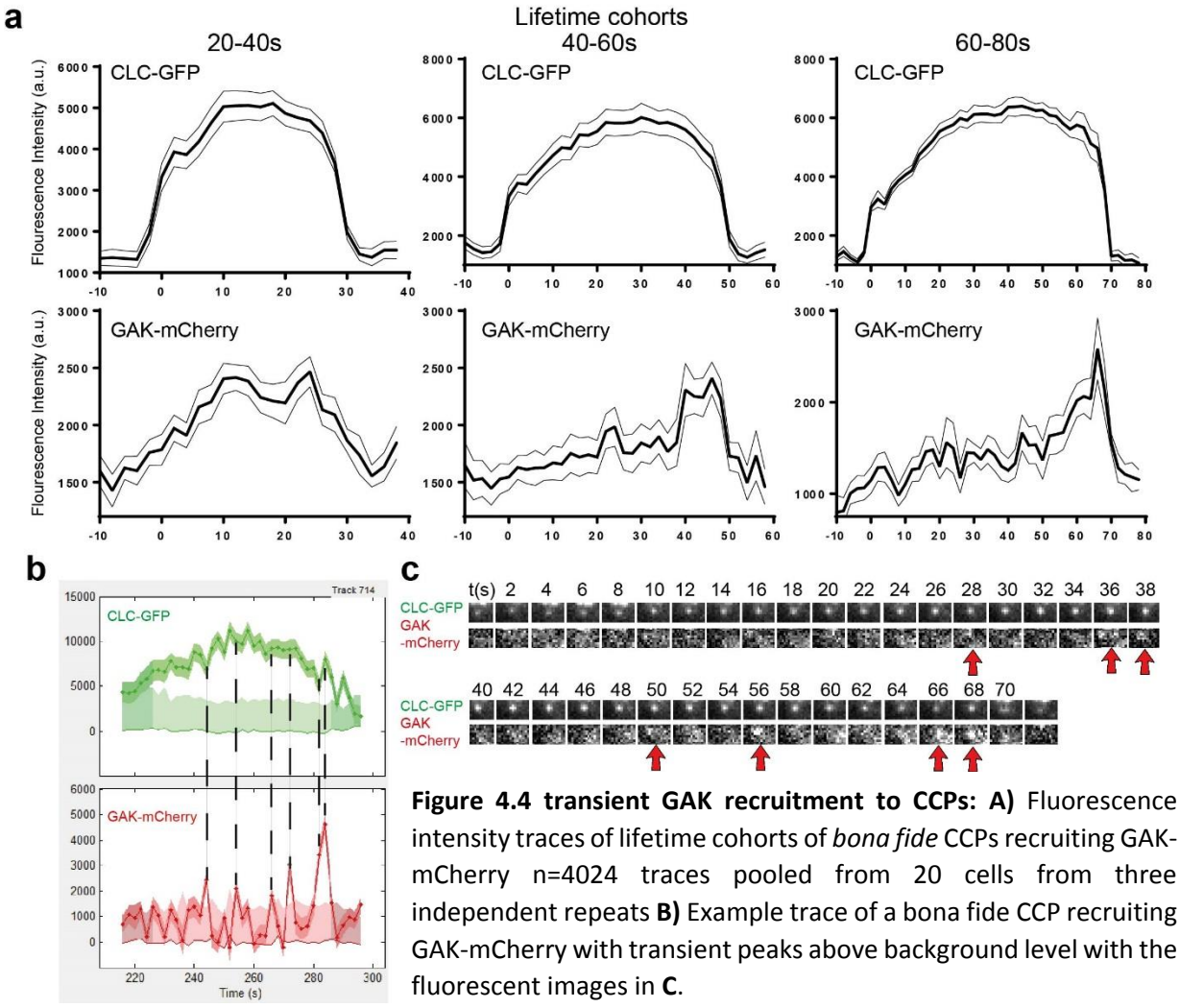

Figure 4.4 transient GAK recruitment to CCPs: A) Fluorescence intensity traces of lifetime cohorts of *bona fide* CCPs recruiting GAK-mCherry n=4024 traces pooled from 20 cells from three independent repeats **B)** Example trace of a bona fide CCP recruiting GAK-mCherry with transient peaks above background level with the fluorescent images in **C**.

4.5 HIP1R RECRUITMENT TO PHOSPHORYLATION DEFICIENT CLCB IS UNALTERED

The work conducted in this thesis thus far was clearly able to demonstrate an important role for CLCb phosphorylation in the uptake of the $P2Y_{12}$ receptor, likely through altered interactions with GAK, leading to defects in lattice dynamics and rearrangements.

An alternative role for CLCb phosphorylation could be in the regulation of actin organization and polymerization at endocytic sites. The regulation of actin polymerization during CME in mammalian cells is a complex process, however it has been shown that Hip1R is a crucial regulator of actin at CCPs and links it to the clathrin lattice through binding of the CLCs. Therefore, we tested whether Hip1R recruitment to CCPs is altered in cells expressing CLCb-SallA. Hip1R fused to mCherry was transiently transfected into HeLa cells expressing either CLCb-WT-GFP or CLCb-SallA-GFP and recruitment to CCPs was determined using life cell TIRF microscopy and analysed with the cmeAnalysis package in MATLAB as described previously. In both cell lines Hip1R is readily recruited to *bona fide* CCPs (Fig. 4.5 A). In agreement with the previous results, there is an increase in short lived, abortive, CCPs expressing CLCb-SallA-GFP. Reminiscent to the recruitment of the adaptor proteins shown earlier, these short lived CCPs also do not recruit Hip1R. However, unlike recruitment of GAK, there is no noticeable difference in the lifetime dynamics of CCPs that were positive for Hip1R (Fig 4.5 A). In agreement with this, there is no noticeable difference in the fraction of CCPs that recruit Hip1R, nor in the fluorescent intensity traces between CLCb-WT and CLCb-SallA (Fig 4.5B). Noticeably, Hip1R seems to be recruited at early stages of CCP formation in this cell line, which disagrees with observations by Taylor et al who showed that Hip1R is recruited at late stages during CCV formation. This discrepancy might be due to different levels of overexpression and use of different cell lines. Importantly, there does not seem to be a difference in Hip1R recruitment between cells expressing CLCb-WT or CLCb-SallA.

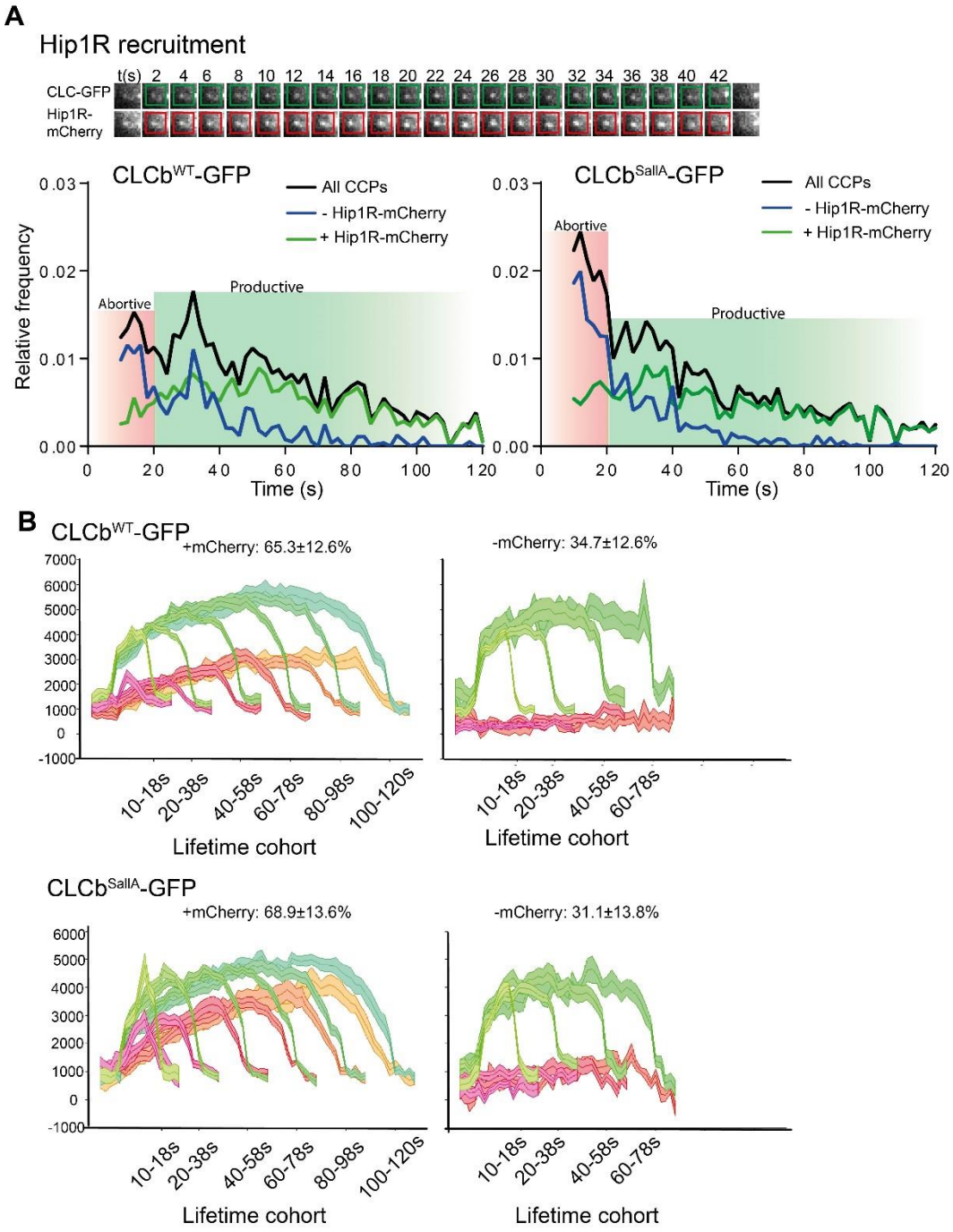

Figure 4.5 Hip1R recruitment to CLCb-SallA-GFP expressing cells is unaltered: A) HeLa cells stably expressing either CLCb-WT-GFP or CLCb-SallA-GFP were transfected with Hip1R-mCherry, and imaged by TIRF microscopy. The lifetime of CCPs was measured and binned for traces with (+Hip1R-mCherry) and without (−Hip1R-mCherry) detection of Hip1R **B)** Fluorescent intensity traces of different lifetime cohorts of cells overexpressing CLCb-WT-GFP or CLCb-SallA GFP with and without detection of Hip1R-mCherry. Lifetimes were analysed using the MATLAB script cmeAnalysis. n= 6488 (WT), 5418 (SallA) traces from 19–16 cells from three independent experiments.

4.6 ACTIN DYNAMICS ARE NOT REQUIRED FOR $P2Y_{12}$ UPTAKE

To further address whether actin polymerization would be required for the uptake of the $P2Y_{12}$ receptor, we used Latrunculin A (LatA) to depolymerize the actin cortex and measured $P2Y_{12}$ uptake. We first verified that treatment with 2.5 µM LatA leads to robust depolymerisation of the actin cortex by transfecting 1321N1 cells with fluorescently labelled LifeAct as marker for actin cytoskeleton. 1321N1 cells were then treated with 2.5 µM LatA or DMSO and imaged by life cell TIRF microscopy. Treatment with LatA lead to fast collapse of the actin cortex with complete depolymerisation after 600 s, whereas treatment with 2.5 µM DMSO had no effect (Fig 4.6 A). We therefore treated 1321N1 cells that stably overexpress the $P2Y_{12}$ receptor with either 2.5 µM LatA or DMSO for 10 min, stimulated P2Y12 uptake for 10 min with ADP and immunostained against the $P2Y_{12}$ receptor and EEA1. In both treatments, the $P2Y_{12}$ receptor is taken up into EEA1 positive endosomes to the same degree, as analysed by image segmentation using the ImageJ plugin SQUASSH (Fig 4.6C). Therefore, actin polymerization is unlikely to be a major contributor for ADP stimulated uptake of the $P2Y_{12}$ receptor into EEA1 positive endosomes in these cells and under the specific conditions tested.

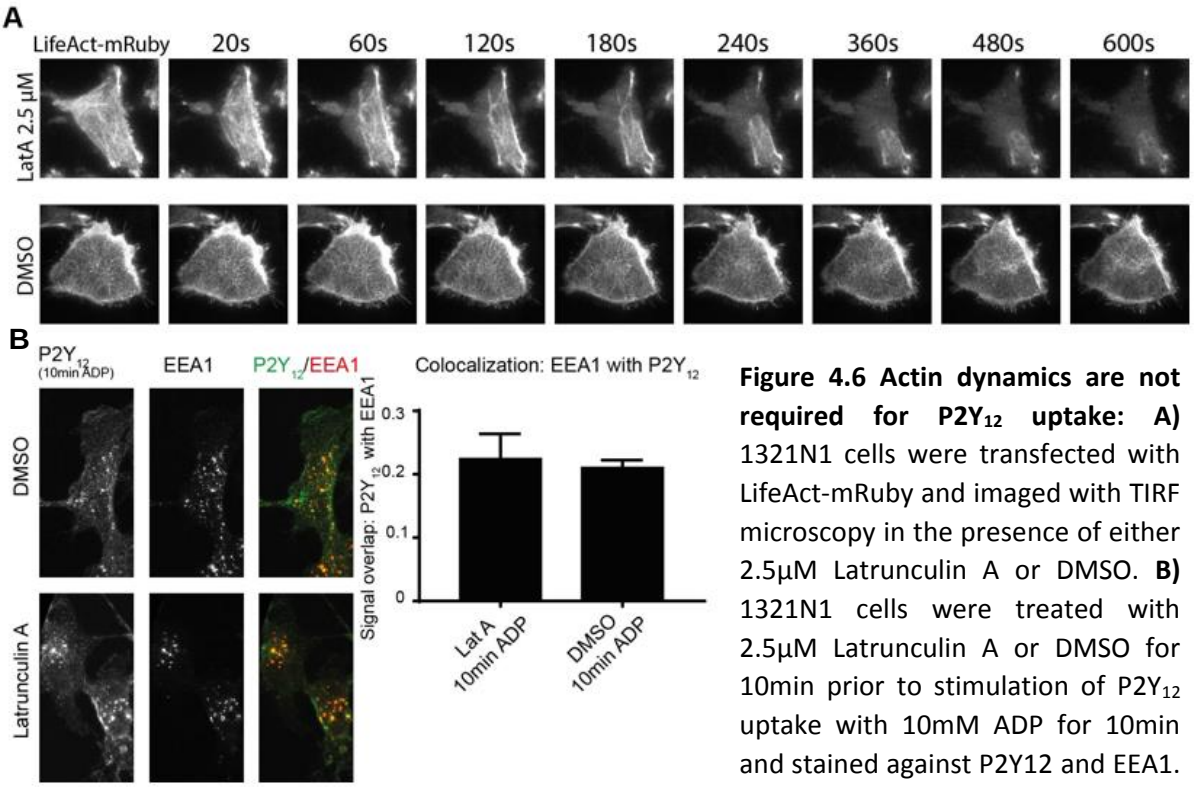

Figure 4.6 Actin dynamics are not required for $P2Y_{12}$ uptake: A) 1321N1 cells were transfected with LifeAct-mRuby and imaged with TIRF microscopy in the presence of either 2.5µM Latrunculin A or DMSO. **B)** 1321N1 cells were treated with 2.5µM Latrunculin A or DMSO for 10min prior to stimulation of $P2Y_{12}$ uptake with 10mM ADP for 10min and stained against P2Y12 and EEA1. Colocalization was quantified using the ImageJ plugin Squassh from 20-30 different cells from 2 independent repeats. Mean ± SEM

4.7 THREE CRITICAL SALT BRIDGES IN THE CLCB ARE REQUIRED FOR $P2Y_{12}$ UPTAKE

CLCb phosphorylation does not seem to alter Hip1R recruitment and actin polymerization does not appear to be required for $P2Y_{12}$ uptake either. The previous results suggest that the mechanism by which the CLCs control cargo specific uptake is through controlling auxilin (or GAK) mediated lattice rearrangements.

The interactions of CLCb with the CHCs were shown to be mediated through three critical salt bridges at their N-Terminus and to regulate lattice (dis)assembly though alteration of the CHC knee angle (Wilbur et al., 2010). We therefore sought to identify whether these interactions are also required for $P2Y_{12}$ receptor uptake. To test this we overexpressed a mutant version of CLCb tagged with GFP in which the three charged residues EED, which form the salt bridges with the CHC, were mutated to the uncharged amino acids QQN. The 1321N1 cells overexpressing this CLCb mutant failed to take up the $P2Y_{12}$ receptor into EEA1 positive endosomes after 10 min of ADP stimulation (Fig. 4.7). Therefore, the formation of these three critical salt bridges between the CLCs and the CHC seem to also regulate the uptake of this CLC dependent receptor.

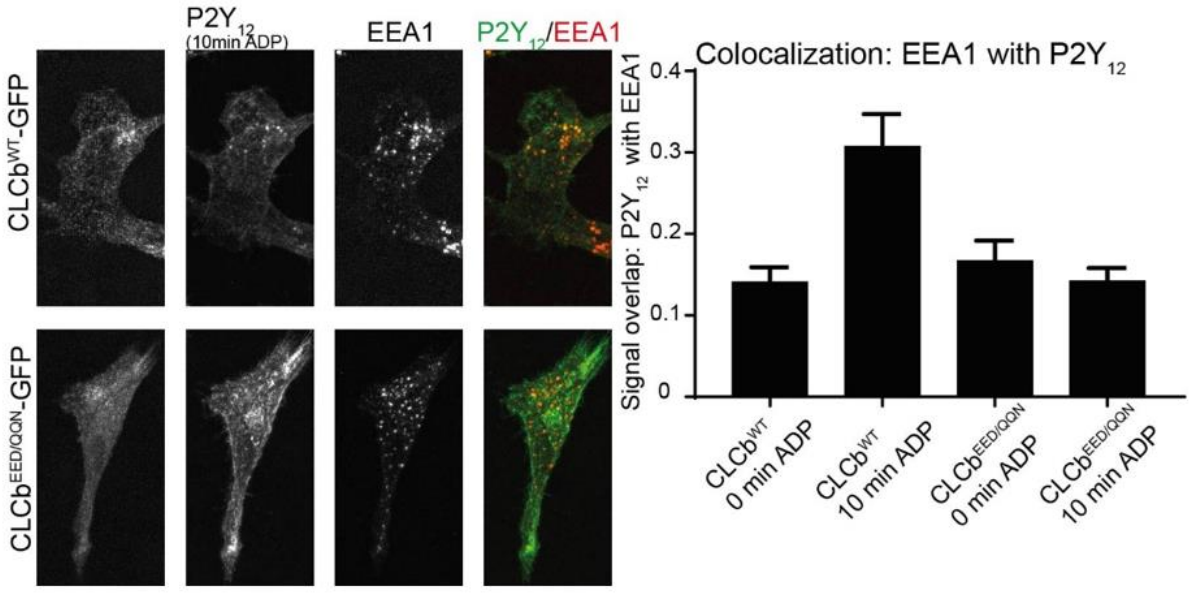

Figure 4.7 $CLCb^{EED/QQN}$-GFP overexpression leads to block of $P2Y_{12}$ uptake: 1321N1 cells were transfected with either CLCb-WT-GFP or CLCb-EED/QQN-GFP and $P2Y_{12}$ uptake was stimulated with 10mM ADP for 10min or unstimulated as control. Cells were fixed and immunostained against the $P2Y_{12}$ receptor and EEA1. Colocalization was measured using the ImageJ plugin Squassh from 20-30 cells for each timepoint from three independent repeats. Error bar ± SEM

4.8 TIGHT INTERACTIONS OF CLCB WITH CHC ARE REQUIRED FOR EFFICIENT CLATHRIN EXCHANGE

The three salt bridges between the CLCs and the CHC have been shown to be important for Hip1R binding and organization of the actin cytoskeleton at sites of CME (Chen et al., 2005). However, actin polymerization does not seem to be required for $P2Y_{12}$ uptake and CLCb phosphorylation does not affect Hip1R recruitment but alters the exchange rate between membrane bound and cytosolic clathrin. We therefore wondered whether the effect on $P2Y_{12}$ uptake in cells expressing EED/QQN mutant of CLCb might also be due to altered clathrin exchange. Consequently the FRAP experiments were repeated in 1321N1 cells expressing CLCb-EED/QQN-GFP before and directly after stimulation of $P2Y_{12}$ uptake by ADP. In the absence of ligand, the fluorescent signal of clathrin coated structures at the plasma membrane recovered rapidly, with a $t_{1/2}$ of 5.3s. However, after ligand stimulation, the exchange rate slowed down drastically with a $t_{1/2}$ of 10.02s, while the mobile fraction remained unchanged (Fig. 4.8). This increase in the halftime of recovery is similar to that observed in 1321N1 cells expressing CLCb-S204A-GFP and suggests that the formation of the three critical salt bridges of CLCb with the CHC might be a deciding factor that regulates clathrin exchange and lattice rearrangement.

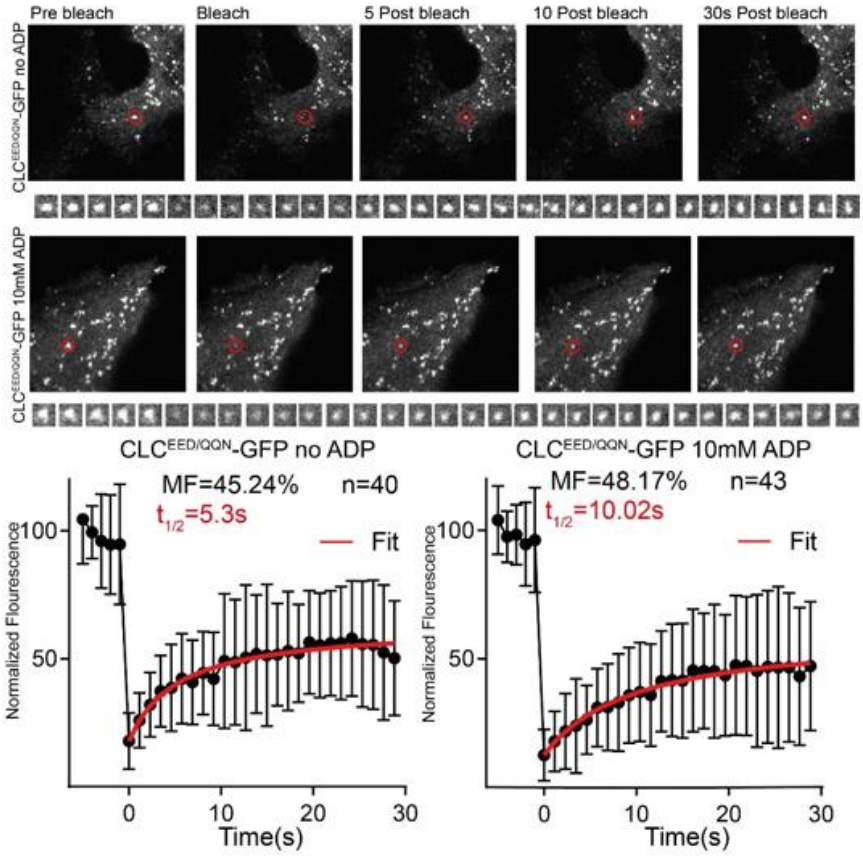

Figure 4.8 Clathrin exchange is decreased after ligand stimulation in CLCb$^{EED/QQN}$-GFP expressing cells: 1321N1 cells were transfected with either CLCb^{WT}-GFP or CLCb$^{EED/QQN}$-GFP, and fluorescence recovery of a single CCS was measured following incubation in serum-free medium before and directly after addition of 10 mM ADP. Top: Typical traces with the cumulative data from three independent repeats in the bottom panels. Error bars are mean ± SD

4.9 ATOMIC FORCE MICROSCOPY IS A SUITABLE TOOL TO INVESTIGATE THE MECHANICAL PROPERTIES OF CCPS

What determines whether the CLCs are required for the uptake of some cargo vs others? This question was discussed in the article published in JCB and one of the deciding factors could be the local properties of the plasma membrane inside of CCPs. Differences in the physical properties of individual CCPs are difficult to determine but one method to measure them could be atomic force microscopy (AFM). AFM relies on the contact of a small cantilever tip with the surface of the sample. Once the cantilever is in close proximity to the sample, it will be deflected, which provides information about the height profile of the sample with nanometre precision. Additionally, AFM is able to provide information about the deformability of the sample. This is done by pushing the cantilever past the point of contact with the sample and measuring the force it is experiencing. The force withstanding deformation by the cantilever is the elasticity of the sample and is measured in Pascal (Pa= kg m^{-1} s^{-2}). By combining the information of the initial contact point of the cantilever with the sample as well as its deformability, a map of cell surface can be obtained that describes its height profile as well as the local Young's modulus. By combining this method with fluorescence microscopy, it should be possible to determine the local deformability of individual CCPs.

To set up this method, the AFM Nanowizard4 from JPK (Berlin) was used in Quantitative Imaging (QI) mode to simultaneously determine the height profile and Young's modulus of live HeLa cells. Due to the slow acquisition time of AFM in QI mode, a low resolution of 311nm step size was chosen for an overview of the cell (Fig. 4.9.1). At higher magnifications, individual structures at the plasma membrane of the cell became apparent. These include filamentous structures as well as small indentations of ~311nm diameter and ~200nm depth. These regions also showed a decrease in the local Young's modulus (Fig. 4.9.1 inserts).

The size and depth of these structures is well in line with that of CCPs at the cell surface and the decrease in the local Young's modulus compared to the surrounding membrane is an intriguing observation. However, to test whether these structures are really CCPs, optical microscopy must be correlated to the AFM measurements. Since the AFM cantilever approaches the sample from the "top", it is easily combined with an optical lens that images the sample from below. HeLa cells expressing CLCb-WT-GFP were grown in glass bottom petri dishes, fixed with 4% PFA and imaged using a fluorescence microscopy combined with AFM. Due to the slow acquisition time of AFM in QI mode and the fast dynamics of CME, the cells had to be fixed in order to correlate the fluorescence signal with AFM measurements. Since the cells were fixed, images were acquired at a high resolution of 18nm step size and a 20µm x 20µm region on the edge of a cell was chosen for imaging overnight.

Using the imaging software from JPK instruments, the optical images were aligned with the AFM measurements (Fig 4.9.2 A) and clathrin puncta were detected using ImageJ and overlaid onto the AFM measurements. It is important to note, that not all spots detected are actual CCPs at the apical cell surface. Due to the nature and poor Z-resolution of epifluorescence imaging, a lot of these clathrin spots are from intracellular structures as well as from CCPs at the basal cell surface. In order to quantify which structures are corresponding to CCPs, the AFM measurements where clathrin puncta were detected were manually examined for small circular indentations in the height profile that agree with the known dimensions of CCPs (Fig 4.9.2 B and C (circular regions with asterisk are potential CCPs)). Through this low-throughput approach, 23 potential CCPs of ~50nm depth, were identified and the Young's modulus was determined and normalized to the surrounding membrane. In agreement with the results from the life cell measurements, the Young's modulus inside these putative CCPs was decreased compared to the surrounding membrane. Intriguing, the local Young's modulus of the individual CCPs differs greatly from each other, as apparent by the large error bars. Thus it is conceivable that the local properties of individual CCPs could be quite variable.

It is therefore possible to determine the Young's modulus of CCPs. However, due to the tremendous technical challenges und low throughput of this approach, I was not able to take this work further. Combining multicolour fluorescent imaging of differently labelled cargo proteins together with fluorescent CLCb would be required to correlate differences in the Young's modulus of CCPs to different cargo compositions. Even though this is theoretically possible, it is practically very difficult and requires proper expertise in atomic force imaging and data analysis. Additionally, the low scan speed of AFM in QI mode and the fast dynamics of CCP maturation, makes it almost impossible to perform these measurements on live cells. Chemical fixation is required to identify CCPs and to correlate them with AFM measurements in QI mode and the effect of PFA fixation on the physical properties of CCPs and the surrounding plasma membrane is a problem that would need to be resolved. Furthermore, the plasma membrane is only ~4nm thick and for determination of the Young's modulus, Cells need to be indented several times the thickness of the plasma membrane. Therefore, the resulting Young's moduli represent more the measurements the actin cortex, just below the membrane, than the actual properties of the plasma membrane itself. Therefore, it was decided not to pursue this method of determining the physical properties of CCPs. Alternative approaches are discussed in the Discussion section of this thesis but they were not able to be tested due to time constraints.

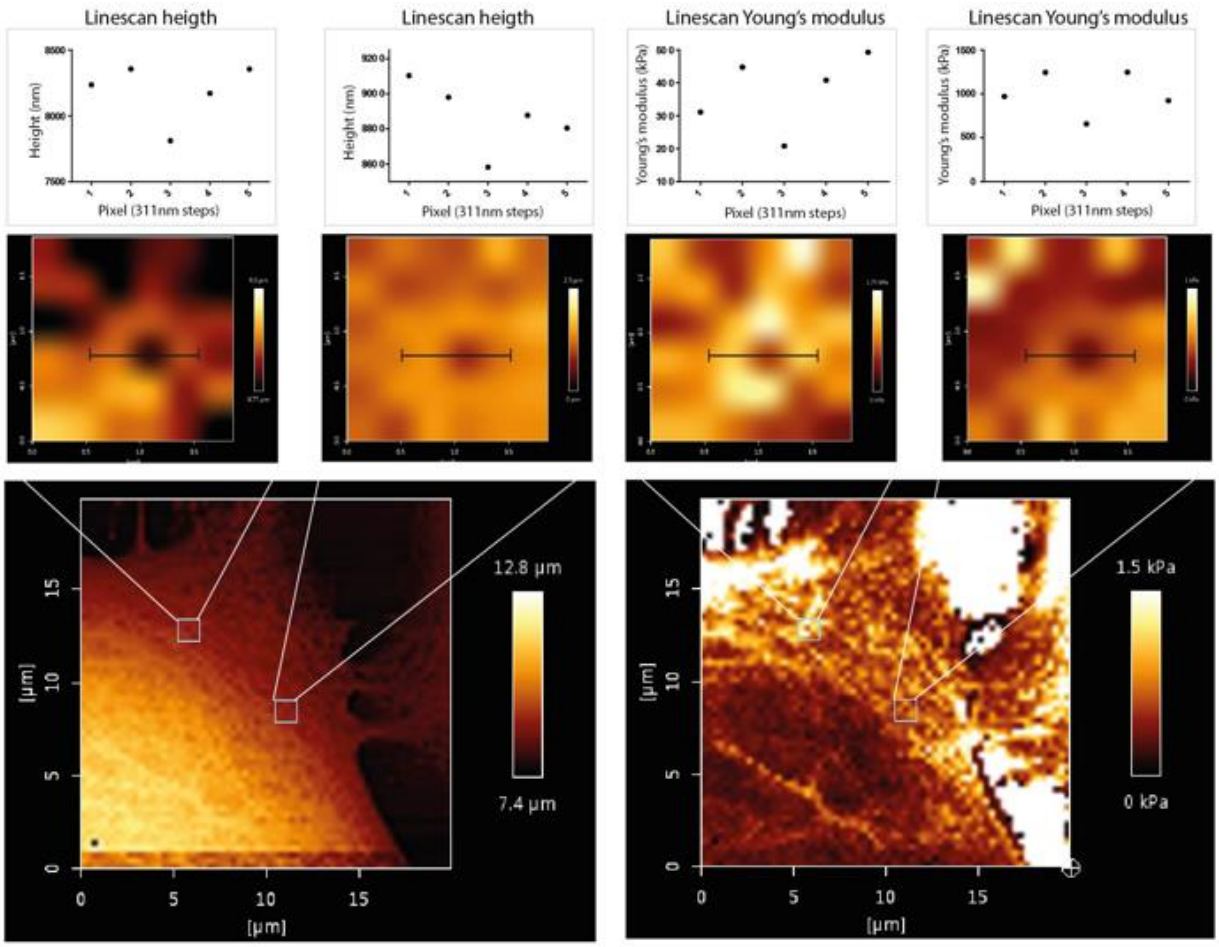

Figure 4.9.1 AFM measurements on life HeLa cells: Live HeLa cells were probed by AFM in QI mode to simultaneously measure the height profile as well as local Young's modulus at 311nm step size. Top panels show two example measurements heights (left) and Young's modulus (right) obtained from the linescans of potential CCPs shown in the middle panels. Bottom panels show overview of the measured cell region with heights profile (left) and Young's modulus (right).

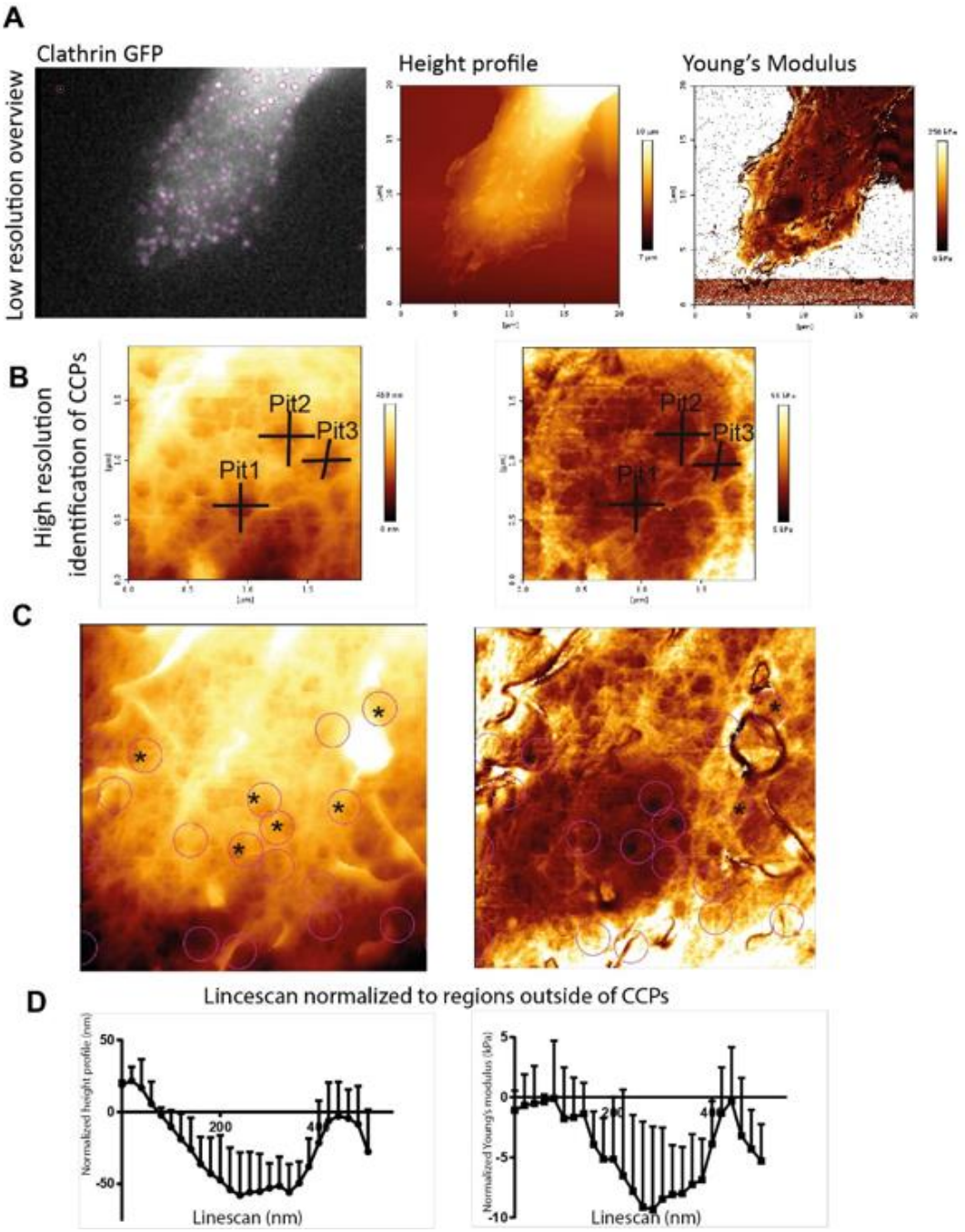

Figure 4.9.2 Correlative fluorescence and AFM measurements on fixed HeLa cells: A) HeLa cells overexpressing CLCb-WT-GFP were imaged using an Epifluorescence microscope with a mounted AFM head. Left panel show fluorescent signal from CLCb-WT-GFP, middle panel shows the height profile and right panel the local Young's modulus at 18nm step size. **B)** High magnification overview of three potential CCPs that were correlated with fluorescent detections from CLCb-WT-GFP. Left panel shows height profile and right panel the Young's modulus. **C)** Fluorescent detections (pink circles) were overlaid onto AFM data with asterisks marking potential CCPs at the cell surface. Left panel shows height profile and right panel the Young's modulus. **D)** Cumulative linescan profiles of 23 potential CCPs, normalized to regions outside of the CCP with height profile (left) and Young's modulus (right). Error bars are ±SD.

5 DISCUSSION

Most of the major results of this thesis have been published and the discussion section of the article covers the main points that needed to be addressed. However, due to the word limit of the article and the generation of new data, after its publication, not all ideas could be discussed. Additionally, the discussion in the article had to be of a more "conservative" nature, and therefore some of the more explorative ideas will be discussed in this section. I apologize to the reader for some repetitions in this discussion section with that of the published article.

5.1 REGULATION OF CLATHRIN EXCHANGE BY THE CLCS

The data presented thus far highlights a requirement for CLCb phosphorylation for efficient clathrin exchange and lattice rearrangement. Intriguingly, this process seems to be required for the uptake of the $P2Y_{12}$ receptor but not the Transferrin receptor. The major reasons why these two different cargo proteins may require differential mechanisms of lattice assembly have been discussed extensively in the manuscript. However, the mechanism(s) by which the CLCs can control lattice rearrangement are less well understood. One possibility is that the phosphorylation status of CLCb modulates the interaction of GAK (or auxilin) with the clathrin lattice. This notion is supported by the increase in short-lived clathrin coated structures that are positive for GAK, as well as the previously published observation that GAK binding to reconstituted clathrin cages is altered in the background of phosphorylation deficient CLCb (Ferreira *et al.*, 2012). Both of these points have been discussed in the manuscript and will therefore not be further addressed in this section.

Strikingly, the results from overexpressing the phosphorylation deficient CLCb could be phenocopied by overexpression of mutated CLCb (CLCb-EED/QQN) which cannot form the three critical salt bridges with the CHCs. As described in the introduction section, these three salt bridges are crucial for the regulatory functions of the CLCs on lattice assembly and regulate the alteration of the knee angle of the CHCs after Hsc70 binding. Using fluorescent microscopy, we could show that overexpression of this CLCb mutant also led to a decrease in $P2Y_{12}$ uptake after ligand stimulation. Previous studies were able to demonstrate that overexpression of CLCb-EED/QQN leads to an altered interaction with Hip1R, resulting in disorganization of the actin cytoskeleton at sites of CME (Chen et al., 2005). Importantly, actin polymerization does not seem to be required for the uptake of the $P2Y_{12}$ receptor as evidenced by the unchanged receptor uptake after Latrunculin A treatment. Additionally, Hip1R recruitment is

unchanged in cells overexpressing phosphorylation deficient CLCb. These observations argue against a strong contribution of actin polymerization in $P2Y_{12}$ uptake. Therefore, the observed deficiency in $P2Y_{12}$ uptake in cells overexpressing CLCb-EED/QQN is unlikely to be due to altered interactions with the cytoskeleton.

Overexpression of phosphorylation deficient CLCb leads to a drastic decrease in the exchange rate of clathrin at the plasma membrane with the cytosolic pool. Importantly, this effect was only apparent after stimulation of $P2Y_{12}$ uptake with ADP. We repeated these experiments for cells expressing CLCb-EED/QQN and could observe a similar delay in the exchange rate of clathrin. Therefore, these distinct mutations in CLCb lead to the same result for $P2Y_{12}$ uptake and clathrin exchange, making it likely that they are involved in the same process. However, the Serine residue that needs to be phosphorylated for uptake of the $P2Y_{12}$ receptor is at aa204, close to the C-terminus of CLCb and in proximity to the trimerization domain of the triskelia. This places it in proximity to the regions that bind the auxilin/Hsc70 complex and could alter their interaction with the lattice. The EED/QQN mutation on the other hand is located between aa22-41 of CLCb, at the N-terminus, close to the knee segment of the CHC, far away from the trimerization domain and GAK binding sites. It is therefore unlikely that these residues directly interact with the Auxilin/Hsc70 complex. Structural data however, was able to demonstrate that upon Hsc70 binding to clathrin cages, structural changes occur at the C-terminus of the CLCs, close to the position of the CHC knee (Wilbur et al., 2010, Young et al., 2013). Furthermore, the salt bridges at these positions have been shown to regulate the alterations of the knee angle of the CHCs and to control the pH-dependent control of clathrin assembly by the CLCs (Ybe et al., 1998). It is therefore likely that these salt bridges are also required for efficient clathrin exchange and lattice rearrangement at endocytic sites. This places the CLCs at an important intersection in the regulation and fine tuning of lattice dynamics.

A potential model of how the CLCs could regulate lattice dynamics is presented in Figure 5.1.1. After formation of a flat clathrin lattice, auxilin (or GAK) bind sub stoichiometrically to the internal site of the trimerization domain of the CHCs. These interactions of the uncoating complex with the lattice are modulated by the phosphorylation status of CLCb. The removal of the triskelia from the lattice then requires breaking the connections with neighbouring triskelias through complex conformational changes of the CHCs. These involve the straightening of the knee angle, which requires the tight interactions with the CLCs through the three salt bridges. The conformational state of the CHCs with “straight” knees is incompatible with being part of the clathrin lattice and would be removed from the structure. After removal of the individual triskelia, new triskelia can be incorporated into the array and the lattice is able to rearrange and form either hexagons or pentagons, according to the local curvature of the membrane. Here it is important to note that clathrin exchange does not necessarily

lead to the generation of curvature. This becomes apparent by elegant experiments by Lois Greene that were able to show that clathrin constantly exchanges at CCPs even when curvature cannot be generated. Therefore, flat clathrin lattices are very plastic and dynamic structures that are able to locally rearrange in order to adapt to changes in local curvature. The mechanism(s) by which curvature is generated from these flat lattices is still somehow unclear but recruitment of adaptor proteins with membrane bending properties, like CALM and Epsin, could be major factors for the deformation of the membrane. If the clathrin lattice is not able to adapt to these changes in curvature, through rapid clathrin exchange and local rearrangements, then CCVs might not be able to form from flat lattices.

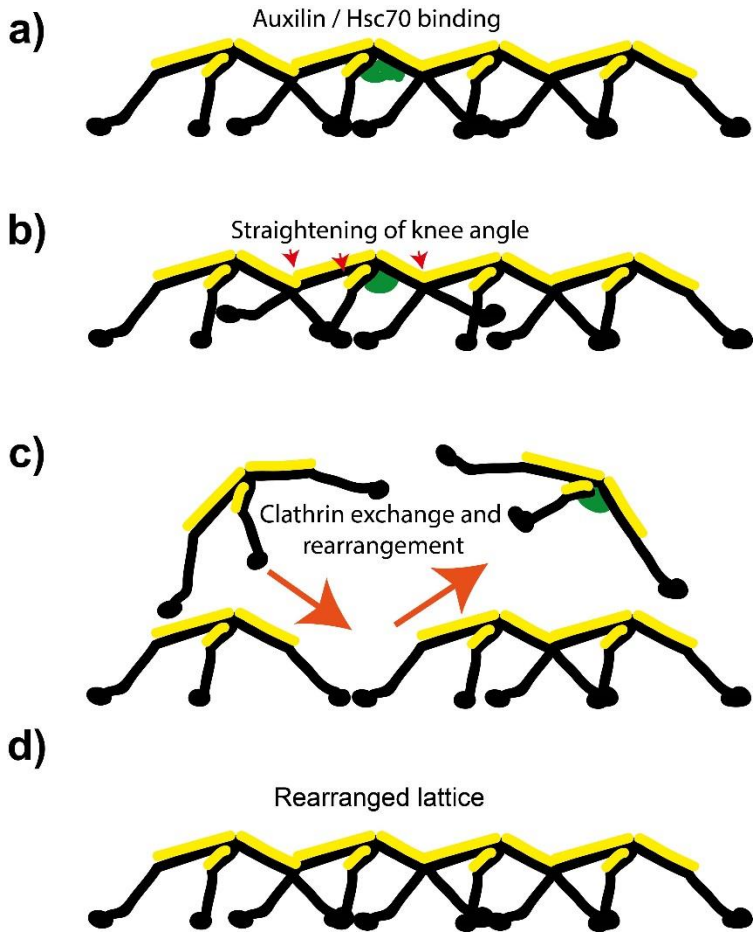

Figure 5.1 Potential model for CLC and auxilin dependent rearrangement of flat clathrin lattices: A) Auxilin and Hsc70 bind to the trimerization domain of some triskelia in the lattice. **B)** Binding of the uncoating complex leads to long range conformational changes in the triskelia, including straightening of the knee angle. **C)** Individual triskelia are removed from the clathrin lattice and new triskelia are incorporated. Leading to rearrangement of the lattice, if necessary. **D)** The rearranged lattice allows for generation of curvature through incorporation of pentagons into the array.

In this model, it is important that the Auxilin/Hsc70 complex only binds to some of the triskelias in the lattice, if the amount of auxilin/Hsc70 recruitment is too high, the lattice would disassemble completely. This is in line with the observation that transient peaks of GAK recruitment could be observed throughout the lifetime of CCPs. However, at the stage of CCVs uncoating, a burst of strong GAK recruitment initiates the complete removal of the clathrin coat. This high level of GAK binding is most likely due to the altered PIP composition of CCVs vs CCPs (Kangmin et al., 2017).

5.2 Influence of cargo identity on the local properties of CCPs

The data presented in this thesis has established a link between the CLCs, clathrin exchange and curvature generation from flat lattices. Previous work has clearly demonstrated that the CLCs are required for the uptake of a subset of GPCRs, while being dispensable for uptake of the Transferrin receptor. Although several possible explanations for this differential requirement have been discussed in the published article, here alternative and more explorative ideas will be discussed.

As mentioned earlier, in *in vitro* systems, the CLCs are required for the deformation of membranes with high bending rigidity. These findings lead to the initial hypothesis, that ligand induced clustering of GPCRs could modify the local rigidity of the CCP that they reside in. One of the main factors that modulates the rigidity of the lipid bilayers is their lipid content. High levels of sphingolipids and cholesterol increase the bending rigidity of the membrane and thereby counteract its deformation. Intriguingly, numerous GPCRs that are CLC dependent, also bind to cholesterol and have historically been associated with the so-called “lipid rafts”. There are currently 5 GPCRs known to be dependent on the CLCs for their uptake: The $P2Y_1$ and $P2Y_{12}$ receptors, the δ-opioid receptor, transforming growth factor β receptor 2 (TGFβR2) and C-X-C chemokine receptor 4 (CXCR4). However, both the C-X-C chemokine receptor 5 (CXCR5) and the β2-adrenergic receptor, also GPCRs, do not require the CLCs for their uptake. What could be the reason behind these differential requirements? The family of the purinergic receptors (of which both $P2Y_1$ and $P2Y_{12}$ are a members of) have been shown to bind to cholesterol and form high order oligomers after ligand activation (Savi *et al.*, 2006). The interactions of GPCRs with cholesterol has been a controversial topic for a while, with most of the data depending on cholesterol depletions with beta cyclodextrin or extraction of detergent resistant membranes. However, both of these techniques are highly debatable and depletion of cholesterol from the plasma membrane has detrimental effects on the structural integrity of the plasma membrane and the extraction of detergent resistant membranes has been shown to be highly prone to artefacts. Nevertheless, cholesterol appears to have differential effects on different GPCRs. While it facilitates

formation of high order oligomers for the $P2Y_{12}$ receptor, it inhibits dimerization of the β2-adrenergic receptor (Prasanna, Chattopadhyay and Sengupta, 2014).

These differences in lipid binding and oligomerizations of GPCRs could have a significant effect on the local properties of the membrane inside CCPs. In an elegant computational study Stachowiak et al were able demonstrate that high cholesterol concentrations as well as cargo crowding inside a CCP increase the local bending rigidity of the membrane (Stachowiak, Brodsky and Miller, 2013). Therefore, it is possible that the oligomerization as well as the lipid binding properties of distinct GPCRs could determine the local properties of CCPs. For GPCRs that form high order oligomers and reside in cholesterol enriched microdomains the local membrane rigidity would be increased due to high cargo loading, compared to those that do not form high order oligomers or are excluded from these microdomains. The deformation of these membranes, with higher rigidity, would then require the contributions of the CLCs to bend the membrane during CME, as discussed in the article.
Along the line of this hypothesis, two "extreme" scenarios are plausible when comparing the uptake of the Transferrin and $P2Y_{12}$ receptors. As mentioned above, the $P2Y_{12}$ receptor forms high order oligomers, binds cholesterol and is partitioned in cholesterol enriched microdomains after ligand binding. The TfR on the other hand does not form high order oligomers, nor binds to cholesterol and is continuously cycled between the plasma membrane and endosomal recycling compartments, independently of ligand binding. Additionally, the structure of these two transmembrane proteins is highly different; while the $P2Y_{12}$ receptor is a classical seven-(pass)-transmembrane receptor with small extracellular domains, the TfR is a single pass transmembrane receptor with a large extracellular domain that binds to two Transferrin molecules. Therefore, under normal conditions, only few TfRs are packed into CCPs due to the steric hindrance of their ectodomains. Interestingly, when TfRs are artificially crosslinked, through a sophisticated biotin-streptavidin approach, the cargo loading of individual CCPs is increased, which leads to an increased lifetime of CCPs (Liu *et al.*, 2010). Unlike the TfR, the $P2Y_{12}$ receptor naturally forms oligomers and is able to pack tightly into CCPs, which also have a longer lifetime compared to those that traffic non-crosslinked TfRs. As discussed in the article, the lifetime of CCPs is indicative towards the mode of lattice assembly, further supporting the notion that high cargo loading could influence the mode of curvature generation by CCPs.

In line with this notion, when measured in serum free media, TfR uptake does not require the presence of the CLCs. Under these conditions the TfR cycles continuously between the plasma membrane and endosomal compartments, while ligand dependent receptors are retained at the plasma membrane. However, if measured in the presence of full media, several agonists in the serum trigger the uptake of a wide array of cargo proteins that will be partially co-packed into the same CCPs as the TfRs. This would increase the cargo loading of CCPs and possibly raise the rigidity of the membrane, making it

dependent on the CLCs for membrane deformation. In line with this, the rate of transferrin uptake is reduced in the presence of full media in cells expressing phosphorylation deficient CLCb. To understand which ligands in the serum could be responsible for this effect, we tested the presence of 10ng/ml EGF on the rate of TfR uptake in HeLa cells expressing phosphorylation deficient CLCb. The rate of TfR uptake under these conditions was only mildly affected. Making it unlikely that the copacking of TfR with EGF Receptors has a significant effect on cargo loading and membrane rigidity. An alternative approach to modulate the physical properties of the plasma membrane is by increasing its tension. Addition of hypotonic media to cells, leads to their swelling which is thought to increase membrane tension. However, no difference in the rate of Tf uptake was detectable between HeLa cells expressing CLCb-WT or CLCb-SallA under these conditions. Treatment with hypotonic media is a complicated because it alters the ion homeostasis and cells have been show to adapt quickly to the increase in membrane tension (Bucher *et al.*, 2018). This adaptation is most likely due to Caveolae (Sinha *et al.*, 2011), which act as membrane reservoirs and flatten out after hypotonic shock. Therefore, we measured the uptake of Tf in serum free media at lower temperatures. At lower temperatures the bending rigidity of the membrane will be increased and in agreement with our hypothesis, the rate of Tf uptake was decreased under these conditions in cells expressing CLCb-SallA. At increased membrane rigidity the constant area model should be favoured for curvature generation of CCPs. As discussed, both Auxilin and GAK are required for CCPs to gain curvature along the constant area pathway. To test this, we depleted 1321N1 cells of auxilin using siRNA and measured Tf uptake in serum free media at 19˚C. Contrary to our expectations, no difference in the rate of Tf uptake was observed under these conditions. However, 1321N1 cells express high levels of both Auxilin and GAK and it is therefore possible that GAK is sufficient to compensate for the loss of Auxilin for the uptake of Tf at low temperatures. Intriguingly, GAK is not able to compensate for the loss of Auxilin for the uptake of the $P2Y_{12}$ receptor. These differential requirements might point towards differential functions of Auxilin and GAK for the trafficking of different receptors and hence warrants further inspections.

A potential model of how cargo packing could influence the local properties of CCPs is presented in Figure 5.2. If the extreme cases are considered of CCPs only trafficking low amounts of TfR compared to CCPs trafficking ligand activated $P2Y_{12}$ receptors, then two different scenarios are plausible. CCPs with low amount of cargo loading, trafficking only few TfRs, would have a lower bending rigidity due to low cargo crowding and low amounts of cholesterol. Due to the low bending rigidity, the membrane could then directly be deformed by polymerization of the clathrin triskelias into spherical buds, along the constant curvature pathway. This mode of curvature generation would be independent of the CLCs and does not require auxilin/GAK mediated clathrin exchange and rearrangement. In the other

case, CCPs that traffic ligand activated $P2Y_{12}$ receptors will show high cargo crowding, due to the oligomeric nature of the $P2Y_{12}$ receptor and higher concentrations of cholesterol. These factors are predicted to increase the local bending rigidity and counteract the polymerization energy of the clathrin triskelia, leading to the formation of a flat clathrin lattice. Curvature generation from these CCPs is than dependent on the phosphorylation of CLCb and efficient clathrin exchange and lattice rearrangement mediated by auxilin and/or GAK. Of course, as shown in the article, in cellular systems cargo composition of CCPs will be more complex, with a mix of different receptors incorporated into CCPs. Therefore, the mode of curvature generation and dependency on the CLCs could differ between CCPs, depending on the local cargo composition and the cellular context.

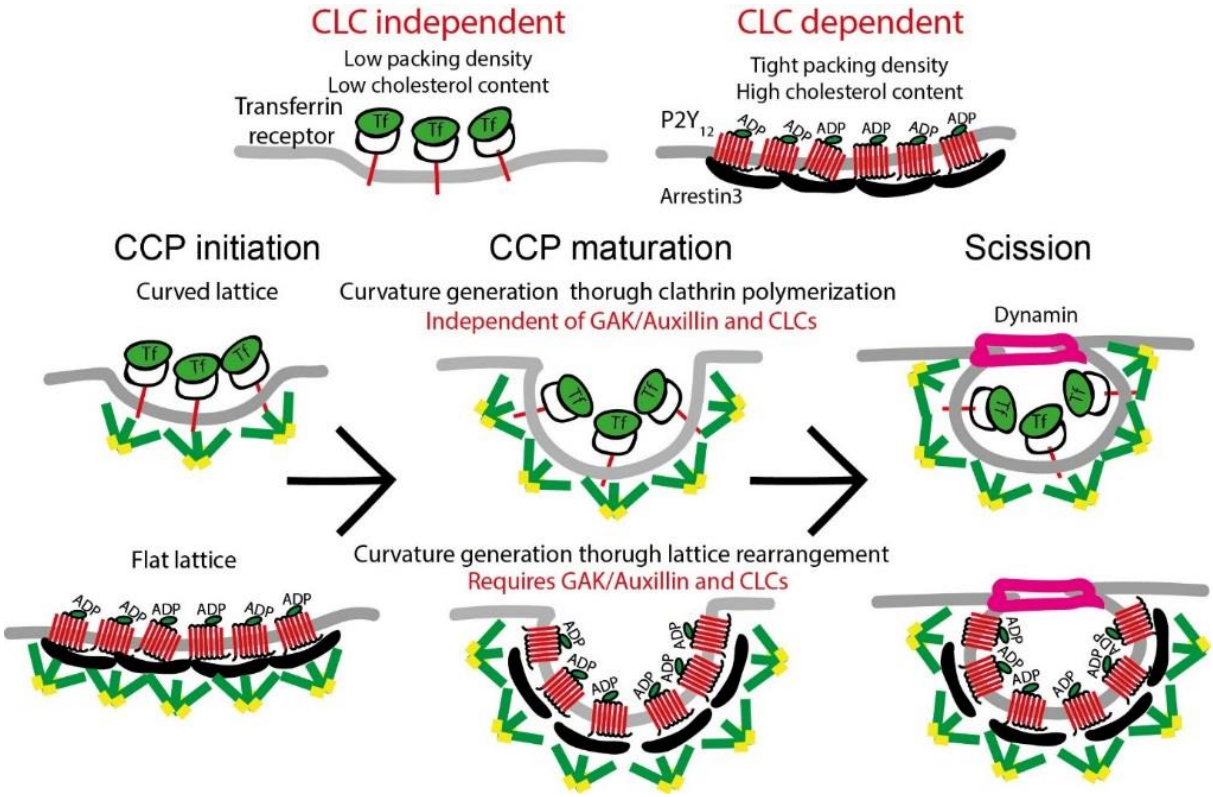

Figure 5.2 Model for cargo dependent curvature generation: Cargo composition determines mode of clathrin assembly. Curvature generation of CCPs containing low amounts of TfR could occur directly through clathrin polymerization along the constant curvature mode while CCPs with high cargo crowding and higher cholesterol content would follow the constant area mode. This mode is dependent on CLC phosphorylation and GAK/Auxilin mediated clathrin exchange and lattice rearrangements.

5.3 ALTERNATIVE APPROACHES TO MEASURE PHYSICAL PROPERTIES OF CCPS

To test the hypothesis that different amounts of cargo loading could affect the physical properties of CCPs, an approach using Atomic Force Microscopy (AFM) combined with fluorescence microscopy was applied. To identify CCPs, HeLa cells expressing CLCb-GFP were imaged using an Epifluorescence microscope with a Nanowizard 3 AFM head. On whole cells AFM is only able to probe the apical surface of cells, while the fluorescence signal of the CLCb-GFP is a mixture of clathrin structures from the basal surface, intracellular vesicles as well as apical structures, making it difficult to directly correlate the fluorescence signal to the AFM measurements. Therefore, the fluorescent structures detected by light microscopy were overlaid onto the AFM map and the AFM measurements were manually screened for structures that correspond to the known dimensions of CCPs. Using this somewhat biased approach, we were able to measure the Young's modulus of several potential CCPs on the apical surface of fixed HeLa cells. Unsurprisingly, the Young's modulus of these potential CCPs is decreased compared to their surrounding area. This is most likely due to the local organization of the Actin cortex at endocytic sites. Due to the indentation depth of AFM in QI mode, it is nigh impossible to measure the deformation of the plasma membrane without probing the underlying actin cortex. For CME to occur, the actin cortex needs to be locally remodelled to make space for the budding CCVs. Therefore, the decreased Young's modulus at potential site of CME is likely to represent a less dense actin cortex. Interestingly, the measurements inside those regions were highly variable when different potential CCPs are compared with each other. Due to the low throughput and ambiguous nature of these measurements it is difficult to draw any concrete conclusions, but it is likely that the local Young's modulus varies between individual CCPs.

As mentioned before, due to the slow acquisition time of AFM and high turnover rate of CME, it is difficult to correlate the AFM measurements to fluorescent signal in real-time. Therefore, these measurements were done on cells fixed with 4% PFA, which alters the physical properties of cellular structures significantly, due to the permanent crosslinking of epitopes. A more elegant and refined approach to measure the physical properties of CCPs at different stages of maturation is presented in Figure 5.3. 1321N1 cells expressing CLCb-GFP and Dynamin2-mCherry, grown on coverslips, could be treated with or without ADP for short timepoints and unroofed by sonification as to standard protocols. The unroofed cells could then be analysed using a combined approach of fluorescence imaging with AFM as before, but with several advantages. Firstly, the internal site of the basal membrane is accessible for AFM and the fluorescent signal can easily be correlated with the measurements because they are bound to be from the basal membrane. Secondly, by comparing clathrin coated structures with and without detection of dynamin-2, information about the differences

of the mechanical properties of CCPs throughout their maturation is available. Finally, by comparing the measurements of cells treated with or without ADP, information about the effect of high cargo loading on the deformability of CCPs would also be assessed. Additionally, this approach does not necessarily require chemical fixation of the sample if the measurements are performed directly after unroofing.

Unfortunately, due to time constraints these exciting experiments could not be performed.

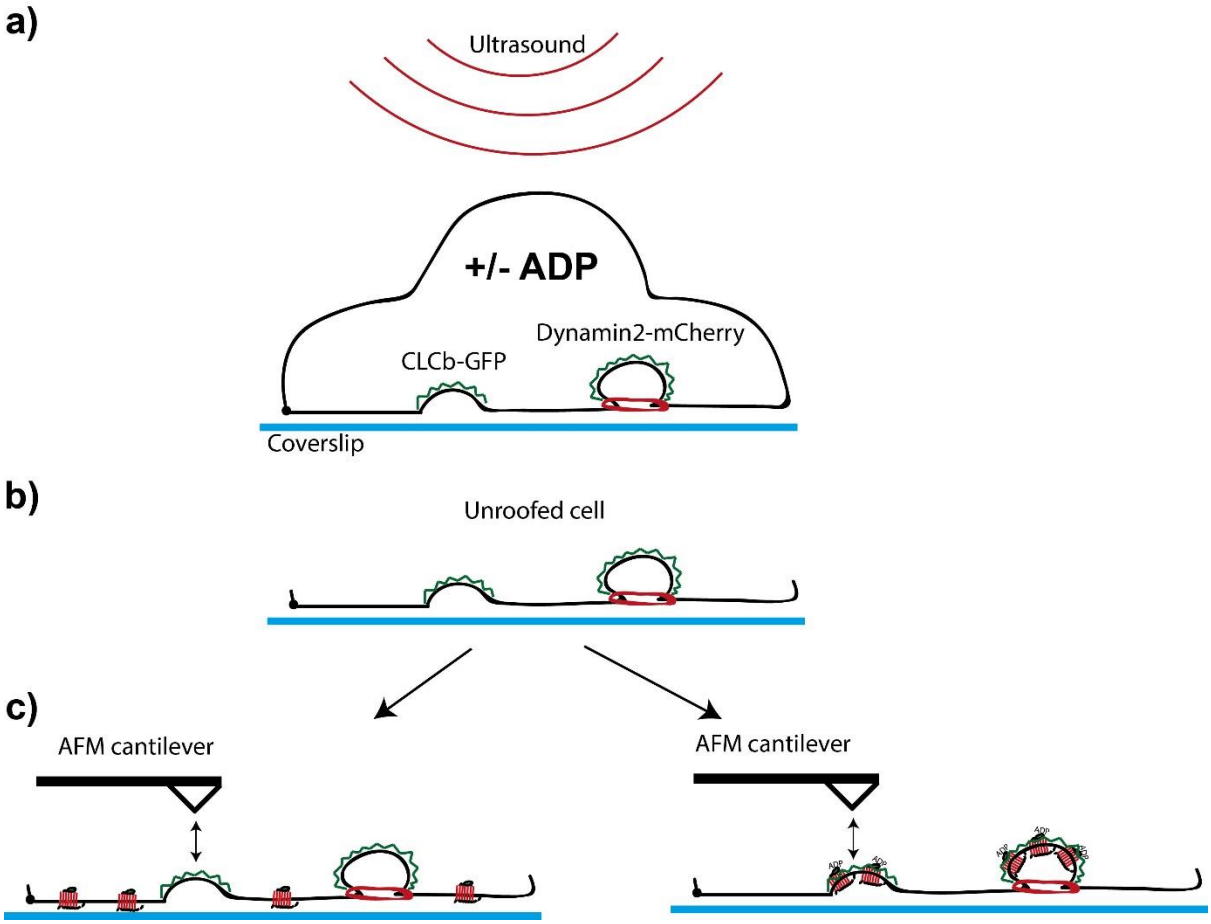

Figure 5.3 Potential approach to measure physical properties of CCPs: A) Cells are grown on coverslips, treated with or without ADP and unroofed by sonification. **B)** Membrane sheets with fluorescently labelled clathrin and dynamin are generated. **C)** AFM measurements on either conditions would allow to detect changes in the physical properties of CCPs with different cargo loading.

6 SUMMARY

To conclude this Thesis, in this thesis I have demonstrated novel mechanisms by which the CLCs and cargo influence the process of clathrin mediated endocytosis. The role of the CLCs for CME has long been elusive, partly because the field has focused on trafficking of the Transferrin and EGF receptors as readout for CME. However, we (and others) could show that, while the CLCs were not needed for the uptake of these classical receptor proteins, they are required for the uptake of a range of GPCRs, such as the $P2Y_{12}$ receptor. The aim of this work was to investigate the mechanism(s) behind this differential requirement. Firstly, we addressed whether the recruitment of cargo and adaptor proteins is affected by the phosphorylation state of the CLCs and demonstrate that cargo as well as adaptors are recruited normally, whether CLCb can be phosphorylated or not. We then investigated the lifetime dynamics of *bona fide* CCPs and could observe an increase in short lived CCPs with lifetimes of 10-20s in the background of phosphorylation deficient CLCb. By testing the recruitment of a range of adaptor proteins to these short lived events, we could identify the clathrin uncoating and rearranging protein GAK, to be involved in this process. This led us to investigate the morphologies of CCPs in the background of phosphorylation deficient CLCb, which showed an increase in the number of shallow CCPs as well as large, flat clathrin lattices. For these flat lattices to gain curvature, pentagons have to be incorporated into the flat hexagonal array, which requires clathrin exchange and rearrangement. We therefore tested whether CLCb phosphorylation affected this process and detected a decreased rate of exchange between cytosolic and membrane bound clathrin if CLCb cannot be phosphorylated. Intriguingly, this process was cargo specific following stimulation of $P2Y_{12}$ uptake. To further test the requirement of clathrin exchange on the uptake of $P2Y_{12}$ vs Transferrin receptor, we depleted 1321N1 cells of Auxilin and were able to show that $P2Y_{12}$ uptake was abolished while the TfR was trafficked normally. These findings lead us to postulate a model in which the cargo that is incorporated into CCPs dictates the way it can be deformed. For cargo such as the $P2Y_{12}$ receptor, CCPs would assemble as flat lattices that require clathrin rearrangement (mediated by GAK and/or Auxilin) and CLCb phosphorylation. However, for cargo such as transferrin, CCPs could invaginate independently of lattice rearrangement and the CLCs.

Additionally, we have shown that the three critical salt bridges between the CLCs and the CHCs, that regulate alterations in the knee angle of the CHCs, are also required for the uptake of the $P2Y_{12}$ receptor and regulate lattice dynamics and clathrin exchange in a similar manner to CLCb phosphorylation. These findings place the CLCs at an important position to fine tune and regulate clathrin lattice dynamics in a cargo dependent manner.

In future work, it would be exciting to further address whether the nature of cargo incorporated into CCPs, changes the physical properties of it. AFM is a promising tool to investigate the physical properties of individual CCPs and initial findings as well as alternative approaches have been discussed. Finally, it would be exciting to properly investigate the mechanisms of lattice rearrangement during CME and exactly how it is possible to rearrange a flat hexagonal array into a curved lattice without dissembling the lattice completely. This requires a fine balance between exclusion and incorporation of triskelia and is properly regulated through the CLCs and Auxilin/GAK. A potential approach to address this challenging topic would be the use of an assay that uses unroofed cells expressing fluorescently labelled CLCs with in vitro purified clathrin triskelia labelled with a different fluorescent tag (Fig 6.1). One of the advantages of this approach would be that the clathrin lattices on the unroofed cells are directly accessible to a wide range of biochemical manipulations. By incubating the membrane sheets with cell lysate depleted of out single components of the rearranging machinery (e.g. Auxillin, GAK or HSC70) the effect on these factors on the rearranging of the lattice could be address by monitoring the change of fluorescent signal of individual lattices. In an orthogonal approach, the minimal components for lattice rearrangement could be identified in a bottom up approach, where only reconstituted proteins are added to the membrane sheets along with the fluorescently labelled triskelia (Fig 6.1). Finally, by combining super resolution microscopy with platinum EM replicas (as demonstrated by the Taraska lab the NIH) it would also be possible to determine at what positions in the lattice, rearrangement occurs by staining for the newly incorporated triskelias.

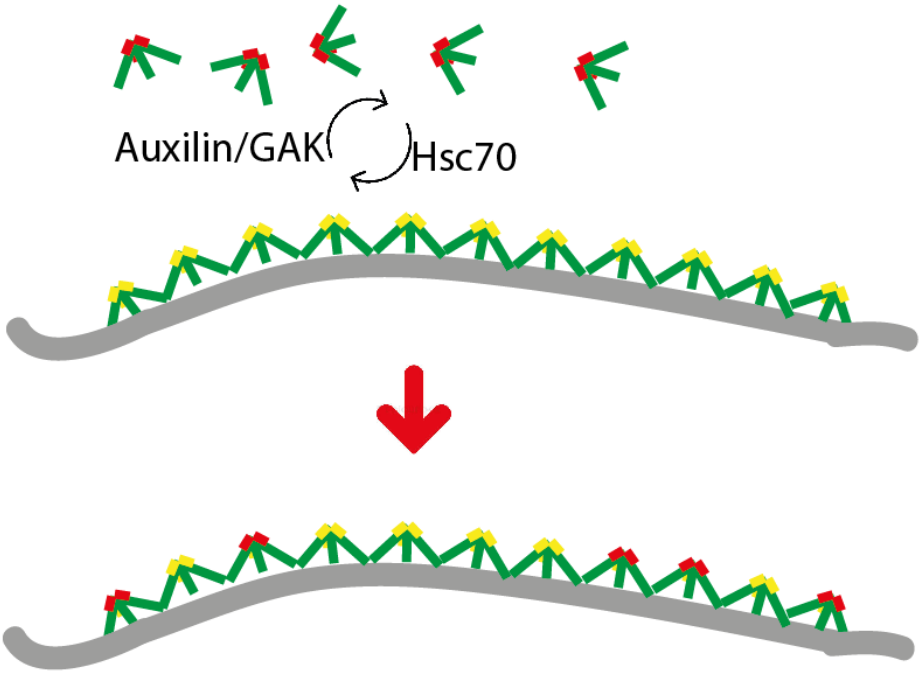

Figure 6.1: Microscopy based approach to determine clathrin exchange. Membrane sheets of cells expressing fluorescently labelled CLC are incubated with differently labelled triskelia in the presence or absence of components of the rearranging machinery to characterise clathrin exchange and lattice rearrangement in real time

7 REFERENCES

Acton, S. L. and Brodsky, F. M. (1990) 'Predominance of clathrin light chain LCb correlates with the presence of a regulated secretory pathway.', *The Journal of cell biology*, 111(4), pp. 1419–26. Available at: http://www.ncbi.nlm.nih.gov/pubmed/2211818 (Accessed: 3 December 2018).

Aggeler, J., biology, Z. W.-T. J. of cell and 1982, undefined (no date) 'Initial events during phagocytosis by macrophages viewed from outside and inside the cell: membrane-particle interactions and clathrin.', *jcb.rupress.org*. Available at: http://jcb.rupress.org/content/94/3/613.abstract (Accessed: 4 December 2018).

Aghamohammadzadeh, S. and Ayscough, K. R. (2009) 'Differential requirements for actin during yeast and mammalian endocytosis', *Nature Cell Biology*, 11(8), pp. 1039–1042. doi: 10.1038/ncb1918.

Akisaka, T. *et al.* (2003) 'Clathrin sheets on the protoplasmic surface of ventral membranes of osteoclasts in culture', *Journal of Electron Microscopy*. Oxford University Press, 52(6), pp. 535–543. doi: 10.1093/jmicro/52.6.535.

Akisaka, T. *et al.* (2008) 'Adhesion structures and their cytoskeleton-membrane interactions at podosomes of osteoclasts in culture', *Cell and Tissue Research*, 331(3), pp. 625–641. doi: 10.1007/s00441-007-0552-x.

Akisaka, T. *et al.* (no date) 'Adhesion structures and their cytoskeleton-membrane interactions at podosomes of osteoclasts in culture', *Springer*. Available at: https://link.springer.com/article/10.1007/s00441-007-0552-x (Accessed: 4 December 2018).

Almeida-Souza, L. *et al.* (2018) 'A Flat BAR Protein Promotes Actin Polymerization at the Base of Clathrin-Coated Pits', *Cell*, 174(2), p. 325–337.e14. doi: 10.1016/j.cell.2018.05.020.

Avinoam, O. *et al.* (2015) 'ENDOCYTOSIS. Endocytic sites mature by continuous bending and remodeling of the clathrin coat.', *Science (New York, N.Y.)*. American Association for the Advancement of Science, 348(6241), pp. 1369–72. doi: 10.1126/science.aaa9555.

Baschieri, F. *et al.* (2018) 'Frustrated endocytosis controls contractility-independent mechanotransduction at clathrin-coated structures', *Nature Communications*, 9(1), p. 3825. doi: 10.1038/s41467-018-06367-y.

Bonazzi, M. *et al.* (2011) 'Clathrin phosphorylation is required for actin recruitment at sites of bacterial adhesion and internalization', *J Cell Biol*. Rockefeller University Press, 195(3), pp. 525–536. doi: 10.1083/JCB.201105152.

Boulant, S. *et al.* (2011) 'Actin dynamics counteract membrane tension during clathrin-mediated endocytosis', *Nature Cell Biology*, 13(9), pp. 1124–1131. doi: 10.1038/ncb2307.

Brodsky, F. M. (1988) 'Living with clathrin: its role in intracellular membrane traffic.', *Science (New York, N.Y.)*, 242(4884), pp. 1396–402. Available at: http://www.ncbi.nlm.nih.gov/pubmed/2904698 (Accessed: 3 December 2018).

Brodsky, F. M. *et al.* (1991) 'Clathrin light chains: arrays of protein motifs that regulate coated-vesicle dynamics.', *Trends in biochemical sciences*, 16(6), pp. 208–13. Available at: http://www.ncbi.nlm.nih.gov/pubmed/1909824 (Accessed: 3 December 2018).

Bucher, D. *et al.* (2018) 'Clathrin-adaptor ratio and membrane tension regulate the flat-to-curved transition of the clathrin coat during endocytosis.', *Nature communications*. Nature Publishing Group, 9(1), p. 1109. doi: 10.1038/s41467-018-03533-0.

Chen, C.-Y. and Brodsky, F. M. (2005) 'Huntingtin-interacting Protein 1 (Hip1) and Hip1-related Protein (Hip1R) Bind the Conserved Sequence of Clathrin Light Chains and Thereby Influence Clathrin Assembly *in Vitro* and Actin Distribution *in Vivo*', *Journal of Biological Chemistry*, 280(7), pp. 6109–6117. doi: 10.1074/jbc.M408454200.

Chen, P.-H. *et al.* (2017) 'Crosstalk between CLCb/Dyn1-Mediated Adaptive Clathrin-Mediated Endocytosis and Epidermal Growth Factor Receptor Signaling Increases Metastasis', *Developmental Cell*, 40(3), p. 278–288.e5. doi: 10.1016/j.devcel.2017.01.007.

Cheng, Y. *et al.* (2007) 'Cryo-electron Tomography of Clathrin-coated Vesicles: Structural Implications for Coat Assembly', *Journal of Molecular Biology*, 365(3), pp. 892–899. doi: 10.1016/j.jmb.2006.10.036.

Cocucci, E. *et al.* (2012) 'The first five seconds in the life of a clathrin-coated pit.', *Cell*. NIH Public Access, 150(3), pp. 495–507. doi: 10.1016/j.cell.2012.05.047.

Collawn, J. F. *et al.* (1990) 'Transferrin receptor internalization sequence YXRF implicates a tight turn as the structural recognition motif for endocytosis.', *Cell*, 63(5), pp. 1061–72. Available at: http://www.ncbi.nlm.nih.gov/pubmed/2257624 (Accessed: 4 December 2018).

Collins, A. *et al.* (2011) 'Structural Organization of the Actin Cytoskeleton at Sites of Clathrin-Mediated Endocytosis', *Current Biology*, 21(14), pp. 1167–1175. doi: 10.1016/j.cub.2011.05.048.

Cossart, P. and Helenius, A. (2014) 'Endocytosis of viruses and bacteria.', *Cold Spring Harbor perspectives in biology*. Cold Spring Harbor Laboratory Press, 6(8). doi: 10.1101/cshperspect.a016972.

Crowther, R. A., Pinch, J. T. and Pearse, B. M. F. (1976) 'On the structure of coated vesicles', *Journal of Molecular Biology*. Academic Press, 103(4), pp. 785–798. doi: 10.1016/0022-2836(76)90209-6.

Dannhauser, P. N. *et al.* (2015) 'Effect of Clathrin Light Chains on the Stiffness of Clathrin Lattices and Membrane Budding', *Traffic*, 16(5), pp. 519–533. doi: 10.1111/tra.12263.

Dannhauser, P. N. *et al.* (2017) 'CHC22 and CHC17 clathrins have distinct biochemical properties and display differential regulation and function.', *The Journal of biological chemistry*. American Society for Biochemistry and Molecular Biology, 292(51), pp. 20834–20844. doi: 10.1074/jbc.M117.816256.

Dannhauser, P. N. and Ungewickell, E. J. (2012) 'Reconstitution of clathrin-coated bud and vesicle formation with minimal components', *Nature Cell Biology*, 14(6), pp. 634–639. doi: 10.1038/ncb2478.

DeLuca-Flaherty, C. *et al.* (1990) 'Uncoating protein (hsc70) binds a conformationally labile domain of clathrin light chain LCa to stimulate ATP hydrolysis', *Cell*. Cell Press, 62(5), pp. 875–887. doi: 10.1016/0092-8674(90)90263-E.

Ebisuya, M., Kondoh, K. and Nishida, E. (2005) 'The duration, magnitude and compartmentalization of ERK MAP kinase activity: mechanisms for providing signaling specificity.', *Journal of cell science*. The Company of Biologists Ltd, 118(Pt 14), pp. 2997–3002. doi: 10.1242/jcs.02505.

Ehrlich, M. *et al.* (2004) 'Endocytosis by Random Initiation and Stabilization of Clathrin-Coated Pits', *Cell*, 118(5), pp. 591–605. doi: 10.1016/j.cell.2004.08.017.

Eisenberg, E. and Greene, L. E. (2007) 'Multiple Roles of Auxilin and Hsc70 in Clathrin-Mediated Endocytosis', *Traffic*, 8(6), pp. 640–646. doi: 10.1111/j.1600-0854.2007.00568.x.

Elkhatib, N. *et al.* (2017) 'Tubular clathrin/AP-2 lattices pinch collagen fibers to support 3D cell migration.', *Science (New York, N.Y.)*, 356(6343), p. eaal4713. doi: 10.1126/science.aal4713.

Erb, L. and Weisman, G. A. (2012) 'Coupling of P2Y receptors to G proteins and other signaling pathways.', *Wiley interdisciplinary reviews. Membrane transport and signaling*. NIH Public Access, 1(6), pp. 789–803. doi: 10.1002/wmts.62.

Ferreira, F. *et al.* (2012) 'Endocytosis of G Protein-Coupled Receptors Is Regulated by Clathrin Light Chain Phosphorylation', *Current Biology*, 22(15), pp. 1361–1370. doi: 10.1016/j.cub.2012.05.034.

Fotin, A., Cheng, Y., Sliz, P., *et al.* (2004) 'Molecular model for a complete clathrin lattice from electron cryomicroscopy', *Nature*, 432(7017), pp. 573–579. doi: 10.1038/nature03079.

Fotin, A., Cheng, Y., Grigorieff, N., *et al.* (2004) 'Structure of an auxilin-bound clathrin coat and its implications for the mechanism of uncoating', *Nature*. Nature Publishing Group, 432(7017), pp. 649–653. doi: 10.1038/nature03078.

Franck, A. *et al.* (2018) 'Mechanosensitive clathrin platforms anchor desmin intermediate filaments in skeletal muscle', *bioRxiv*. Cold Spring Harbor Laboratory, p. 321885. doi: 10.1101/321885.

Fujimoto, L. M. *et al.* (2000) 'Actin Assembly Plays a Variable, but not Obligatory Role in Receptor-Mediated Endocytosis', *Traffic*. Wiley/Blackwell (10.1111), 1(2), pp. 161–171. doi: 10.1034/j.1600-0854.2000.010208.x.

Gkouvatsos, K., Papanikolaou, G. and Pantopoulos, K. (2012) 'Regulation of iron transport and the role of transferrin', *Biochimica et Biophysica Acta (BBA) - General Subjects*, 1820(3), pp. 188–202. doi: 10.1016/j.bbagen.2011.10.013.

Grove, J. *et al.* (2014) 'Flat clathrin lattices: stable features of the plasma membrane', *Molecular Biology of the Cell*. Edited by S. L. Schmid and J. Lippincott-Schwartz, 25(22), pp. 3581–3594. doi: 10.1091/mbc.e14-06-1154.

ter Haar, E. *et al.* (1998) 'Atomic structure of clathrin: a beta propeller terminal domain joins an alpha zigzag linker.', *Cell*. NIH Public Access, 95(4), pp. 563–73. Available at: http://www.ncbi.nlm.nih.gov/pubmed/9827808 (Accessed: 3 December 2018).

He, K. *et al.* (2017) 'Dynamics of phosphoinositide conversion in clathrin-mediated endocytic traffic', *Nature*. Nature Publishing Group, 552(7685), pp. 410–414. doi: 10.1038/nature25146.

Henry, A. G. *et al.* (2012) 'Regulation of Endocytic Clathrin Dynamics by Cargo Ubiquitination', *Developmental Cell*, 23(3), pp. 519–532. doi: 10.1016/j.devcel.2012.08.003.

Heuser, J. (1980) 'Three-dimensional visualization of coated vesicle formation in fibroblasts.', *The Journal of cell biology*. Rockefeller University Press, 84(3), pp. 560–83. doi: 10.1083/JCB.84.3.560.

Hill, B. L. *et al.* (1988) 'Identification of the phosphorylation sites of clathrin light chain LCb.', *The Journal of biological chemistry*, 263(12), pp. 5499–501. Available at: http://www.ncbi.nlm.nih.gov/pubmed/3128543 (Accessed: 3 December 2018).

Hinrichsen, L. *et al.* (2003) 'Effect of clathrin heavy chain- and alpha-adaptin-specific small inhibitory RNAs on endocytic accessory proteins and receptor trafficking in HeLa cells.', *The Journal of biological chemistry*, 278(46), pp. 45160–70. doi: 10.1074/jbc.M307290200.

Hirst, J. *et al.* (2008) 'Auxilin Depletion Causes Self-Assembly of Clathrin into Membraneless Cages *In Vivo*', *Traffic*, 9(8), pp. 1354–1371. doi: 10.1111/j.1600-0854.2008.00764.x.

Irannejad, R. and von Zastrow, M. (2014) 'GPCR signaling along the endocytic pathway', *Current Opinion in Cell Biology*, 27, pp. 109–116. doi: 10.1016/j.ceb.2013.10.003.

Jackson, A. P. *et al.* (1987) ‘Clathrin light chains contain brain-specific insertion sequences and a region of homology with intermediate filaments’, *Nature*, 326(6109), pp. 154–159. doi: 10.1038/326154a0.

Kanaseki, T. and Kadota, K. (1969) ‘The "vesicle in a basket". A morphological study of the coated vesicle isolated from the nerve endings of the guinea pig brain, with special reference to the mechanism of membrane movements.’, *The Journal of cell biology*, 42(1), pp. 202–20. Available at: http://www.ncbi.nlm.nih.gov/pubmed/4182372 (Accessed: 3 December 2018).

Keyel, P. A. *et al.* (2006) ‘A Single Common Portal for Clathrin-mediated Endocytosis of Distinct Cargo Governed by Cargo-selective Adaptors’, *Molecular Biology of the Cell*. Edited by S. Schmid, 17(10), pp. 4300–4317. doi: 10.1091/mbc.e06-05-0421.

Kirchhausen, T. *et al.* (1987) ‘Clathrin light chains LCA and LCB are similar, polymorphic, and share repeated heptad motifs.’, *Science (New York, N.Y.)*, 236(4799), pp. 320–4. Available at: http://www.ncbi.nlm.nih.gov/pubmed/3563513 (Accessed: 3 December 2018).

Kirchhausen, T. *et al.* (2008) ‘Location and distribution of the light chains in clathrin trimers.’, *PNAS*. National Academy of Sciences, 80(9), pp. 2481–2485. doi: 10.1073/pnas.80.9.2481.

Kirchhausen, T. (2009) ‘Imaging endocytic clathrin structures in living cells’, *Trends in Cell Biology*, 19(11), pp. 596–605. doi: 10.1016/j.tcb.2009.09.002.

Kirchhausen, T., Harrison, S. C. and Heuser, J. (1986) ‘Configuration of clathrin trimers: evidence from electron microscopy.’, *Journal of ultrastructure and molecular structure research*, 94(3), pp. 199–208. Available at: http://www.ncbi.nlm.nih.gov/pubmed/3805786 (Accessed: 3 December 2018).

Kirchhausen, T., Owen, D. and Harrison, S. C. (2014) ‘Molecular structure, function, and dynamics of clathrin-mediated membrane traffic.’, *Cold Spring Harbor perspectives in biology*. Cold Spring Harbor Laboratory Press, 6(5), p. a016725. doi: 10.1101/cshperspect.a016725.

Kochman, K. (2014) ‘Superfamily of G-protein coupled receptors (GPCRs) – extraordinary and outstanding success of evolution’, *Postępy Higieny i Medycyny Doświadczalnej*, 68, pp. 1225–1237. doi: 10.5604/17322693.1127326.

Lampe, M., Vassilopoulos, S. and Merrifield, C. (2016) ‘Clathrin coated pits, plaques and adhesion’, *Journal of Structural Biology*, 196(1), pp. 48–56. doi: 10.1016/j.jsb.2016.07.009.

Leyton-Puig, D. *et al.* (2017) ‘Flat clathrin lattices are dynamic actin-controlled hubs for clathrin-mediated endocytosis and signalling of specific receptors’, *Nature Communications*, 8, p. 16068. doi: 10.1038/ncomms16068.

Liu, A. P. *et al.* (2010) ‘Local clustering of transferrin receptors promotes clathrin-coated pit initiation.’, *The Journal of cell biology*. Rockefeller University Press, 191(7), pp. 1381–93. doi: 10.1083/jcb.201008117.

Lock, J. G. *et al.* (2018) ‘Reticular adhesions are a distinct class of cell-matrix adhesions that mediate attachment during mitosis’, *Nature Cell Biology*. Nature Publishing Group, 20(11), pp. 1290–1302. doi: 10.1038/s41556-018-0220-2.

Ma, L. *et al.* (2016) ‘Transient Fcho1/2· Eps15/R· AP-2 Nanoclusters Prime the AP-2 Clathrin Adaptor for Cargo Binding.’, *Developmental cell*. Elsevier, 37(5), pp. 428–43. doi: 10.1016/j.devcel.2016.05.003.

Maib, H. *et al.* (2018) ‘Cargo regulates clathrin-coated pit invagination via clathrin light chain phosphorylation’, *The Journal of Cell Biology*, 217(12), pp. 4253–4266. doi: 10.1083/jcb.201805005.

Mamedova, L. K., Gao, Z.-G. and Jacobson, K. A. (2006) 'Regulation of death and survival in astrocytes by ADP activating P2Y1 and P2Y12 receptors', *Biochemical Pharmacology*, 72(8), pp. 1031–1041. doi: 10.1016/j.bcp.2006.07.017.

Maupin, P., biology, T. P.-T. J. of cell and 1983, undefined (no date) 'Improved preservation and staining of HeLa cell actin filaments, clathrin-coated membranes, and other cytoplasmic structures by tannic acid-glutaraldehyde-saponin', *jcb.rupress.org*. Available at: http://jcb.rupress.org/content/96/1/51.abstract (Accessed: 4 December 2018).

Miaczynska, M. (2013) 'Effects of membrane trafficking on signaling by receptor tyrosine kinases.', *Cold Spring Harbor perspectives in biology*. Cold Spring Harbor Laboratory Press, 5(11), p. a009035. doi: 10.1101/cshperspect.a009035.

Miller, K. *et al.* (no date) 'Transferrin receptors promote the formation of clathrin lattices', *Elsevier*. Available at: https://www.sciencedirect.com/science/article/pii/009286749190094F (Accessed: 4 December 2018).

Miller, S. E. *et al.* (2015) 'CALM regulates clathrin-coated vesicle size and maturation by directly sensing and driving membrane curvature.', *Developmental cell*. Elsevier, 33(2), pp. 163–75. doi: 10.1016/j.devcel.2015.03.002.

Moore, C. S. *et al.* (2015) 'P2Y12 expression and function in alternatively activated human microglia', *Neurology - Neuroimmunology Neuroinflammation*, 2(2), p. e80. doi: 10.1212/NXI.0000000000000080.

Mundell, S. J. *et al.* (2006) 'Distinct Clathrin-Coated Pits Sort Different G Protein-Coupled Receptor Cargo', *Traffic*, 7(10), pp. 1420–1431. doi: 10.1111/j.1600-0854.2006.00469.x.

Musacchio, A. *et al.* (1999) 'Functional organization of clathrin in coats: combining electron cryomicroscopy and X-ray crystallography.', *Molecular cell*, 3(6), pp. 761–70. Available at: http://www.ncbi.nlm.nih.gov/pubmed/10394364 (Accessed: 3 December 2018).

Nicol, A., biology, M. N.-E. journal of cell and 1987, undefined (no date) 'A new type of substratum adhesion structure in NRK cells revealed by correlated interference reflection and electron microscopy.', *europepmc.org*. Available at: https://europepmc.org/abstract/med/3113954 (Accessed: 4 December 2018).

Nisar, S. *et al.* (2011) 'An intact PDZ motif is essential for correct P2Y12 purinoceptor traffic in human platelets.', *Blood*, 118(20), pp. 5641–51. doi: 10.1182/blood-2011-02-336826.

Ohno, H. *et al.* (1995) 'Interaction of tyrosine-based sorting signals with clathrin-associated proteins.', *Science (New York, N.Y.)*, 269(5232), pp. 1872–5. Available at: http://www.ncbi.nlm.nih.gov/pubmed/7569928 (Accessed: 4 December 2018).

den Otter, W. K. and Briels, W. J. (2011) 'The Generation of Curved Clathrin Coats from Flat Plaques', *Traffic*, 12(10), pp. 1407–1416. doi: 10.1111/j.1600-0854.2011.01241.x.

Pearse, B. M. (1975) 'Coated vesicles from pig brain: purification and biochemical characterization.', *Journal of molecular biology*, 97(1), pp. 93–8. Available at: http://www.ncbi.nlm.nih.gov/pubmed/1177317 (Accessed: 3 December 2018).

Picco, A. *et al.* (2015) 'Visualizing the functional architecture of the endocytic machinery.', *eLife*, 4. doi: 10.7554/eLife.04535.

Poupon, V. *et al.* (2008) 'Clathrin light chains function in mannose phosphate receptor trafficking via regulation of actin assembly.', *Proceedings of the National Academy of Sciences of the United States of America*, 105(1), pp. 168–73. doi: 10.1073/pnas.0707269105.

Prasanna, X., Chattopadhyay, A. and Sengupta, D. (2014) 'Cholesterol modulates the dimer interface of the β_2-adrenergic receptor via cholesterol occupancy sites.', *Biophysical journal*. The Biophysical Society, 106(6), pp. 1290–300. doi: 10.1016/j.bpj.2014.02.002.

Pumplin, D. W. and Bloch, R. J. (1990) 'Clathrin-coated membrane: A distinct membrane domain in acetylcholine receptor clusters of rat myotubes', *Cell Motility and the Cytoskeleton*, 15(2), pp. 121–134. doi: 10.1002/cm.970150208.

Ranjan, R., Gupta, P. and Shukla, A. K. (2016) 'GPCR Signaling: β-arrestins Kiss and Remember.', *Current biology : CB*. Elsevier, 26(7), pp. R285-8. doi: 10.1016/j.cub.2016.02.056.

Rapoport, I. *et al.* (2008) 'A motif in the clathrin heavy chain required for the Hsc70/auxilin uncoating reaction.', *Molecular biology of the cell*. American Society for Cell Biology, 19(1), pp. 405–13. doi: 10.1091/mbc.e07-09-0870.

Saffarian, S., Cocucci, E. and Kirchhausen, T. (2009) 'Distinct Dynamics of Endocytic Clathrin-Coated Pits and Coated Plaques', *PLoS Biology*. Edited by F. Hughson. Public Library of Science, 7(9), p. e1000191. doi: 10.1371/journal.pbio.1000191.

Saffarian, S. and Kirchhausen, T. (2008) 'Differential Evanescence Nanometry: Live-Cell Fluorescence Measurements with 10-nm Axial Resolution on the Plasma Membrane', *Biophysical Journal*. Cell Press, 94(6), pp. 2333–2342. doi: 10.1529/BIOPHYSJ.107.117234.

Saleem, M. *et al.* (2015) 'A balance between membrane elasticity and polymerization energy sets the shape of spherical clathrin coats', *Nature Communications*. Nature Publishing Group, 6(1), p. 6249. doi: 10.1038/ncomms7249.

Sanan, D. A. and Anderson, R. G. (1991) 'Simultaneous visualization of LDL receptor distribution and clathrin lattices on membranes torn from the upper surface of cultured cells.', *The journal of histochemistry and cytochemistry : official journal of the Histochemistry Society*. SAGE PublicationsSage CA: Los Angeles, CA, 39(8), pp. 1017–24. doi: 10.1177/39.8.1906908.

Savi, P. *et al.* (2006) 'The active metabolite of Clopidogrel disrupts P2Y12 receptor oligomers and partitions them out of lipid rafts.', *Proceedings of the National Academy of Sciences of the United States of America*, 103(29), pp. 11069–74. doi: 10.1073/pnas.0510446103.

Schmid, S. L. *et al.* (no date) 'A role for clathrin light chains in the recognition of clathrin cages by "uncoating ATPase".', *Nature*, 311(5983), pp. 228–31. Available at: http://www.ncbi.nlm.nih.gov/pubmed/6148701 (Accessed: 3 December 2018).

Scott, B. L. *et al.* (2018) 'Membrane bending occurs at all stages of clathrin-coat assembly and defines endocytic dynamics', *Nature Communications*. Nature Publishing Group, 9(1), p. 419. doi: 10.1038/s41467-018-02818-8.

Signoret, N. *et al.* (2005) 'Agonist-induced Endocytosis of CC Chemokine Receptor 5 Is Clathrin Dependent', *Molecular Biology of the Cell*, 16(2), pp. 902–917. doi: 10.1091/mbc.e04-08-0687.

Sinha, B. *et al.* (2011) 'Cells respond to mechanical stress by rapid disassembly of caveolae.', *Cell*. NIH Public Access, 144(3), pp. 402–13. doi: 10.1016/j.cell.2010.12.031.

Smith, S. M. *et al.* (2017) 'Weak Molecular Interactions in Clathrin-Mediated Endocytosis', *Frontiers in Molecular Biosciences*. Frontiers Media SA, 4. doi: 10.3389/FMOLB.2017.00072.

Sochacki, K. A. *et al.* (2017) 'Endocytic proteins are partitioned at the edge of the clathrin lattice in mammalian cells', *Nature Cell Biology*, 19(4), pp. 352–361. doi: 10.1038/ncb3498.

Soohoo, A. L. and Puthenveedu, M. A. (2013) 'Divergent modes for cargo-mediated control of clathrin-coated pit dynamics', *Molecular Biology of the Cell*. Edited by D. G. Drubin, 24(11), pp. 1725–1734. doi: 10.1091/mbc.e12-07-0550.

Sorokin, A. *et al.* (2018) 'Rule-based modelling provides an extendable framework for comparing candidate mechanisms underpinning clathrin polymerisation', *Scientific Reports*. Nature Publishing Group, 8(1), p. 5658. doi: 10.1038/s41598-018-23829-x.

Stachowiak, J. C., Brodsky, F. M. and Miller, E. A. (2013) 'A cost–benefit analysis of the physical mechanisms of membrane curvature', *Nature Cell Biology*, 15(9), pp. 1019–1027. doi: 10.1038/ncb2832.

Tuteja, N. (2009) 'Signaling through G protein coupled receptors.', *Plant signaling & behavior*. Taylor & Francis, 4(10), pp. 942–7. Available at: http://www.ncbi.nlm.nih.gov/pubmed/19826234 (Accessed: 4 December 2018).

Umasankar, P. K. *et al.* (2012) 'Distinct and separable activities of the endocytic clathrin-coat components Fcho1/2 and AP-2 in developmental patterning.', *Nature cell biology*. NIH Public Access, 14(5), pp. 488–501. doi: 10.1038/ncb2473.

Unanue, E. R., Ungewickell, E. and Branton, D. (1981) 'The binding of clathrin triskelions to membranes from coated vesicles.', *Cell*, 26(3 Pt 1), pp. 439–46. Available at: http://www.ncbi.nlm.nih.gov/pubmed/7034962 (Accessed: 3 December 2018).

Ungewickell, E. *et al.* (1995) 'Role of auxilin in uncoating clathrin-coated vesicles', *Nature*, 378(6557), pp. 632–635. doi: 10.1038/378632a0.

Ungewickell, E. and Branton, D. (1981) 'Assembly units of clathrin coats.', *Nature*, 289(5796), pp. 420–2. Available at: http://www.ncbi.nlm.nih.gov/pubmed/7464911 (Accessed: 3 December 2018).

Ungewickell, E. and Ungewickell, H. (1991) 'Bovine brain clathrin light chains impede heavy chain assembly in vitro.', *The Journal of biological chemistry*, 266(19), pp. 12710–4. Available at: http://www.ncbi.nlm.nih.gov/pubmed/2061336 (Accessed: 3 December 2018).

Vassilopoulos, S. *et al.* (2009) 'A Role for the CHC22 Clathrin Heavy-Chain Isoform in Human Glucose Metabolism', *Science*, 324(5931), pp. 1192–1196. doi: 10.1126/science.1171529.

Wang, L. *et al.* (2016) 'Eps15 membrane-binding and -bending activity acts redundantly with Fcho1 during clathrin-mediated endocytosis.', *Molecular biology of the cell*. American Society for Cell Biology, 27(17), pp. 2675–87. doi: 10.1091/mbc.E16-03-0151.

Watts, C. (1985) 'Rapid endocytosis of the transferrin receptor in the absence of bound transferrin.', *The Journal of cell biology*. Rockefeller University Press, 100(2), pp. 633–7. doi: 10.1083/JCB.100.2.633.

Wilbur, J. D. *et al.* (2008) 'Actin Binding by Hip1 (Huntingtin-interacting Protein 1) and Hip1R (Hip1-related Protein) Is Regulated by Clathrin Light Chain', *Journal of Biological Chemistry*, 283(47), pp. 32870–32879. doi: 10.1074/jbc.M802863200.

Wilbur, J. D. *et al.* (2010) 'Conformation switching of clathrin light chain regulates clathrin lattice assembly.', *Developmental cell*. NIH Public Access, 18(5), pp. 841–8. doi: 10.1016/j.devcel.2010.04.007.

Willox, A. K. and Royle, S. J. (2012) 'Functional Analysis of Interaction Sites on the N-Terminal Domain of Clathrin Heavy Chain', *Traffic*, 13(1), pp. 70–81. doi: 10.1111/j.1600-0854.2011.01289.x.

Wu, S. *et al.* (2016) 'Clathrin light chains' role in selective endocytosis influences antibody isotype switching', *Proceedings of the National Academy of Sciences*, 113(35), pp. 9816–9821. doi: 10.1073/pnas.1611189113.

Wu, X. *et al.* (2001) 'Clathrin exchange during clathrin-mediated endocytosis.', *The Journal of cell biology*. Rockefeller University Press, 155(2), pp. 291–300. doi: 10.1083/jcb.200104085.

Wu, X. *et al.* (2003) 'Adaptor and Clathrin Exchange at the Plasma Membrane and *trans* -Golgi Network', *Molecular Biology of the Cell*. Edited by R. Schekman, 14(2), pp. 516–528. doi: 10.1091/mbc.e02-06-0353.

Xu, C. and Min, J. (2011) 'Structure and function of WD40 domain proteins', *Protein & Cell*, 2(3), pp. 202–214. doi: 10.1007/s13238-011-1018-1.

Ybe, J. A. *et al.* (1998) 'Clathrin self-assembly is regulated by three light-chain residues controlling the formation of critical salt bridges', *The EMBO Journal*, 17(5), pp. 1297–1303. doi: 10.1093/emboj/17.5.1297.

Ybe, J. A. *et al.* (2003) 'Contribution of Cysteines to Clathrin Trimerization Domain Stability and Mapping of Light Chain Binding', *Traffic*. John Wiley & Sons, Ltd, 4(12), pp. 850–856. doi: 10.1046/j.1600-0854.2003.0139.x.

Yim, Y.-I. *et al.* (2005) 'Exchange of clathrin, AP2 and epsin on clathrin-coated pits in permeabilized tissue culture cells', *Journal of Cell Science*, 118(11), pp. 2405–2413. doi: 10.1242/jcs.02356.

Young, A. *et al.* (2013) 'Hsc70-induced changes in clathrin-auxilin cage structure suggest a role for clathrin light chains in cage disassembly.', *Traffic (Copenhagen, Denmark)*. Wiley-Blackwell, 14(9), pp. 987–96. doi: 10.1111/tra.12085.

Zhang, C. X. *et al.* (2005) 'Multiple Roles for Cyclin G-Associated Kinase in Clathrin-Mediated Sorting Events', *Traffic*, 6(12), pp. 1103–1113. doi: 10.1111/j.1600-0854.2005.00346.x.

Zuidema, A. *et al.* (2018) 'Mechanisms of integrin αVβ5 clustering in flat clathrin lattices', *Journal of Cell Science*, 131(21), p. jcs221317. doi: 10.1242/jcs.221317.